Universidade do Porto

Faculdade de Engenharia

FEUP

Departamento de Engenharia Electrotecnica e de Computadores

Time-Domain Impedance-Based Fault Location for HVDC Transmission Lines

Luis de Andrade de Freitas

Electrical Engineer, Universidad Simón Bolívar, Venezuela (2002)

M.Sc., Universidad Simón Bolívar, Venezuela (2008)

Doctoral dissertation submitted to the
Faculty of Engineering of the University of Porto

Supervisor
Prof. Maria Teresa Ponce de Leão Ph.D.

Co-supervisors
Prof. Helder Leite Ph.D.
Prof. Paulo De Oliveira Ph.D.

Departamento de Engenharia Electrotecnica e Computadores
Faculdade de Engenharia da Universidade do Porto

October, 2013
Porto — Portugal

This thesis was funded by a Ph.D. Grant SFRH/BD/33788/2009
FCT Fundação para a Ciência e a Tecnologia
MINISTÉRIO DA EDUCAÇÃO E CIÊNCIA

Time-Domain Impedance-Based Fault Location for HVDC Transmission Lines

Luis de Andrade de Freitas

Departamento de Engenharia Electrotecnica e Computadores
Faculdade de Engenharia da Universidade do Porto

To my family Mary, Gaby and Leo

Acknowledgments

I would like to express my gratitude to Prof. Dr. Maria Teresa Ponce de Leão for her invaluable ideas, advice, suggestions, guidance and encouragement since the beginning of this research project. This Thesis owes to her a sense of ambition and innovation that would have being impossible to attain without her leadership and support, providing the means to stablish a good friendship.

I would like to acknowledge the MIT-Portugal Program, specially Prof. Dr. João Peças Lopes and Prof. Dr. Eduardo Oliveira Fernandes for providing me the opportunity to participate in this program to develop this research work.

I'm also very thankful for the support provided by the Department of Electrical and Computer Engineering of the Faculty of Engineering of University of Porto (DEEC-FEUP), and the Power Systems Unit of INESC Porto (Instituto de Engenharia de Sistemas e Computadores do Porto). Specially, Prof. Dr. João Tome Saraiva and Prof. Dr. Manuel Matos.

Generous funding was provided by the Portuguese Fundação para a Ciência e a Tecnología with a Doctorate Scholarship.

Sincere thanks to Prof. Dr. Helder Leite at University of Porto and Prof. Dr. Paulo De Oliveira at Simón Bolívar University in Venezuela, for serving as co-advisers of this research and for their time invested with valuable advice and guidance.

I also wish to thank two important companies for their help: Eletrobras Furnas of Brazil, especially to Eng. Guilherme Sarcinelli Luz, and Eng. Ronaldo dos Santos for allowing me to use both actual fault records and model's data from their transmission line Foz do Iguaçu-Ibiuna. And from ABB Eng. Andre Balzi for providing technical and financial information about fault location equipment commercialized by them.

Great appreciation goes to Prof. Elmer Sorrentino at Simón Bolívar University for being my counsellor and guide throughout this journey.

I don't want to forget my great office mates at "J" building of FEUP campus, for helping me sort through the administrative hurdles and for their friendship. Many thanks to Célia Couto at MIT-Portugal Program. Colleagues and friends are also acknowledged for their support.

Last but not least, to my wife: for your patience, for your love and help. Without you I would be nowhere.

To my family.

Summary

In the last decades, High Voltage Direct Current (HVDC) systems have had extensive growth due to the great development that has occurred in AC-DC-AC conversion technology based on power electronics, and also for being strongly promoted as a great solution for the connection of renewable energy sources through long distances, both offshore and onshore.

However, there are still problems in the operation and maintenance of HVDC systems that can be reviewed and updated. Such is the case of automated methods of fault location. All currently available commercial methods are based on traveling wave technologies. These methods can have good accuracy, but they also have some disadvantages, such as the need for expensive measuring equipment dedicated exclusively to this purpose, and problems for detecting high impedance faults or faults close to the line terminals.

This thesis develops a method for fault location on HVDC lines based on line impedance estimation, as a proposal to complement the current methods in cases where commercial methods are not capable to give a satisfactory result. The reason to develop this method based on a different technology than traveling wave, is because it's intended to prevent the problems that affect these type of technologies.

The proposed method uses a mathematical model of the transmission line as a basis for estimating the line's impedance. This model was specifically attained to use in this project, and it was deducted from the transmission line differential equations in the time-domain. For this deduction is not required any approximation, so it was obtained a model that brings high accuracy to the fault location method.

The method's behavior is evaluated from the technical point of view, using both actual fault records and simulated fault records. The results are compared with results obtained by traditional methods in order to verify the performance of the different methods.

The proposed method aims to assist in the operation process of HVDC systems, providing a robust fault locator, with high accuracy, and low cost. This method is intended to replace the current traveling wave-based methods, or at least complement them in cases where traditional methods have not performed well.

Resumen

En las últimas décadas, los sistemas de Alto Voltaje en Corriente Directa (HVDC) han tenido un amplio crecimiento debido al gran desarrollo que se ha dado en la tecnología de conversión AC-DC-AC basado en electrónica de potencia y también gracias a que han sido fuertemente impulsado como una gran solución para la conexión de fuentes de energías renovable, tanto offshore como onshore, a través de largas distancias.

Sin embargo, existen aun problemas en la operación y mantenimiento de los sistemas HVDC que pueden ser revisados y actualizados. Tal es el caso de los métodos automáticos de localización de fallas. Todos los métodos comerciales actualmente disponibles se basan en tecnologías de ondas viajeras. Estos métodos pueden llegar a tener buena precisión, pero también poseen algunas desventajas tales como la necesidad de costosos equipos de medición dedicados exclusivamente a este fin y problemas para detección de fallas de alta impedancia o de fallas cercanas a los terminales de la línea.

Esta tesis desarrolla un método de localización de fallas en líneas HVDC basado en cálculo de impedancia de línea como propuesta para complementar los actuales métodos en aquellos casos donde los métodos comerciales no sean capaces de dar una respuesta satisfactoria. El hecho de desarrollar este método basado en una tecnología diferente al de onda viajera tiene como objetivo evitar los problemas que afectan a estos tipos de tecnologías.

El método propuesto utiliza un modelo matemático de la línea de transmisión como base para el cálculo de la impedancia de la línea. Este modelo fue específicamente deducido para su aplicación en este trabajo. El modelo fue deducido a partir de las ecuaciones diferenciales en el dominio del tiempo de la línea de transmisión. En esta deducción no se requirió de ninguna aproximación, por lo que se obtuvo un modelo que brida alta precisión al método de localización de fallas.

El comportamiento del método es evaluado desde el punto de vista técnico, utilizando tanto registros de fallas reales como registros de fallas simuladas. Los resultados son luego comparados con los resultados obtenidos mediante métodos tradicionales a fin de comprobar el desempeño de los diferentes métodos.

El método propuesto tiene como objetivo ayudar en el proceso de operación de los sistemas HVDC, ofreciendo un localizador de fallas robusto, de alta precisión y bajo costo. Con este método se pretende reemplazar los actuales métodos basados en onda viajera o, al menos, complementarlos en aquellos casos donde los métodos tradicionales no tengan buen desempeño.

Resumo

Nas últimas décadas, os sistemas de Alta Tensão em Corrente Continua (HVDC) tiveram um amplo crecimento devido ao grande desenvolvimento que tem acontesido na tecnologia de conversão AC-DC-AC baseado na electrónica de potência e também devido a que têm sido fortemente impulsionado como uma grande solução para a conecção de fontes de energias sustentaveis, quer offshore quer onshore, por longas distâncias.

No entanto, ainda há problemas na operação e manutenção de sistemas HVDC que podem ser revistos e atualizados. Tal é o caso dos métodos automatizados de localização de defeitos. Todos os métodos comerciais disponíveis atualmente são baseados em tecnologias de onda viajante. Esses métodos podem ter boa precisão, mas também têm algumas desvantagens, como a necessidade de dispendiosos equipamentos de medição dedicados unicamente para esse fim, alem de problemas de detecção de defeitos de alta impedância ou defeitos crecanos aos terminais da linha.

Esta dissertação desenvolve um método de localização de defeitos em linhas HVDC baseado no cálculo da impedância de linha, como proposta para complementar os métodos existentes nos casos em que os métodos comerciais não são capases de dar uma resposta satisfatória. O fato de desenvolver este método baseado numa tecnologia diferente ao de onda viajante se destina a evitar que os problemas que afetam esses tipos de tecnologias.

O método proposto utiliza um modelo matemático da linha de transmissão como base para calcular a impedância da linha. Este modelo foi derivado especificamente para sua aplicasión neste trabalho. O modelo foi derivado a partir das equações diferenciais no domínio do tempo da linha de transmissão. Nesta derivação não foi necessario o uso de qualquer aproximação, pelo que foi obtido um modelo que traz alta precisão ao método de localização de defeitos.

O comportamento do método é avaliado do ponto de vista técnico, com o uso quer de registros de defeitos reais quer de registros de defeitos simulados. Os resultados são então comparados com os resultados obtidos pelos métodos tradicionais com o fim de verificar o desempenho dos diferentes métodos.

O método proposto têm como objectivo auxiliar o processo da operação dos sistemas HVDC, proporcionando um localizador de defeitos robusto, de alta precisão e baixo custo. Este método destina-se a substituir os atuais métodos baseados em onda viajante, ou pelo menos suplementa-lhos nos casos em que os métodos tradicionais não tiveram um bom desempenho.

Publications

Publications in International Journals

1. L. de Andrade, H. Leite and M.T. Ponce de Leão. Time-Domain Distributed Parameters Transmission Line Model for Transient Analysis. *Progress In Electromagnetics Research B Journal*, Vol. 53, pp. 25-46, 2013.

2. L. de Andrade and M.T. Ponce de Leão. Fault Location for Transmission Lines Using Wavelet . *IEEE Latin America Trasactions*, Vol. 12, No. 6, p. 6, 2014.

Publications in International Congress & Conferences

1. L. de Andrade and E. Sorrentino, Inclusion of the Zero-Sequence Mutual Impedance in a Distributed Parameter Model of Transmission Lines, *In Proceedings of IEEE 9th International Conference on Environment and Electrical Engineering, Prague, Czech Republic*, pp. 242-245, May 2010,

2. L. de Andrade, P. De Oliveira and M. Ponce de Leão, Current Strategic Environmental Assessment in the Electrical Industry, *In Proceedings of IEEE 11th International Conference on Electrical Power Quality and Utilisation, Lisbon, Portugal*, p. 6, October 2011

3. L. de Andrade and M. Ponce de Leão, Faults Location Methods Reviews for Transmission Lines, *In Proceedings of CIGRÉ III Congreso Venezolano de Redes y Energía Eléctrica, Caracas, Venezuela*, p. 8, March 2012

4. L. de Andrade and M. Ponce de Leão, Travelling Wave Based Fault Location Analysis for Transmission Lines, *In Proceedings of 2nd European Energy Conference, Maastricht, Netherlands*, p. 9, April 2012

5. L. de Andrade and M. Ponce de Leão, Impedance-Based Fault Location Analysis for Transmission Lines, *In Proceedings of IEEE PES Transmission and Distribution Conference, Orlando, USA*, p. 6, May 2012

6. L. de Andrade and M. Ponce de Leão, A Brief History of Direct Current in Electrical Power Systems, *In Proceedings of IEEE History of Electro-technology Conference, Pavia, Italy*, p. 6, September 2012

7. L. de Andrade and M. Ponce de Leão, Current Interoperability of Electrical Systems, *In Proceedings of IEEE IV International Congress on Ultra Modern Telecommunications and Control Systems, St. Petersburg, Russia*, pp. 423-427, October 2012,

8. L. de Andrade and M. Ponce de Leão, Direct Current Power Systems, *In Proceedings of CIGRÉ Smarts Grids: Next Generation Grids for New Energy Trends International Symposium, Lisbon, Portugal*, p. 8, April 2013

9. L. de Andrade, Y. Blanco and M. Ponce de Leão, Using Power Systems Simulation Software for Fault Analysis, *In Proceedings of Encontro Regional Ibero-americano do CIGRE, Foz do Iguaçu, Brasil*, p. 8, May 2013

Acronyms

ABB	Asea Brown Boveri Group
AC	Alternating Current
ANN	Artificial Neural Networks
ASCII	American Standard Code for Information Interchange
ASEA	Allmänna Svenska Elektriska Aktiebolaget
BBC	Brown Boveri & Cie
BHEL	Bharat Heavy Electricals Ltd.
BM	Bergeron's Model
CIGRÉ	International Council on Large Electric Systems (in French: Conseil International des Grands Réseaux Électriques)
CIRED	Congrès International des Réseaux Électriques de Distribution
COMTRADE	IEEE Standard Common Format for Transient Data Exchange
CT	Current Transformer
DC	Direct Current
DG	Distributed Generation
DM	Developed Transmisson Line Model
EMTP	Electro-Magnetic Transients Programs
EU	European Union
FDTD	Finite Difference Time Domain Method
G.E.	General Electric
GPS	Global Positioning System
HVDC	High Voltage Direct Current
IEEE	Institute of Electrical and Electronics Engineers
IGBT	Insulated-Gate Bipolar Transistor
LCC	Line-Commutated Converters
PT	Potential Transformer
PV	Photovoltaics
SCADA	Supervisory Control and Data Acquisition
SEL	Schweitzer Engineering Laboratories Inc.
SO	System Operator
T&D	Transmission & Distribution
UHVDC	Ultra High Voltage DC
USA	United States of America
VSC	Voltage-Source Converters

List of Symbols

$^{+}$	Denote the Positive-sequence Component
^{0}	Denote the Zero-sequence Component
α	Attenuation Constant
β	Phase Constant
Γ	Reflection Coefficient
γ	Line Propagation Constant
γ_{RG}	Line Propagation Constant with Low Frequency Components of the Frequency Domine Coeficients ($\gamma_{RG} = \sqrt{RG}$)
ϵ_o	Absolute Magnetic Permeability in a Vacuum (8.85×10^{-12})
μ_o	Absolute Dielectric Permittivity of Vacuum ($4\pi \times 10^{-7}$)
π	Ratio of a Circle's Circumference to its Diameter (3.14159)
τ	Total Travel Time from one end of the Line to the Other ($\tau = l/v = l\sqrt{LC}$)
ω	Line Frequency
C	Capacitance Per Unit Length
c	Speed of Light in Vacuum ($\approx 3 \times 10^8$ m/sec.)
d	Distance Between the Measurement Point and the Fault Point
F	Fault Point
$f_1(x,t)$, $f_2(x,t)$	Denote a General Function Relative to x and t
G	Conductsnce Per Unit Length
I	Current
I_1	Current Measured in $x = 0$ at $t = t_1$
I_2	Current Measured in $x = 0$ at $t = t_2$
I_F	Fault Current
I_{Re}	Residual Current
j	Imaginary Unit ($\sqrt{-1}$)
K_1, K_2, K_a, K_b, K_c, K_d	Constant of the General Solution of Differential Equations
L	Inductance Per Unit Length
l	Total Length of the Line

R	Denote the Receiver Line-end
R	Resistance Per Unit Length
R_a, R_b	Variable Resistances Used in a Bridge Circuit
R_T	Total Line Series Resistance
S	Denote the Sender Line-end
S_{mode}	Signal Vector in Mode Domine
S_{phase}	Signal Vector in Phase Domine
t	Time Variable. Denote any Time Inside the Time Interval Analized
t_1	wavefront Arrival Time 1
t_2	wavefront Arrival Time 2
V	Voltage
v	Velocity
v_t	Travelling Wave Velocity
V_1	Voltage Measured in $x = 0$ at $t = t_1$
V_2	Voltage Measured in $x = 0$ at $t = t_2$
V_F	Fault Voltage
X	Axis on which the Distance Variable x Moves
x	Distance Variable. Denote any Point Inside the Transmission Line
Y	Total Shunt Admittance of the Line
y	Shunt Admittance Line Per Unit Length
Z	Total Series Impedance of the Line
z	Serie Impedance Line Per Unit Length
Z_o	Line Characteristic Impedance
Z_a	Impedance of the Medium a
Z_{LC}	Line Characteristic Impedance with High Frequency Components of the Frequency Domine Coeficients ($Z_{LC} = \sqrt{\frac{L}{C}}$)
Z_{RG}	Line Characteristic Impedance with Low Frequency Components of the Frequency Domine Coeficients ($Z_{RG} = \sqrt{\frac{R}{G}}$)

Contents

List of Tables

List of Figures

Chapter 1

Introduction

The operation and control of transmission networks is of crucial importance when guaranteed sustainability is desired, security of supply, and competitiveness. Solutions to optimize the interoperability of the grids must be developed in order to accommodate different sources of energy, some of them from natural resources, and of intermittent nature. As a consequence, power systems are becoming more and more complex with the increasing need to integrate renewable energy at large scales.

During the last decade, world non-hydro renewable electricity generation has gradually increased from 1.7% of total electricity generation in year the 2000, to 4.6% in the year 2009 [1]. This number is expected to increase since many countries try to get 20% of their electricity generation from renewable resources by 2020 [1]. In Europe, almost 70% of all new installed capacity during 2012 came from renewable energy [2]. This statistic shows a huge leap of EU countries to move away from fossil fuels and nuclear power. Among renewable energy sources, wind energy is one of the fastest growing energy technologies, due to its cost-competitiveness, reliability, and efficiency[1]. At the end of year 2000, there are 18 GW installed capacity of wind energy around the globe; by the end of year 2010, this number has increased tremendously to 195 GW [1], with 39% of the global installed wind energy capacity in 2012, Europe becomes the global leader in wind energy technology [3].

The structure and management of present electricity grids are not entirely suitable for the deployment of these low carbon technologies that, in general, present great uncertainty regarding their production profile, strongly dependent on the availability of natural resources. Therefore, any improvement in the management and operation of systems is important to help ensure the service. In this regard, in the last years systems operations have increased in an interconnected manner, in order to handle in an optimized way the different sources of energy and to respond efficiently to wide system disturbances.

The trend in power system planning uses tight operating margins with less redundancy, because of new constraints placed by economical and environmental factors. At the same time, additions of non-utility generators and independent power producers, an increase in interconection of systems, and an increasing competitive environment, make the power system difficult to operate and, consequently, more vulnerable to disturbances.

Also the increased availability of sophisticated computer, communication and measure-

[1] "Benefits of wind energy." Website, 2013. available at http://www.nrgsystems.com/AboutWind.aspx

ment technologies, are changing how to control and operate the power systems. However, the implementation of technologies that take into account these changes hasn't been exploited sufficiently and it continues to be a subject of the utmost importance for a society with growing energetic requirements and power systems with growing needs that do not endanger the environment. The current research work aims to investigate these unexplored fields to find solutions to the problems posed by modern power systems topologies.

In the development of these large power systems, AC transmission lines have traditionally been used, but in recent years a rapid development of power electronics and control technology has allowed the use of direct current lines (HVDC). The characteristics of the HVDC lines make them ideal for applications of interconnections between systems, and transportation of large blocks of energy.

Some of the advantages of HVDC, are greater capacity per equivalent conductor, simpler line construction, reduction of transmission losses, not contribution to AC faults, and no need of synchronous operation, then, when carrying a large amount of power, they can be used to interconnect AC systems with different frequencies or where asynchronous operation is desirable. Therefore, some common applications for these lines are the transmission of large amounts of power over long distances by overhead lines, for system interconnection through cables crossing bodies of water, or for interconnecting AC systems having different frequencies, or where asynchronous operation is desired.

This investigation will be concentrated in the development of a methodology oriented towards the support of the operation and maintenance of HVDC transmission systems that can be adapted to the high penetration of renewable energy current trends, based on communication technology to support the decision making process that aids the power system's security.

This work deals with the research in the field of HVDC systems with the objective of improving procedures for fault management. It also aims to accomplish the reduction of response times, the optimization of the location of the faults, with the implementation of simpler procedures in an economically viable way.

1.1 HVDC Historical Background

This section summarizes a brief history of the use of Direct Current (DC) in power systems, and the various problems associated with its commercial implementation. DC technology has been associated with power systems since the early uses of electricity; it has boomed and then fell into disuse in several occasions.

This section aims to show the causes that led to the evolution of electrical systems as are known today. To this end, the evolution of DC systems is presented since its beginnings to its replacement by Alternating Current (AC) systems as the standard for energy commerce, and the legacy left by these first DC systems that still persists to these days. Then, the HVDC systems are presented as a natural solution to preserve the advantages of DC systems in the AC era. A brief summary of converter technology is presented since their application in HVDC systems dictates the way these systems have been implemented. Also, it's shown the evolution this technology has had and the main projects built around the world with the implementation of DC technology.

Previous works have shown a review of DC history [4–7] so this section follows and

compliments this information with current data. Finally, is analyzed the new DC technology boom in recent decades and the promising development expectations that this technology brings to power systems.

1.1.1 The Beginnings

The practical applications of electricity began with DC. The basic discoveries of Galvani, Volta, Ampere or Ohm were on DC [6]. The first widespread practical application was DC telegraphy, but electric lighting also began with DC powered by dynamos. First came carbon arc lamps operated in series at constant current and fed from series-wound generators, later came carbon-filament incandescent lamps operated in parallel at constant voltage and supplied from shunt-wound generators.

The first electric central station in the world was built on Pearl Street in New York by Thomas A. Edison in 1882 [8]. It supplied DC at 110 V to an area roughly of 1.6 km in radius, and it had DC generators driven by steam engines (Figure 1.1). Within a few years similar stations were in operation in the central districts of most large cities throughout the world.

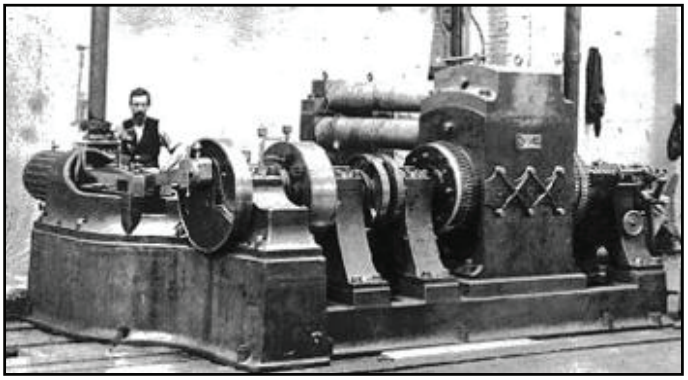

Figure 1.1: 100 kW Engine-driven dynamo
of the type installed at the Pearl Street station.

1.1.2 DC System Decline Causes

The mid-1880s AC systems began to compete with DC systems. Inventors such as Nicola Tesla, William Stanley, Michael Von Dolivo-Dobrowolsky, Elihu Thomson, Lucien Gaulard, John Gibbs, and others working in Europe and North America all contributed to AC technology.

In 1889, René Thury developed the first commercial system for high-voltage DC transmission in Europe, supplying Genoa, Italy from Gorzente River hydro turbines. The system was composed by generators in series to attain high transmission voltages. When loads were added to the system, other generators were added to maintain the voltage in the load.

In 1889, the first long distance transmission of DC electricity in the United States was switched on at Willamette Falls Station in Oregon. Later in 1890 a flood destroyed the Willamette Falls DC power station. This unfortunate event paved the way for the first long

distance transmission of AC electricity in the world when Willamette Falls Electric Company installed experimental AC generators from Westinghouse in 1890. In 1896, the first AC generation and transmission system was finished in the Niagara Falls using Westinghouse equipment [9].

The race between AC and DC systems was faced by great personalities of the time, in what would become the first standards war (Figure 1.2) [10]. Much has been written about the so called "war of currents", but this conflict was more a media fight than a conflict that had real importance in the selection of the winning system. Final decisions on the type of system to be applied always ended up being based on technical reasons, and AC systems of the time offered greater advantages than DC systems given the needs and available technology of the time.

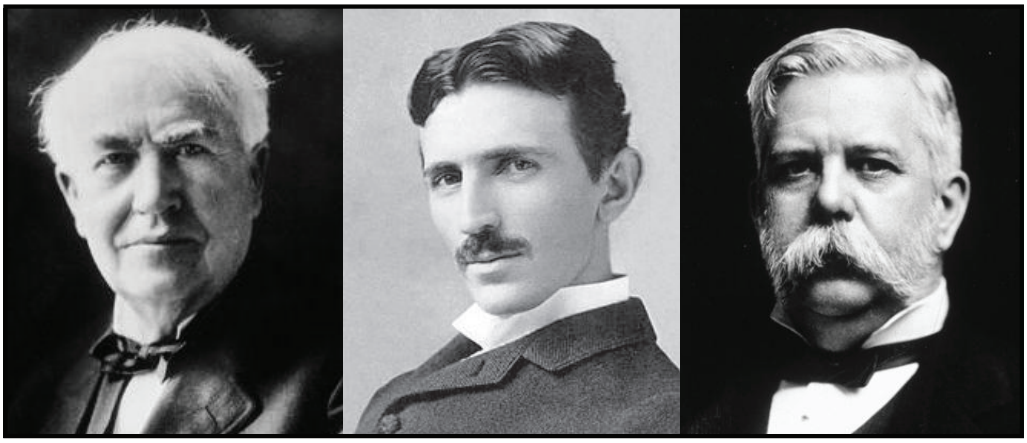

Figure 1.2: The three man faced in the first standards war.
From left to right: T. Edison, N. Tesla and G. Westinghouse.

N. Tesla's work contributed greatly to demonstrate the benefits of the use of AC systems, like the invention of the induction motor in 1888 [11]. Increasingly, promoted by industrialists such as George Westinghouse, the advantages of AC electric utility service became obvious, and by the end of the 19th century DC systems began an inevitable decline.

The advent of the transformer, tree-phase circuits, and the induction motor promoted the strengthening of AC electric systems as the world standard.

The transformer made possible the use of different voltage levels for generation, transmission, distribution, and use -particularly important for the high-voltage power transmission over long distances-. The 1890s DC systems required wire for each voltage level, making a city's streets look like a spider web of wire. With the use of three-phase networks it was possible to ensure a smooth, non-pulsating flow of power and also bring an easy way to interrupt current on high-voltage equipment.

The induction motor is rugged, cheap, and serves the majority of industrial and residential purposes. Also, the advent of steam turbines, which are best at high speeds, gave a great advantage to AC generators since the commutators of DC motors and generators impose limitations on the voltage, size, and especially in the speed of these machines.

The victory of AC over DC was almost complete. But some vestiges of DC distribution can be found in the electric traction system (trolley bus, railways or subway). Also, some cities continued to use DC well into the 20th century. For example, in Europe, Helsinki had

a DC network until the late 1940s, Stockholm lost its dwindling DC network as late as the 1970s, and London had some loads on DC as late as 1981. In USA, certain locations in Boston still used 110 volts DC in the 1960s. In 2007, the last DC circuit, a vestige of 19th century DC system of New York City was shut down [12].

1.1.3 DC Application at the Beginning of the AC Era

Despite the general acceptance of AC systems, some people never forgot the obvious advantages of DC, so they proposed not to replace AC but to complement it with DC, introducing a DC link on AC systems. This is how the HVDC systems came about.

All HVDC systems are composed by four mains parts, as shown in Figure 1.3:

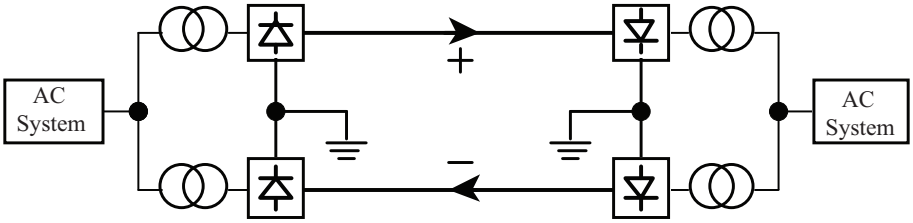

Figure 1.3: General scheme of a bipolar HVDC system.

- Transformers: responsible for bringing the AC system voltage to values that are manageable by the converters.
- Converters: are the devices that make the connection between AC and DC systems. A converter is basically an assemblage of controlled switches that commutes the different AC phases with the DC system as the AC phases vary. Therefore, the HVDC requires at least a converter at the sending end (called rectifier), and other at the receiver end (called inverter).
- Conductors: the systems can be classified according the number of conductors they have: mono-polar (with one conductor, usually of negative polarity), bipolar (with two conductors, one positive and other negative), or homo-polar (with two or more conductors all having the same polarity, usually negative).
- Protection and control: both always at the level of the converters which bring a high potential of control over voltage, current, power (active and reactive), and frequency.

The HVDC systems have many advantages over its AC counterpart, like:

- Greater capacity per equivalent conductor and simpler line construction.
- Each conductor can be operated as an independent circuit.
- Reduction of transmission losses and no skin effect.
- Improvement of the stability system.
- No problem with reactive power and voltage regulation.

- No Ferranti effect problems.
- No need of synchronous operation.

But also HVDC systems have some disadvantages like:

- Converters generate harmonics.
- Converters require greater reactive power.
- Converters have little overload capability.

Based on these advantages and disadvantages, many applications were found for HVDC, the most important are shown below:

- For transmitting large amounts of power over long distances.
- For interconnecting AC systems having different frequencies or where asynchronous operation is desired.
- For cables crossing bodies of water.

1.1.4 Converters Evolution

The converters are one of the most complex and important devices in a HVDC system. Since a DC transmission scheme requires currents to be converted from AC to DC or vice versa, the feasibility and advantageousness of DC transmission depended on the development of suitable converters. The converters in a HVDC system have proved to be reliable but expensive. They also constitute a bottle neck to the power transmissible since valves have little overload capability.

1.1.4.1 Firsts High Voltage Converters

Three of the most serious attempts to develop a converter suitable to DC transmission are the transverter, the electrolytic, and the atmospheric-arc converter.

The transverter, developed by W. Highfield and J. Calverley in 1920 [13], was an electromechanical switch that consisted essentially of polyphase transformers commutated by synchronously rotating brush gear. It performed the three basic operations of voltage transformation, phase multiplication, and commutation, and could be used either as a rectifier or as an inverter. Several experimental transverters were built; the largest of which was rated at 2 MW 100 kV DC but none has been used commercially.

The electrolytic rectifier was patented by G. Carpenter in 1928 [14]. Based on an electrochemical method where two different metals are suspended in an electrolyte solution, and direct current flowing one way through the solution sees less resistance than in the other direction. Despite several attempts, this device was not produced for high voltage applications because of the low breakdown voltage and the risk of electric shock.

The atmospheric-arc converter, devised by E. Marx in 1932, is a switching device in which an arc between two like water-cooled main electrodes are ignited by a high-frequency spark between auxiliary electrodes in the path of the main arc, and is extinguished after a zero

current by a blast of air that is continually released on the arc's path. A 5 km experimental line using atmospheric-arc converter was successfully operated in Germany with 16 MW and ±40 kV. The main difficulty encountered was that the main electrodes were consumed regularly requiring periodic replacement.

1.1.4.2 Converters Applied Commercially

The first commercial converter technology that came to be was the mercury-arc valves [15]. It was based on the early works of P. Cooper Hewitt in 1903 [16], but it was U. Lamm[2] in 1933 who develop a commercial high voltage mercury-arc valve [17]. A mercury-arc valve consists of an evacuated chamber containing a pool of mercury at the bottom forming the cathode. The anode is a carbon electrode at the top of the chamber. When the mercury pool is heated an arc can be struck within the chamber which conducts electrons from the cathode to the anode but not in the other direction. Hence, the device operates as a rectifier. The mercury-arc rectifier was used for power transmission and industrial processing between 1930 and 1975, when it was replaced by thyristor valves.

With the advent of the thyristor the converters evolution moved from electrochemical to solid state technology. It was developed in 1956 by engineers at General Electric (G.E.) led by R. Hall [18], but the firsts high voltage applications were in the middle of 1970s. The thyristor quickly replaced the mercury-arc valves as standards converters because of lower maintenance costs, simpler converter stations, and easier control system.

The thyristor is a silicon solid-state semiconductor device with four layers of alternating N and P type materials. They act as bi-stable switches, conducting when their gate receives a current pulse, and continuing to conduct as long as the voltage across the device is not reversed. In HVDC applications, many devices are placed in series/parallel configurations to achieve the desired voltage and current ratings. The thyristor rectifier was used from 1975 to 2000 when it was replaced by Insulated-Gate Bipolar Transistor (IGBT).

IGBT is a three-terminal silicon semi-conductor device, noted for high efficiency and fast switching. The IGBT is a Voltage Source Converter (VSC), meaning that it can be switched off as well as on by gate control. This seemingly small difference has completely revolutionized HVDC systems. The use of IGBT instead of thyristors is not a development comparable with the transition from mercury-arc valves to thyristor valves, but a rupture that required a complete change of the layout and design philosophy of the converter stations, and that greatly expanded the range of applications of HVDC. IGBTs allow the implementation of VSC instead of LCC. A main advantage of VSC converter stations is a high degree of flexibility: VSC has the inherent capability to control not only active but also reactive power.

The IGBT is a fairly recent development, first appearing in the 1980s. Third-generation devices were available in the late 1990s and quickly gained a reputation for excellent ruggedness and tolerance of overloads. In HVDC applications many devices are placed in series/parallel configurations to achieve the desired voltage and current ratings.

[2]Lamm is sometimes called "The Father of HVDC lines" due to its contribution to the current DC systems configuration. In 1933 he worked for ASEA.

1.2 HVDC Projects Around the World

1.2.1 Current HVDC Projects

It's difficult to quantify how many HVDC projects there are in the world, mainly at the moment of delimiting what HVDC means. The scope of this work only quantifies the projects of a commercial nature (not developed with research purposes) that include every element of a previous HVDC project (back to back projects are not included since they don't have conductors). Also, this work only refers to the beginnings of each project, future updates or extensions of a same project are not included. Finally, all the projects that have been in operation have been accounted for disregarding if they have been dismantled (projects under construction are not included).

There are 65 HVDC projects that interconnect power systems around the world [19]. Most of these projects are found in Europe (33.9%), Asia (32.3%), and America (24.6%), other projects have been built in Oceania (6.1%), and Africa (3.1%). Most European HVDC projects involve submarine cables, while Asia is dominated by overhead lines.

Although the commercial application of HVDC has existed since 1954, 58.5% of the projects have been developed in the last 20 years. This increase in the construction of HVDC systems in recent years is due mainly to the growth of the electrical network in Asia. Figure 1.4 shows the distribution of the HVDC projects throughout the continents and how these have increased in recent years, especially in the Asian region.

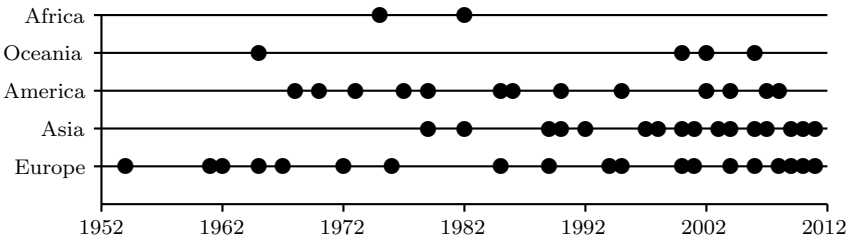

Figure 1.4: HVDC projects distribution.

In the manufacturing field of HVDC systems, the most important companies in charge of this task are ABB, Siemens, and Alstom. In the beginning, G.E. was an important manufacturer of HVDC systems, but in the mid 1990s the HVDC division at G.E. was absorbed by Alstom. Other manufacturers like Hitachi, Toshiba, and BHEL, among others, have had an important role in the construction of certain projects.

The first HVDC applications were built using mercury-arc converters. The initiative in exploring the HVDC applications were taken by G.E., in 1936 they used a 27 km line with 5.25 MW and 30 kV to connect the Mechanicville hydroelectric plant with the G.E. factory in New York [20]. This line was also the first that proved a feature of HVDC systems: frequency conversion (from 60 Hz to 40 Hz). Although it is the first application of a complete HVDC system, it's not considered the first commercial application since it supplied the G.E. factory.

The Gotland I[3] project is considered the first truly commercial HVDC scheme in the

[3]Gotland is between Västervik Converter Station (57^{o}43'41"N 16^{o}38'51"E) and Ygne Converter Station (57^{o}35'13"N 18^{o}11'44"E). Today is on service after many upgrades.

world. It was built by ASEA (now part of ABB), operated at 20 MW at ±100 kV, and consisted of 96 km of underwater cable between Västervik and Ygne in Sweden. This site is the most significant heritage site in the development of HVDC systems because it showed the progress made by mercury-arc technology (Figure 1.5[4]).

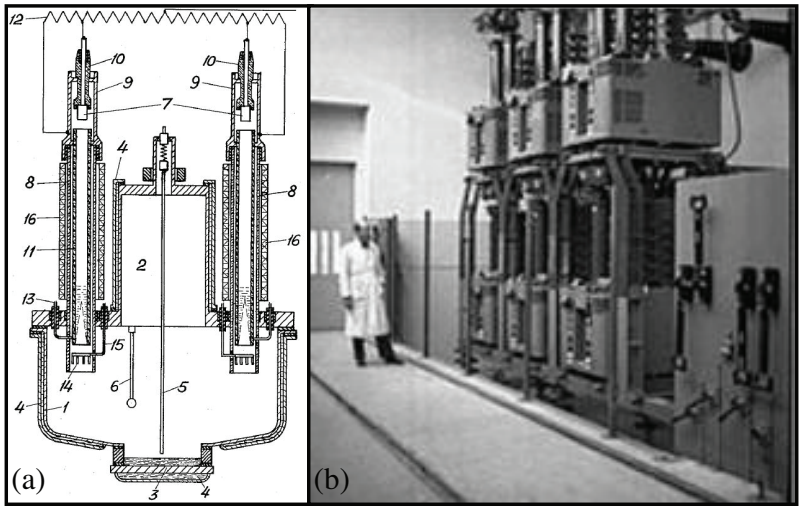

Figure 1.5: Mercury-arc converter diagram shown in Lamm's patent (a) that was also used in the Gotland I project (b).

In spite of the achievements of this project, HVDC did not immediately become a commercial success. Just until the 1960s more HVDC projects appeared. The most important of these projects was the Volgograd-Donobass[5] line [21] and was developed in 1965. It was a 473 km overhead line with 720 MW at ±400 kV built by the Russian government. It was the largest and with the highest voltages during these times.

During these years the Sardinia[6] HVDC system was also built in Italy between Sardinia and the mainland [22], which was the first HVDC system in the Mediterranean. It was a 413 km underwater cable with 200 MW at 200 kV constructed by English Electric (now part of Alstom). It was built in 1967 based on mercury-arc valves, but in 1993 it was upgraded with thyristor valves and it was added a third terminal towards Corsica, France, becoming the first multi-terminal HVDC system in the world.

In 1970 was built the Pacific Intertie[7] overhead line with 1440 MW, ±400 kV, and 1362 km of length [23]. It was the first HVDC of USA and was built by G.E. and ASEA. After some upgrades, it now has 3100 MW and ±500 kV.

In 1975 was built the Cahora-Bassa[8] overhead line with 1920 MW, ±563 kV, and 1456 km

[4]Photo source: ABB web site

[5]Volgograd-Donobass is between Volzhskaya Converter Station (48^{o}49'34"N 44^{o}40'20"E) and Mikhailovskaya Converter Station (48^{o}39'13"N 38^{o}33'56"E). The scheme is today in a bad state and only operated with a voltage of 100 kV. Nevertheless, it is being modernized.

[6]Sardinia is between Suvereto Converter Station (43^{o}03'10"N 10^{o}41'42"E) and Codrongianos Converter Station (40^{o}39'07"N 8^{o}42'48"E). Today is operational after many upgrades.

[7]Pacific Intertie is between Celilo Converter Station (45^{o}35'39"N 121^{o}6'51"W) and Sylmar Converter Station (34^{o}18'39"N 118^{o}29'21"W). Today is operational after many upgrades.

[8]Cahora-Bassa is between Songo Converter Station (15^{o}36'41"S 32^{o}44'59"E) and Apollo Converter Station (25^{o}55'11"S 28^{o}16'34"E). Today is on service after some upgrades.

in length between Mozambique and South Africa [24]. It was the first HVDC system in Africa. This project was a breakthrough in technology for several reasons: it was the second to use thyristor valves (the first was the Kingsnorth in England, but had half the voltage and a third of the power), and it was built in cooperation by three important manufacturers: BBC (now part of ABB), Siemens, and AEG (now part of Alstom). The Cahora-Bassa was also the most powered, with the highest voltage, and longest HVDC system of the world for almost a decade until the construction of the Itaipu project.

Itaipu[9] was built in Brazil in 1986 [25]. It was an overhead line with 3150 MW, ±600 kV, and 800 km of length built by ASEA. It was the first HVDC system in South America and was built in order to connect the Itaipu dam (the biggest hydroelectric dam between 1984 and 2008) to São Paulo city (Figure 1.6[10]).

Figure 1.6: Foz do Iguaçu converter station.
The Itaipu hydroelectric plant can be seen in the background.

The first uses of IGBT valves in high voltage were in 2000 in Australia. The project called Directlink[11] was an underground cable with 180 MW, ±80 kV, and 59 km built by ABB [26]. This project demonstrated the great advantages in control that IGBT technology can bring to HVDC systems, but this technology is still limited to lower level applications.

The state-of-the-art in high level HVDC is the Ultra High Voltage DC (UHVDC), and the largest project in this area is the Xiangjiaba-Shanghai[12] in China [27]. It was built by ABB in 2011. Nowadays is the most powered, with the highest voltage, and longest HVDC

[9]Itaipu is between Foz do Iguaçu Converter Station (25^{o}27'58"S 54^{o}32'33"W) and Ibiúna Converter Station (23^{o}40'02"S 47^{o}06'19"W). Today is on service.

[10]Photo source: ABB web site

[11]Directlink is between Mullumbimby Converter Station (28^{o}34'15"S 153^{o}27'8"E) and Bungalora Converter Station (28^{o}15'20"S 153^{o}28'20"E). Today is on service.

[12]Xiangjiaba-Shanghai is between Fulong Converter Station (28^{o}32'47"N 104^{o}25'04"E) and Fengxia Converter Station (30^{o}55'32"N 121^{o}46'16"E).

system of the world. It has 6400 MW, 800 kV, and 2071 km. Table 1.1 shows a summary of the most important HVDC projects to date. Figure 1.7 shows how the voltage levels of the projects have increased since Gotland to recent years.

Table 1.1: Summary of main HVDC projects.

Project Name	Location	Year	Characteristics		
			MW	kV	km
Gotland	Sweden	1954	20	±100	96
Volgograd-Donbass	Russia	1962	720	±400	473
N. Z. Inter Island	N. Zealand	1965	600	±250	609
Sardinia	Italy	1967	200	200	413
Pacific Intertie	USA	1970	1440	±400	1362
Nelson River	Canada	1973	1854	±463	890
Cahora-Bassa	MZ-ZA	1975	1920	±533	1456
Hokkaido-Honshu	Japan	1979	300	250	167
Itaipu	Brazil	1986	3150	±600	785
Quebec-N. England	Canada-USA	1990	2250	±450	1500
Directlink	Australia	2000	180	±80	59
East-South	Intercon. India	2003	2000	±500	1450
Celilo	USA	2004	3100	±400	1200
Norned	NO-NL	2008	700	±450	580
Yunnan-Guangdong	China	2010	5000	±800	1418
Xiangjiaba-Shanghai	China	2011	6400	800	2071

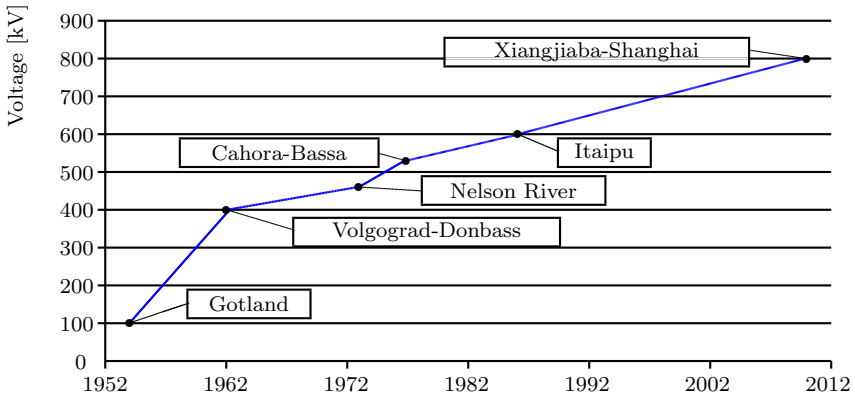

Figure 1.7: Evolution of voltage levels in HVDC projects.

1.2.2 The Next HVDC Projects

The growing needs of electrical systems, such as the load increases, the interconnection of large networks, the integration of renewable energy sources, and changes in operation and management of the systems, bring a high development potential for HVDC systems.

The coming years will see the construction of projects that will go over 2500 km in length, that will surpass 7000 MW or that will break the ±1000 kV barrier [28].

Throughout the world, projects are being planned that were unthinkable 15 years ago. These projects plan to connect large generation centers with mega-cities over thousands of kilometers. Like in China [29], Brazil [30], and India, that expect to harness the vast hydroelectric potential they posses.

Another important reason for the undertaking of these projects is the connection of large electric markets, such as USA where it's planned to take advantage of price differentials between the three great markets of the region [31]. Also in Europe a major project is in development that aims to connect all electrical markets of the EU and also to take advantage of the wind energy potential of the North Sea, creating a HVDC network with the largest underwater HVDC cables of the world [32].

Table 1.2 shows the most significant HVDC projects expected in the coming years:

Table 1.2: Summary of main HVDC projects under construction.

Project Name	Location	Year	Characteristics		
			MW	kV	km
Rio Madeira	Brazil	2013	3150	±600	2500
Jinping-Sunan	China	2013	7600	±800	2090
Tres Amigas	USA	2014	5000	300	—
North-East Agra	India	2015	6000	±800	1728
NorthConnect	Norway-UK	2020	1400	—	711

In the early 20th century, AC systems were imposed over DC systems due to the benefits they offered and because these benefits could not be reproduced by DC systems with the available technology of the time. Some of these benefits have to do with the ease of changing voltages and current interruption.

These benefits allowed AC systems the transmission of energy over long distances, but with the growth of electrical networks, these AC systems are operated to their limit and DC systems have proven to be of great help to solve the problems that large electrical systems have, including distance limitations.

The natural descendants of DC systems of the early 20th century are the current HVDC systems. The HVDC systems have evolved considerably since their inception in the mid 20th century based on mercury-arc technology to become an ideal solution for large block transmission over long distances. This ensures a great future for the HVDC systems and a great development potential for large electrical systems.

The development of power electronics has enabled the growth that HVDC systems have had in recent years, and have helped to show the great value that DC systems have for modern networks. As more than one hundred years ago, today's DC technology remains a fundamental part of several modern electrical systems.

1.3 Justification and Statement of the Problem

The power system's behavior has become increasingly difficult to analyze and predict for the utility industry because of the large scale and the complexity of modern systems. In the most important electrical systems of the world such as Brazil, Canada, China, India, USA and many European systems [30, 32–38], the longest lines are also the most important, because they carry large amounts of energy from generation centers to consumption places, making these lines vital to the correct operation of their systems.

Traditionally, AC transmission lines have been used in the development of these large systems, but the last year has seen rapid advances in power electronics and control technology, that allow the use of HVDC lines. The characteristics of the HVDC lines make them ideal for applications in systems interconnection and transmission of large blocks of energy.

But even with all the potential advantages of HVDC system applications, they are still lines that require special attention when problems arise. Inability to quickly locate and remove faults on a HVDC line could destroy the stability of the power system and lead to serious social and economic consequences.

1.3.1 Motivation

When a major power system disturbance occurs in HVDC lines, protection and control actions need to take place to prevent power system degradation and restore the system to a normal state within a minimum time. But in most cases, the service outages of these lines inevitably lead to the loss of large blocks of loads. So, a quick repair to recover the line service is vital for the system's operators. The operators must deal with a very complex situation where they perform a series of procedures to achieve breakdown service. These procedures always carry a significant expenditure of time.

Once the fault has been cleared and the HVDC lines isolated by the protection systems, most of the following processes are carried out by the maintenance crews. They need the most sophisticated equipment and methods to locate and repair the fault in an economically viable way and as quickly as possible. One of the first steps in the repair of the faults always is locating the fault. Therefore, in these cases it is extremely difficult to determine directly by line inspections where a fault occurred, because they are used as an interconnection between different power systems over long distances by overhead lines or by cables crossing bodies of water.

Most HVDC lines inevitably cross through complex terrain or in deep sea, and work under harsh weather conditions, so the time required to physically check the lines is much greater than the faults in the sub-transmission and distribution systems. However, researches about fault location techniques for transmission lines show that accurate and fast methods are of great significance and of practical engineering value [39, 40]. Prompt and accurate fault location in a HVDC system can accelerate the system's restoration, reduce the outage time,

and improve the system's reliability.

Fault locators provide estimates for both sustained and transient faults. Generally, transient faults cause minor damage that is not easily visible on inspection. Fault locators help identify these locations for early repairs to prevent recurrence and consequent major damages.

For AC systems, a lot of impedance based fault location methods have been implemented. Unfortunately, these methods were developed in a frequency domain and cannot be used for HVDC transmission lines. Currently, fault location methods commercially available for HVDC lines are all based on traveling wave without exception.

The traveling-wave based methods have fast response and high accuracy, where the time it takes for the traveling wave head to propagate from the fault point to the terminals implies the fault distance. There are highly accurate traveling-wave based methods, but require an analysis from field work with the line isolated from the system. These methods are expensive because they require specialized equipment and field personnel, and also consume a time that is prohibitive for lines as neuralgic as these.

Other traveling-wave based methods used fault records for the fault location, therefore, to have more post-mortem data is not required. These methods, in most cases, have fast response and high accuracy. However, they are also facing some insurmountable technical problems:

- The wave head must be identified when locating the fault, which is often carried out by professionals and cannot be implemented automatically.
- If the wave head could not be captured successfully or does not exist at all, the fault location will fail.
- For instance, when the line is grounded through a large resistance, the traveling-wave signals are too weak to be detected.
- Since the speed at which the wave travels is slightly lower than light speed, in order to achieve higher accuracy, a very high sampling frequency has to be used.
- The traveling-wave fault location is vulnerable to interference signals.
- Another difficulty arises for faults near the buses or for those faults occurring at near zero voltage inception angle.

In general, fault location techniques are classified in two categories depending on their basic essence: those who use traveling waves propagation and those who use impedance-based method. Although the traveling wave-based methods for fault location in HVDC systems is widely used and accepted, there is no doubt that they have problems in the previous cases. Whereas the impedance based fault location methods constitute the class most commonly used in practice for AC systems due to its simplicity and low cost. But its application in HVDC has not been sufficiently studied because of difficulties in the implementation of the DC system models that are necessary for this methodology.

Impedance-based methods can also be classified into those that use data from just one end of the line, and those that use data from both ends of the line. The accuracy of single-ended fault locators is affected by the assumptions that are made about the fault's

impedance, the source impedance and the in-feed into the fault from the remote end source. Two-ended fault location techniques are therefore more accurate than single-ended methods. The unknown fault resistance can be eliminated from the line model equations to estimate the location of the fault.

In spite of the developed research efforts in the literature for fault location studies, to provide a reliable and accurate fault location algorithm is still considered a challenge. This is mainly due to the variety of technical problems that can remarkably affect the behavior of the existing algorithms. Thus, the research of fault location methodologies is an important area of focus, in order to have a better understanding of the problem's essence that lead to the development of advanced solutions.

To increase accuracy, the use of two-ended data is important. Therefore, is proposed a method based on data obtained with synchronized measurements. The potential to improve fault location performance using synchronous measures seems to be great. Also, these measures have greatly improved the observability of the power system's dynamics. By accurately locating a fault, the amount of time spent by line maintenance crews in searching for the fault can be kept at a minimum, restoring the service quickly.

1.3.2 Objectives

In this context, is proposed the development of a new methodology based on impedance models of HVDC lines with two-ended synchronized data, for application in a comprehensive analysis for fault location in AC/DC systems in order to obtain a high accuracy fault location method for HVDC lines that can replace the currently traveling wave-based methods or, at least, complement them in cases when traditional methods don't work. This objective provides advancements in the fault analysis field by offering more accuracy and faster solutions to these problems, leading to improvements in the repair and operational processes of these vital systems.

To accomplish this main objective, several research steps will be raised. These steps will pursue the following specific objectives:

- Exhaustive investigations in the available literature of fault location methods for HVDC lines, to provide a significant contribution in this field of knowledge.
- Research and development of fault location methods to adapt to HVDC systems.
- Research and development of mathematical models of HVDC lines that can be adapted to the fault location methodologies.
- Research of time synchronized measurements technologies to use in fault location methods.
- Development of case studies to evaluate the performance of the proposed solution.
- Comparative analysis of the proposed solution adapted to the studied systems in order to find the solution that best suits the problem.

1.4 Research Approach

In the next section is presented the proposed methodology. This methodology consists of three main stages: problem investigation, method development, and method validation.

1.4.1 Problem Investigation

An exhaustive analysis to the literature in this field was carried out. The results of this critical analysis will be shown in Chapters 2 and 3 in order to better understand the problem and know how electric utilities and researchers have dealt with it. Also a critical analysis in complementary areas that relate directly with the issue raised for this work was done. These areas are:

- Fault location methods: characteristics of currently available methods. Advantages and disadvantages of the most used methods.
- Transmission lines: power transmission line modeling for its implementation in a fault location method oriented to HVDC systems.
- HVDC lines: composition of currently available systems and equipment, and its modeling for transient analysis tests oriented to validating the proposed fault location method.
- Data measurement and collection: Equipment and technologies for collection and management of interest data in the fault location analysis (specifically oscillography), as well as the formats for power systems data storage most commonly used.

With the review of the available literature in these areas, the problems in tracking methods currently applied in HVDC lines were identified. Based on some gaps that these problems present, a new method to improve the way to repair HVDC lines is proposed below.

1.4.2 Method Development

In order to find an alternative method for fault location in HVDC based on traveling-wave, an impedance-based fault location is proposed. In literature, a lot of impedance-based fault location methods have been developed for AC lines. Many impedance-based fault location methods in AC lines are based on the distributed parameter model of transmission lines and they can produce excellent results. Although designed for AC lines, these methods can also be applied to locate faults on DC transmission lines because there is no essential difference in primary line parameters between AC and DC transmission lines. But AC lines models used in these methods are a function of the system's frequency, so they can't be applied directly as HVDC line models because DC lines don't have a fundamental frequency.

The main problem in this formulation is to find a model that fulfills the functions of the traditional frequency-domain line models but in the time-domain in order to adapt it to an impedance based fault locator. So, the first steps for this research is to find a time-domain transmission line model, which can be used for the development of a HVDC line

fault locator. The work done until now for the development of a new time-domain model for transmission lines is shown in Chapter 4.

This time-domain model will be used as the base for the development of the impedance-based fault locator. The proposed approach for fault location will be oriented to calculate the voltage profile through the line at the moment when the fault occurs. This calculation is repeated with data obtained from each end. In a fault condition, the results obtained for the voltage profiles viewed from each end should be different for all points in the line except for one, that point would be the fault point. This methodology is simple, robust, and is little affected by possible errors in measurement or in line parameters. Similar methods have been proposed previously for AC lines [41, 42] and have been very successful.

This high accuracy fault location method for HVDC systems based on a time-domain transmission line model, could replace the currently traveling wave based methods or, at least, complement them in cases when traditional methods don't work. Also, all methods will be compared through a technical economical analysis because it's necessary to test that the new solution does not represent a significant increase in repair costs.

1.4.3 Method Validation

The performance of the new method will be assessed in a series of tests in order to validate its behavior under different scenarios and from different approaches. The first tests will be made based on a comparative analysis between the new method and other existing methods.

For this test, a select group of faults will be analyzed using evaluations with several criteria in order to compare the performance of the new method against other existing methods. The criteria for the analysis will be the location's accuracy and sensitivity of the methods to data errors (such as problems in measuring equipment, synchronization errors or line parameters errors), and implementation costs.

Different types of faults will be analyzed, some will have the specific characteristics where the current HVDC fault location methods are insufficient for the needs of the user, according to the literature. These type of faults will be evaluated in order to verify the problems with current methods presented in the literature, which are referenced in Chapter 2, and also to prove that the proposed method is able to fulfill the need that current methods are not able to fulfill. Additionally, faults where all methods can operate properly will be analyzed in order to compare the accuracy of each method's results.

In order to meet as many scenarios as possible, the faults group to be analyzed will come from different sources. Some tests will be made with actual fault records (in COMTRADE format) occurred in lines currently in service, and other tests will be made with simulated fault records produced by a electromagnetic transients program.

In addition to comparative performance analysis between the proposed method and other methods, a cost-benefit analysis will be made to evaluate the feasibility of the proposed method implementation in the industry, and the impact it could have on the current fault locations procedures.

1.5 Thesis Proposals and Contributions

This Thesis proposes an impedance-based fault location method for a two-terminal HVDC line. This work intends to help maintenance crews in the fault restoration processes by performing an accurate fault location on the line in a quick and easy way. The thesis tries to evaluate how this fault location can be estimated efficiently in order to send crews to the correct area of the line. This approach could significantly reduce the operating costs of HVDC. With accurate location of the fault, repair times can be reduced, also reducing the cost of unavailability.

The impedance-based nature of this proposal lies on the fact that voltage profile trough the line during the fault can be estimated using a time-domain line model. This should allow an accurate method that could overcome existing weaknesses in commercially available fault locators since the proposed method uses a different operating principle than the commercial equipment.

The major contribution of this work is the development of a method that increases the accuracy in fault location. The proposal is founded on the introduction of a new time-domain distributed-parameters transmission line model specifically designed for this method.

The proposed fault location approach is differentiated from other methods in that all commercially available methods are traveling wave-based and not impedance-based. On the other hand, impedance-based methods are vastly used in AC lines, hence they use frequency-domain line models. Few studies have been proposed using time-domain line models, but they use lumped parameters models which decrease the accuracy of the methods.

The transmission line model developed here provides higher accuracy. This is because approximations are not used to solve differential equations, then line parameters appear as a distributed characteristic of the line and not as a lumped modeling. The model is based directly on the transmission line differential equations represented as the distributed parameter model without any approximation. The solution shown here for these differential equations results in a model with certain parallels with the frequency-domain model for long transmission lines, and also with many similarities with others time-domain models, like the Bergeron's model, but in a more detailed way.

A possible benefit of this work, is savings in dedicated measurement equipment that are required for commercial methods, since the proposed method uses conventional fault records for its analysis.

1.6 Supplementary Research

The reasons for the development of the fault location method has implications that require further analysis for its explanation. One specific issue is subject of supplementary research: the perspective of HVDC systems development from point-to-point DC connections to operational HVDC grids.

With an increasing number of point-to-point DC connections, today connected through AC grids, it becomes apparent that it would be beneficial to connect the DC links in a more direct way, so the possibility for a HVDC grid has been discussed [43, 44]. This section aims to contribute to the discussion about the pros and cons of adopting a power system entirely based on DC, and the challenges that this type of technology faces.

1.6.1 Direct Current Power Systems

The vast majority of electric power transmissions systems use three-phase AC over DC. This is due to historical reasons (Sec. 1.1). Although technology has evolved since the invention of electricity, the power infrastructure is based fundamentally in AC. However, because of the development of power converters and DC energy sources, interest in DC has resurfaced.

The development of power converters between DC lines has facilitated the introduction of DC links on AC systems. The use of DC links favors the transmission of large amounts of power over long distances. This use of DC technology has been applied successfully all around the world for many years [45]. The greatest increase has been in countries with emerging economies like China, Brazil, and India [30, 37, 46] where the longest and highest voltage DC lines of the world are under construction. The conditions of these countries are perfect for this type of projects, because these are countries with vast territories where the great consumption centers are located at large distances from areas with high potential for energy exploitation, mainly consisting on renewable resources.

The most ambitious project in DC that is currently being developed because of its complexity, is being undertaken in Europe and includes several independently planned projects. These projects seek to exploit the potential of renewable energy around the continent [38]. The advantage of using DC technology in these projects is the ability to connect remote renewable power resources (Figure 1.8[13]) such as wind power in the North Sea, solar power in North Africa by crossing large bodies of water (North Sea and Mediterranean Sea).

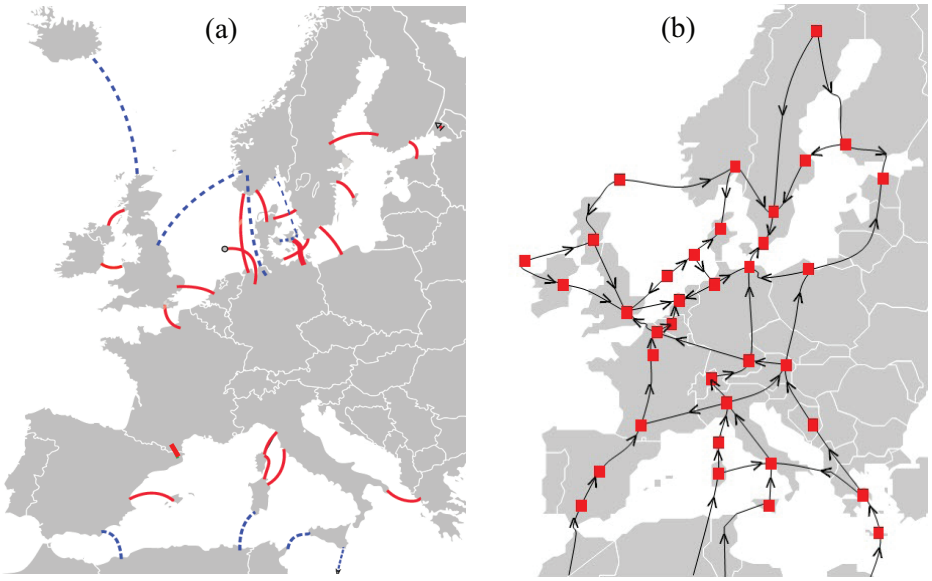

(a) European DC links built (red), and under consideration (blue).

(b) Conceptual interregional HVDC grid proposed by ABB for the EU.

Figure 1.8: European Union HVDC super grid vision.

As mentioned before, one of the reasons for the AC systems victory was the inability of early twentieth century DC systems to transmit large blocks of power from the generation

[13]Photo source: ABB website

centers to consumption centers, over long distances and at high voltage levels. But twenty first century needs have already exceed the operating limits of AC systems. The increase in the amount of transmitted power and greater distances covered by existing electrical systems are beyond the capabilities of the secure and stable operation of AC technology. Recent developments in power electronics applied to converters have made current HVDC systems to provide a better solution than AC systems for the transmission of large blocks of power over long distances, so it's safe to assume that the roles played by AC and DC systems in the early twentieth century have been inverted during the last few years.

These demonstrates that the same reasons that led to the adoption of AC systems as the global standard are the same reasons that now bring back DC systems, and just as more than 100 years ago, is not unreasonable to consider today a drastic change of paradigm in the design of electrical systems.

DC systems of early twentieth century were unable to meet the needs of its time due to two main reasons: its inability to generate, transmit, and distribute power at different voltage levels, and its difficulty to interrupt high levels of current in DC. With the advent of power electronics, these problems were solved. The converters are a powerful tool for the control and protection of HVDC systems [13] and are an easy, safe, and fast way to cut power when needed. Also, this technology can be applied to change in voltage levels with AC/DC converters equipment. The development of such equipment began for low voltage applications, but there are some studies that show its feasibility for high voltage applications and without magnetic-core transformers [14].

1.6.1.1 DC Advantages

The most common arguments in favor of HVDC are:

- Investment cost: It is undeniable that the transmission of large amounts of power over long distances is more cost efficient in DC than AC. This is not so clear in the case of shorter distances, but there are still certain considerations that must be taken into account and that are discussed in more detail below.

- Long distance water crossing: In a long AC transmission cable, the reactive power flow will limit the maximum transmission distance due to the large cable capacitance. With HVDC there is no such limitation so, for long cable links, HVDC is the only viable technical alternative.

- Lower losses: An optimized HVDC transmission line has lower losses than AC lines for the same power capacity. The losses in the converter stations have of course to be added, but since they are only about 0.6% of the transmitted power in each station, the total HVDC transmission losses come out lower than the AC losses in practically all cases.

- Controllability: One of the fundamental advantages with HVDC is that it is very easy to control the active power in the link.

- Stability: It is sometimes difficult or impossible to connect large AC systems due to stability reasons. In these cases, HVDC is the only way to make possible an exchange of power between the two networks. Also, DC systems are more stable and reliable

during faults than AC systems because when a DC system adopts a bi-polar dual-loop configuration, any fault can take one loop out of service, while the other loop can still operate by switch conversion to avoid power interruption in a large area.

- Magnetic pollution: Magnetic fields from HVDC lines are negligible in comparison to corresponding magnetic fields from AC lines.

- Environment: The latest developments in renewable energy are in DC. Improved energy transmission contributes to a more efficient use of existing power plants. Also, the land coverage and the associated right-of-way cost for a HVDC overhead transmission line is not as high as for an AC line, this reduces the visual impact. It is also possible to increase the power transmission capacity for existing rights of way. There are, however, some environmental issues that must be considered for the converter stations, such as: audible noise, visual impact, electromagnetic compatibility, and use of ground or sea return path in mono-polar operation.

1.6.1.2 Economic Considerations

A long HVDC transmission line costs less than a long AC line for the same transmission capacity. However, the terminal stations are more expensive in HVDC because they must perform the conversion from AC to DC and vice versa. On the other hand, the average costs of transmission (overhead lines and cables), and land acquisition/right-of-way costs are lower in HVDC, just like operation and maintenance costs. Initial loss levels are higher in the HVDC system, but they do not vary with distance. In contrast, loss levels increase with distance in a high voltage AC system. Above a certain distance, the so called "break-even distance" (Figure 1.9), the HVDC alternative will always give the lowest costs. The break-even-distance is a lot smaller for submarine cables than for an overhead transmission line, and this distance depends on several factors, such as transmission medium and different local aspects (permits, cost of local labor, etc).

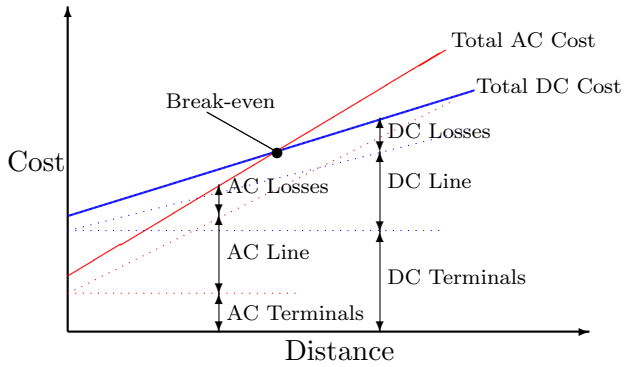

Figure 1.9: Cost comparison between AC and DC lines

In Figure 1.9 is easy to see that for short distance lines, the cost of building in AC is less than the cost of building in DC. This is a fact that may hinder the establishment of DC systems. The major costs in a DC line project are the converters located at each line-end. Even so, with the continuous development that has occurred in recent times in converter technology, this cost is expected to decline in the coming years.

The DC-DC converters are another vital equipment and a cost that should be taken into account. It is becoming accepted that a DC-DC converter will have considerably higher costs and losses than a comparable AC transformer. Another important issue to consider in the DC grid are DC breakers, without this type of equipment would not be possible to pass from two or three terminal HVDC lines to an entire DC grid. A lot of work was done in this area [47], and some manufacturers (especially in Europe) have shown interest in addressing this challenge; where certain proposals have emerged [48] and even the first commercially available DC breaker was manufactured [49]. Nevertheless, because of a range of advantages associated with DC transmission, DC networks may compete with established AC grid topologies.

In the case of distribution systems, several studies have been carried out over the use of a DC distribution system and they show the feasibility of this type of systems, both in isolated topologies [50] and linked to larger networks [51]. Just like in transmission grids, the converters are the most expensive equipment in distribution grids but, since the converters are composed by a series of power electronic valves, when the voltage is lower, fewer valves are needed, so the price decreases; therefore, in distribution networks the total cost is lower than in transmission networks.

The load is a factor that deserves attention in distribution systems. In most systems, the loads are of two main types: electronic devices, and motors. All electronic equipment works in DC and converters are required in order to connect to AC networks. Motors work in AC, but the vast majority use voltage based speed control, which involves using AC-DC-AC converters. If these controls were connected directly to DC, the AC-DC conversion would not be necesary. Therefore, a DC distribution grid would eliminate the need of converters sets for each load, reducing the cost, complexity, and possibly increasing the efficiency.

But beyond this, the choice between AC or DC systems should not be made based only on the costs associated with building the system. There are other operational factors that must be taken into account in the decision making process. The great control of the converters is a powerful tool in the operation of DC systems and the full control of power flow that enables efficient power trading between regions. Whereas in a meshed DC system it might not be possible to directly control currents in all lines. With the use of DC systems, energy markets could reach a precision that is not possible with AC systems.

Due to the growing need for energy in populations, AC electrical systems have become more vulnerable to blackouts. These blackouts have increased in recent years around the world, affecting vast areas and millions of people[14].

- The 2003 blackout in the northeast of USA, and east Canada affected an estimated 45 million people in 8 USA states, and 10 million people in Ontario, caused by a fallen tree branch.
- The 2003 blackout in Italy affected a total of 56 million people between the north of this country and the south of Switzerland.
- The 2005 blackout in Indonesia was a cascading outage across Java and Bali, affecting some 100 million people.
- The 2008 blackout in Venezuela affected more than 10 million people, caused by stability problems in the transmission system.

[14]Source of people affected by blackout estimation by Reuters

- Over 5 million people were affected in 2001 when cascading outages hit parts of California, Arizona, and northwestern Mexico.
- The 2012 blackout in Brazil affected as many as 53 million people across 11 states caused, by a cascading problem in the transmission system.
- The 2012 India blackout was the largest outage in history. The outage affected over 620 million people and was spread across 22 states in northeast India.

Because converters are so controllable, each HVDC line can be operated independently, avoiding stability problems in DC systems, making them safer and virtually immune to large blackouts. The costs incurred by each of the large blackouts of the last years, greatly exceeds the difference in costs of construction between AC and DC systems [52, 53].

1.6.1.3 DC Grids Challenges

Wider use of DC grids will definitely add several important features for handling future sustainable power generation, but it also involves challenges. To a limited extent, these are of a technical nature. The challenges mainly concern adoption of international regulations in order to manage these new grids[15].

When DC grids grow into meshed grids, there will be a need for control and protection schemes as well as for powerful breakers. The basic technologies in these fields are known although further development and verification is needed to fully meet all future needs and regulatory demands. The feasibility of three-terminal HVDC systems has been clearly demonstrated with already operational projects around the world.

Also, standards will be called for in the future to provide greater harmony of HVDC grids, to this end, a work group has been established within CIGRÉ [54] made up of both manufacturers and users. The work group is researching reliability of DC grids, and various grid configurations like radial and meshed grids are being reviewed. Because a grid has more branches than nodes, methodologies for power flow control are also being looked into.

Current conditions of electrical systems around the world present an unique opportunity in the decision making process to establish how the systems of the future are going to be, not only in countries with emerging economies but also in countries with already mature economies.

In countries with emerging economies like China, Brazil, and India, the electrical systems are still being expanded or even under development, so their design is open to great changes of paradigm in their construction.

The expansion of mature electrical systems is quite difficult because of the many permit and land requirements for the building of new lines. There are projects like the one in Europe where the plan is to build a DC grid that connects the European continent, North Africa, and even parts of the Middle East, in order to share the hydro, wind, and solar resources scattered throughout this vast area.

Beyond the likelihood of expansion, mature systems currently present another unique opportunity to foster the change of paradigm in electrical systems. The electrical systems in Europe and the USA base their infrastructure in large projects built with the available

[15]Like ENTSO-E, which already has a working group addressing this.

technology of the mid-twentieth century, and are approaching the end of their useful life and must be replaced in the coming years. This will require a huge investment from these countries to support the needs of their population. So this requires the answer to an important question: If such a large investment should be made, why is not made on a system with the best features and benefits that current technology has to offer?

It is undeniable that DC systems are at least one of the possible roads to take for the construction of the electrical systems of the future, and as such they should be taken into account and evaluated.

1.7 Organization of the Thesis

Originally, it was intended to write this work as a continuous idea, each development of the argument being logically derived from what had come immediately before. This proved to be an impossible ideal. The scope of research areas indicated a number of boundaries where chronological development of this work was not possible. Therefore, it was decided to divide the analysis into sections of chronological development where each section retains its own chronological order, and at points that will reference would be made from more than one section in the future. Figure 1.10 shows a diagram with the organization of the topics covered by this research.

A brief review of the issues addressed in this work is made below. These are the subjects required for the development of this book. Also there is a justification of the order in which this book is structured:

Introduction: This part shows a first approach to the problem of fault location, and justifies their importance for electrical systems in general, and in particular HVDC systems. It is also the framework of the problem and considers how they will be addressed in order to propose a solution. To understand the context in which the work is carried out, a review of the evolution of HVDC systems is made, as well as the prospects that exist for short-term development. This theme conforms the Chapter 1 of the book. The main topics of this part are:

- HVDC systems background
- Justification and statement of the problem
- Research approach
- Thesis proposals and contributions

Fault location review: This section addresses one of the two main themes of the work: the fault location methods. Shows the importance these methods have for the power system operation. A review of existing methods is made and the basis of their operation are explained.

All fault location methods could be classified in two types: impedance-based, and traveling wave-based fault location. The section seeks to study these methods in two ways, one theoretical and other practical. In the theoretical part, a general definition of fault location is presented and a critical analysis of different methods is made. In the practical section, a comparative analysis between two of the most widely used methods is made.

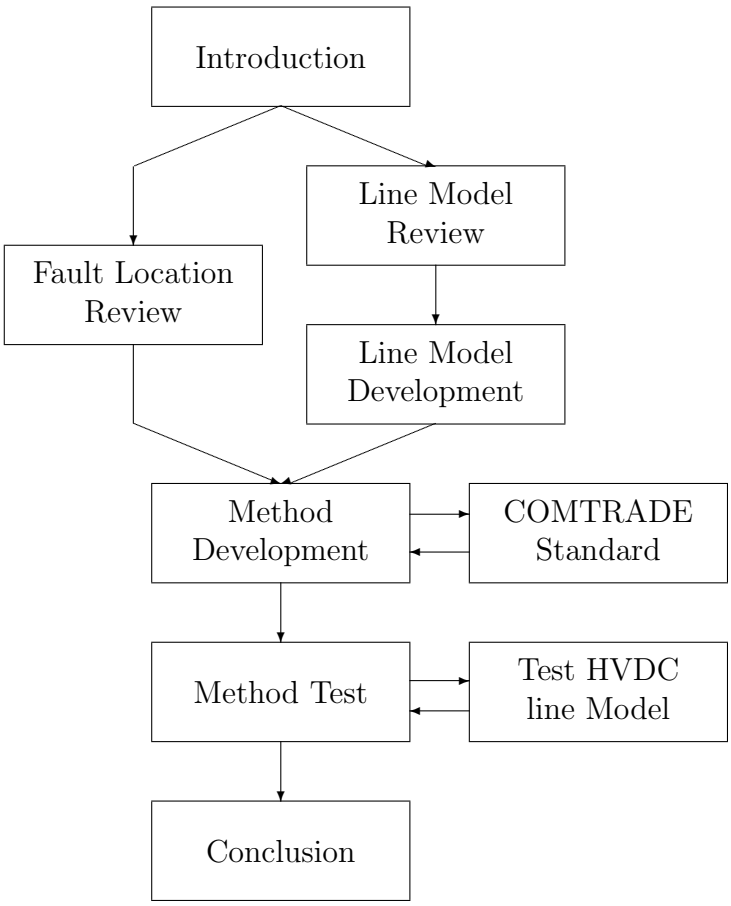

Figure 1.10: Thesis' organization diagram.

The objective of these tests is to deepen the understanding of the different methods by making comparisons between their performances, so as to observe their behavior and test the strengths and weaknesses of each method.

This theme conforms the Chapter 2 of the book. The main topics of this part are:

- Origins, definition and benefits
- Traveling wave-based fault location review
- Impedance-based fault location review
- Principles of operation of the methods
- Comparative analysis of the methods

Line model review: This section addresses the second main theme of the work, the transmission line models. Since the fault location method proposed in this work needs to estimate the voltage and current profiles along the line based on a mathematical model, it is necessary to know the models of transmission lines currently available.

This section addresses the problem of transmission lines modeling, and shows the basic differential equations that describe the lines' behavior. A review of the different methods used to solve these equations is also made and they are grouped into two types of modeling: frequency-domain, and time-domain models.

This theme conforms the Chapter 3 of the book. The main topics of this part are:

- Line model differential equations
- Frequency-domain models
- Time-domain models

Line model development: This part begins the development of the proposal presented in Chapter 1. This part shows the development of a new time-domain distributed parameters transmission line model. Since HVDC lines have no frequency, frequency-domain line models can not be applied. Moreover, the existing time-domain line models are based in solutions that use lumped parameters, therefore, the model's accuracy is lost.

The model deduced here has a structure similar to other time-domain models, but in a more complex way that provides greater accuracy. This is because approximations are not used to solve differential equations. This model was developed specifically to use in the fault location method proposed in this work.

This theme conforms the first part of Chapter 4 of the book. The main topics of this part are:

- Line model deduction
- Model analysis
- Illustrative examples

Method development: This section presents, in a structured manner, all the knowledge presented so far. The principles of operation of the fault location method proposed is explained, and its structure is shown. Also, it explains the selected algorithm for this method, as well as the different stages that is composed of.

The work developed here proposes the implementation of an impedance-based method for locating faults in two-terminal HVDC lines, using the time-domain line model in order to estimate the voltage profile over the line during the fault.

This theme conforms the second part of Chapter 4 of the book. The main topics of this part are:

- Method scheme
- Fault detection
- Impedance-based fault location method

Method test: Fault records of a HVDC line will be analyzed with the developed method in order to validate the method's performance. The results will be compared with two commercially available methods. Tests with records of actual and simulated faults were carried out in order to prove the method with the highest number of possible variations.

This theme conforms the Chapter 5 of the book. The main topics of this chapter are:

- HVDC line used
- Actual fault process and commercial fault location equipment
- Method's performance to actual faults
- Method's accuracy test
- Fault resistance sensitive test

Conclusion: This section provides a summary of the research, and argues quantitative and qualitative conclusions for this work. This part is pretended to give closure to the research and provides an assessment of its results.

This theme conforms Chapter 6 of the book. The topics covered are:

- Conclusions
- Contributions and findings
- Future lines of research

COMTRADE standard: Supplementary information can be obtained here to understand the theme developed in Chapter 4. This part addresses the issue of the IEEE Standard Common Format for Transient Data Exchange (COMTRADE). This standard is intended for use by digital computer based devices which generate or collect transient data from electric power systems. The standard should facilitate exchange of the transient data for the purpose of simulation, testing, validation, or archival storage.

This theme conforms the Appendix B of the book. The topics of this section are:

- COMTRADE standard files summary
- Sampling rate
- Illustrative example

Test HVDC line model: Supplementary information can be obtained here to understand the theme developed in Chapter 5. In this part is done a detailed explanation of the HVDC line model used for the simulation of faults required for the tests. It explains the block diagrams used for modeling of the line and converters systems. It also explains the block diagrams of the control and protection systems that act during the faults.

This theme conforms the Appendix A of the book. The topics covered in this part are:

- Description of the HVDC system
- Control and protection systems

Bibliography Chapter 1

[1] IEA, "Co-generation and renewables: Solutions for a low-carbon energy future," *International Energy Agency*, 2011.

[2] EWEA, "Wind in power: 2012 european statistics," tech. rep., The European Wind Energy Association, Feb. 2013.

[3] GWEC, "Global wind report 2012," tech. rep., Global Wind Energy Council, Apr. 2013.

[4] O. Peake, "The history of high voltage direct current transmission," in *3rd Australasian Engineering Heritage Conference* (U. of Otago, ed.), p. 8, 2009.

[5] G. Asplund, L. Carlsson, and O. Tollerz, "50 years of HVDC. part I: From pioneer to world leader," *ABB Review*, no. 4, pp. 6–8, 2003.

[6] E. Kimbark, *Direct Current Transmission*. New York: Wiley Interscience, 1971.

[7] L. de Andrade and T. Ponce de Leão, "A brief history of direct current in electrical power systems," *IEEE History of Electro-technology Conference*, p. 6, 2012.

[8] C. Sulzberger, "Thomas edison's 1882 pearl street generating station," *IEEE Global History Network*, 2003.

[9] R. Belfield, "The niagara system: The evolution of an electric power complex at Niagara falls, 1883-1896," *Proceedings of the IEEE*, vol. 64, no. 9, pp. 1344–1350, 1976.

[10] T. McNichol, *AC/DC the Savage Tale of the First Standars War*. San Francisco: Jossey-Bass, 2006.

[11] N. Tesla, "A new system of alternate current motors and transformers," in *Transactions of the American Institute of Electrical Engineers*, vol. V, pp. 308–327, 1888.

[12] R. Lobenstein and C. Sulzberger, "Eyewitness to DC history: the first and last days of DC service in New York City," *IEEE Power and Energy Magazine*, vol. 6, no. 3, pp. 84–90, 2008.

[13] W. E. Highfield and J. E. Calverley, "Improvements in and relating to electric converting apparatus," 1921.

[14] G. Carpenter, "Liquid rectifier," *United States Patent Office*, vol. USA, US1671970, 1928.

[15] A. Moglestue, "From mercury arc to hybrid breaker 100 years in power electronics," *ABB Review*, no. 2, pp. 70–78, 2013.

[16] P. Cooper Hewitt, "Method of manufacturing electric lamps," *United States Patent Office*, vol. USA, US682692, p. 7, 1901.

[17] U. Lamm, "Gaseus discharge converter," *United States Patent Office*, vol. USA, US2006053, p. 3, 1935.

[18] R. Hall, "Power rectifiers and transistors," *Proceedings of the IRE*, vol. 40, no. 11, pp. 1512–1518, 1952.

[19] W. G. on HVDC and FACTS, "HVDC projects listing," *IEEE Transmission and Distribution Committee*, 2008.

[20] G. Breuer, M. Morack, L. Morton, and C. Woodrow, "D-C transmission: An american view-point," *Power Apparatus and Systems, Part III. Transactions of the American Institute of Electrical Engineers*, vol. 78, no. 3, pp. 504–512, 1959.

[21] N. Chuprakov, A. Milutin, A. Posse, and V. Shashmurin, "Initial period of operation of the D.C. transmission line between Volgograd and Donbass," *IEE Conf. HVDC Transmission*, 1966.

[22] V. Ciallella, P. Grattarola, A. Taschini, C. Martin, and D. Willis, "Testing and operating experience of the Sardinia-Italian mainland D.C. link," *CICGRE Session*, 1968.

[23] R. Cresap, W. Mittelstadt, D. Scott, and C. Taylor, "Operating experience with modulation of the pacific HVDC intertie," *IEEE Transactions on Power Apparatus and Systems*, vol. PAS-97, no. 4, pp. 1053–1059, 1978.

[24] W. Bayer, K. Habur, D. Povh, D. Jacobson, J. Guedes, and D. Marshall, "Long distance transmission with parallel AC/DC link from Cahora Bassa (Mozambique) to South Africa and Zimbabwe," 1996.

[25] C. Peixoto, "Itaipu 6300 MW HVDC transmission system feasibility and planning aspects," *Symposium on Incorporating HVDC Power Transmission Into System Planning*, pp. 211–236, 1980.

[26] B. Railing, G. Moreau, J. Wasborg, D. Stanley, J. Miller, and Y. Jiang-Häfner, "The directlink VSC-Based HVDC project and its commissioning," 2002.

[27] A. Kumar, V. Lescale, U. Åström, R. Hartings, and M. Berglund, "800 kV UHVDC from test station to project execution," 2009.

[28] R. Nayak, R. Sasmal, Y. Sehgal, M. Rashwan, and G. Flisberg, "Technical feasibility and research & development needs for ±1000 kV and above HVDC system," in *CIGRE Conference*, p. 10, 2010.

[29] K. Zha, X. Wei, and G. Tang, "Research and development of ±800kV/4750A UHVDC valve," in *Second International Conference on Intelligent System Design and Engineering Application*, pp. 1466–1469, 2012.

[30] J. Graham, A. Persson, and G. Biledt, "The integration of remote hydroelectric plants into the brazilian network using HVDC transmission," in *CIGRE Conference*, p. 9, 2006.

[31] M. Reynolds, D. Stidham, and Z. Alaywan, "The golden spike: Advanced power electronics enables renewable development across NERC regions," *IEEE Power and Energy Magazine*, vol. 10, no. 2, pp. 71–78, 2012.

[32] T. Vrana, R. Torres-Olguin, B. Liu, and T. Haileselassie, "The north sea super grid - a technical perspective," in *9th IET International Conference on AC and DC Power Transmission*, pp. 1–5, 2010.

[33] F. Tesche, "On the inclusion of loss in time-domain solutions of electromagnetic interaction problems," *IEEE Transactions on Electromagnetic Compatibility*, vol. 32, no. 1, pp. 1–4, 1990.

[34] R. Dass, B. Linden, S. Rinaldo, and S.-P. Cheung, "Operation experience from bulk power HVDC links from three gorges complex," in *Cigre Conference*, p. 8, 2006.

[35] Z. Alaywan, "The tres amigas superstation: Linking renewable energy and the nation's grid," in *Power and Energy Society General Meeting, 2010 IEEE*, pp. 1–5, 2010.

[36] CAISO, "Trans bay cable project," tech. rep., Board of Governors California Independent System Operator, April 2007.

[37] V. Prasher, D. Kumar, C. Bartzsch, V. Hartmann, and A. Mukherjee, "HVDC east-south interconnector II in India: 2000 MW, +/-500 kV," in *Seventh International Conference on AC-DC Power Transmission*, pp. 78–83, 2001.

[38] G. Asplund, B. Jacobson, B. Berggren, and K. Lindén, "Continental overlay HVDC-Grid," in *CIGRE Conference*, p. 9, 2010.

[39] L. de Andrade and R. Guanipa, "Costs reduction in attention to transmission lines faults using faults location equipment," *I Congreso Venezolano de Redes y Energía Eléctrica*, 2007.

[40] P. Gale, J. Stokoe, and P. Crossley, "Practical experience with travelling wave fault locators on scottish power's 275 & 400 kV transmission system," in *Sixth International Conference on Developments in Power System Protection*, pp. 192–196, 1997.

[41] S. Brahma and A. Girgis, "Fault location on a transmission line using synchronized voltage measurements," *IEEE Transactions on Power Delivery*, vol. 19, no. 4, pp. 1619–1622, 2004.

[42] J. Izykowski, E. Rosolowski, P. Balcerek, M. Fulczyk, and M. Saha, "Accurate noniterative fault location algorithm utilizing two-end unsynchronized measurements," *IEEE Transactions on Power Delivery*, vol. 25, no. 1, pp. 72–80, 2010.

[43] Z. Qianzhi and Y. Defang, "Prediction on future DC power system," in *IEEE 6th International Power Electronics and Motion Control Conference*, pp. 1192–1195, 2009.

[44] D. Larruskain, I. Zamora, A. Mazón, O. Abarrategui, and J. Monasterio, "Transmission and distribution networks: AC versus DC," *Egyptian Solar Research Center*, p. 6, 2005.

[45] G. Wolf, "Renovating the grid for the 21st century," *Transmission & Distribution World*, pp. 10–13, 2012.

[46] V. Lescale, U. Åström, W. Ma, and Z. Liu, "The xiangjiaba-shanghai 800kV UHVDC project status and special aspects," in *CIGRE Conference*, p. 7, 2010.

[47] C. Franck, "HVDC circuit breakers: A review identifying future research needs," *IEEE Transactions on Power Delivery*, vol. 26, no. 2, pp. 998–1007, 2011.

[48] J. Häfner and B. Jacobson, "Proactive hybrid HVDC breakers - a key innovation for reliable HVDC grids," in *The Electric Power System of the Future - Integrating Supergrids and Microgrids International Symposium*, p. 9, Cigré, 2011.

[49] M. Callavik, A. Blomberg, J. Häfner, and B. Jacobson, "Breakthrough! ABB's hybrid HVDC breaker, an innovation breakthrough enabling reliable HVDC grids," *ABB Review*, no. 2, pp. 6–13, 2013.

[50] K. Kurohane, T. Senjyu, Y. Yonaha, A. Yona, T. Funabashi, and K. Chul-Hwan, "A distributed DC power system in an isolated island," in *IEEE International Symposium on Industrial Electronics*, pp. 1–6, 2009.

[51] M. Starke, L. Tolbert, and B. Ozpineci, "AC vs. DC distribution: A loss comparison," in *IEEE/PES Transmission and Distribution Conference and Exposition*, pp. 1–7, 2008.

[52] A. Chowdhury and D. Koval, "Application of customer interruption costs in transmission network reliability planning," in *IEEE Industrial and Commercial Power Systems Technical Conference*, pp. 53–60, 2001.

[53] R. Vajeth and D. Dama, "Methodology for evaluating the cost of a network fault," in *IEEE International Conference on Probabilistic Methods Applied to Power Systems*, pp. 581–587, 2004.

[54] CIGRE, "HVDC grid feasibility study," tech. rep., Study Committee B4, 2011.

Chapter 2

Fault Location Analysis for Transmission Lines

Even the best planned systems are subject to unpredictable events in transmission lines that place the system beyond the planned limits. When a major power system disturbance occurs, protection and control actions need to take place in order to prevent power system degradation, and restore the system to a normal state within a minimum time. In most cases, the service outages of these lines inevitably lead to the loss of large blocks of loads. So, a quick repair for the line service recovery is vital for the system operators. But most lines inevitably cross through complex terrain, and work under difficult weather conditions, so the time required to physically check the lines is long. However, researches about fault location techniques for transmission lines show that accurate and fast methods are of great significance and of practical engineering value [1, 2]. Prompt and accurate fault location in transmission lines can accelerate the system restoration, reduce the outage time and improve the system reliability.

In general, all fault location methods can be classified according to Figure 2.1.

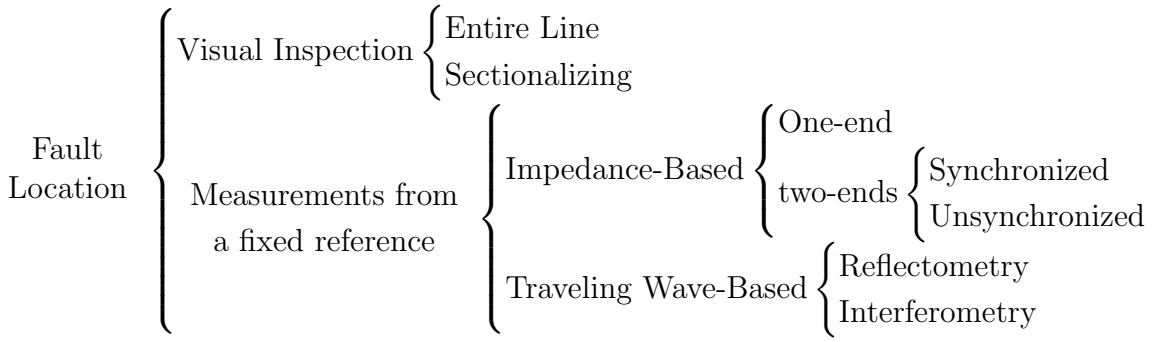

Figure 2.1: Classification of transmission line fault location methods.

This section aims to show the efforts made to meet the needs of fault location in transmission lines that exist in modern power systems. For this, the issue is addressed in two ways, one theoretical and other practical. In the theoretical part, a general

definition of fault location is presented and a critical analysis of different methods is made; showing the advantages and disadvantages of each of them and their most common applications. In the practical part, is made a comparative analysis between two of the most widely used methods, using actual and simulated faults tests as examples to show the method's behavior.

2.1 Fault Location Origins and Definition

The problem of locating transmission line faults is as old as the power industry itself. The first methods for locating electrical faults in lines were developed for submarine telegraph cables [3], and was based on measuring the line's resistance using a bridge circuit and galvanometers[1]. For this bridge circuit, one end of the faulted cable is connected through a pair of resistors to the voltage source. The galvanometer is also connected. The other end of the cable is shorted. The bridge is brought to balance by changing the values of R_a and R_b, which is achieved when:

$$\frac{dR}{lR + (l-d)R} = \frac{R_a}{R_b} \tag{2.1}$$

Then

$$d = 2l\frac{R_a}{R_a + R_b} \tag{2.2}$$

Where d is the distance to the fault and l is the total line length as shown in Figure 2.2[2].

In the beginning of power systems, the fault location was made directly by visual inspections of the line[3]. But the visual inspection of a long line, both on foot or by air, is always extremely slow and is subject to the terrain circumstances and environmental conditions of the moment. Additionally, visual inspection does not always ensure that the location will be found because, in many cases, faults don't let physical evidence.

All events occurred in a transmission line are investigated. Faults are classified as permanent or temporary depending on the impact they have on the system. Permanent faults are those that keep the line out of service and are dealt with immediately because the need to place the line back into operation. Temporary faults also affect the proper operation of the line, but they do it momentarily, so the line can be energized

[1]The Murray loop and the Varley loop were two types of connections for locating faults in cables

[2]Photo source: Wikipedia

[3]In the beginning, most electric utilities companies elected to have little or no investment for improving fault location methods. This is mainly due to a belief that most faults disappeared by themselves when the problem was isolated, needing no information about their locations. Also, the weak or inaccurate behavior of the earlier fault locators may have played a role in this belief. These points of view were changed due to free marketing and deregulation all over the world. These competitive markets force the companies to change their policies to save time and money, as well as to provide a better service.

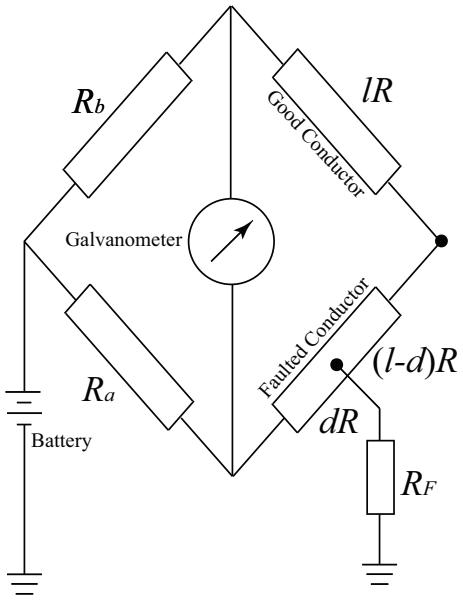

(a) Bridge circuit diagram

(b) Leeds & Northrup instrument used for bridge circuit tests in early XX century.

Figure 2.2: Bridge circuit tests was used at late XIX century for fault location in telegraph cables.

in a short period of time (either through automatic controls such as re-closers, or by indication of the operation personnel). In spite of this, temporary faults should also be investigated to prevent future faults or hidden problems. In these cases, the investigation of faults' causes is not urgent, so it is possible to wait the best time where the most appropriate resources for the investigation are available.

All event investigations inevitably require sending crews for a visual inspection of the line. After finding the origin of the fault is possible to repair the damage (removal of conductive objects, repair poles or insulators, reconnecting conductors, etc.), or other actions that minimize the risk of such events happening again (cut of vegetation, re-tensioning of conductors, repair hot spots, etc.). But checking an entire line requires great effort and it's time consuming, specially in the case of long lines that pass through complex terrain or with difficult access. This investment of resources and time becomes prohibitive when a problem which prevents the correct operation of a line needs to be solved quickly.

In order to minimize the resources and time needed to find the fault's origin, a series of previous analysis are made, so the search area is reduced as much as possible and crews can be sent directly to the line area where is more feasible that the fault took place. These previous analysis are called fault location methods. So fault location methods are a group of techniques that seek to locate, with the highest possible accuracy, all those abnormal network conditions that take the current out of its normal course through a transmission line. These techniques are used before

starting the visual inspection, so that the work area can be delimited to a small section of the line.

For the location, these techniques are based on the impact that faults have on other well-defined points on the same line. In these other previously defined points, different types of data are collected and analyzed to conclude that only an event with certain characteristics may have such effects on the measuring point. The location of this event is the fault location.

Many methods have been developed about fault location in transmission lines and many articles have been published about each of these methods (sections 2.3 and 2.4). The researches discussed below are all pioneers in their respective work areas and all are representative samples of developments that have occurred in the different fault location methods.

2.2 Fault Location Benefits

Once the fault is cleared, the adopted fault locator is enabled to detect the fault's position. Then, the maintenance crews can be informed of that location in order to fix the resultant damage. Later, the line can be re-energized again after finishing the maintenance task. Since transmission line networks spread for some hundreds of kilometers in different environmental and geographical circumstances, locating these faults based on the human experience and the available information about the status of all breakers in the faulted area is not efficient and time consuming. These efforts can effectively help to sectionalized the fault (declare the faulted line section), rather than to locate precisely the fault's position.

Temporary faults are self-cleared and do not affect permanently the supply's continuity, however, the location of such faults is also important. In this case, the fault's location can help to pinpoint the weak spots on the line as well as hidden problems. As a result, the plans of maintenance schedules can be fixed to avoid further problems in the future. Fast and effective maintenance processes lead to improve the power availability to the consumers. This consequently enhances the overall efficiency of the power grids. These concepts of (availability, efficiency, quality, etc) have an increasing importance nowadays due to the marketing policies resulting from deregulation and liberalization of power and energy markets.

All the mentioned benefits of savings in time and effort, improved availability, and assistance to maintenance plans can be reviewed from a economical perspective. There is no doubt that time and effort saving, increasing the power availability, and avoiding future accidents can be directly interpreted as a cost reduction or a profit increase. This is an essential concept for competitive marketing.

2.3 Traveling Wave Based Fault Location

In general, these methods are founded on the work of Carson [4, 5] and are based on measuring the time that takes the wavefront to propagate from the point where a discontinuity occurs in the line to the measuring terminals. If the speed by which the wave travels is known, then is possible to calculate how much distance the wavefront has traveled. The general principles of operation of these methods are explained below.

2.3.1 Principles of Operation

A traveling wave is a wave observed traveling through a medium. This is basically any space containing matter in any given state. When moving, the crest of the wave will move from particle to particle from the incidence of energy transfer. An ideal traveling wave has the moving crest (called wavefront), followed by a drop. This creates a sine wave pattern. The ideal example of a traveling wave is an ocean wave.

When any fault occurs in transmission lines, a traveling wave appears. It means that fault current is divided into two separate currents, and each of these currents goes to each side of the transmission line. Those currents are shaped as a wave, they quickly achieve their peak value but their decrease lasts much longer.

Traveling waves spread along the transmission lines at almost light speed. Because of the resistance of the lines, their peak value of current decreases as they move.

When a traveling wave comes to any crossing, it divides itself into several smaller waves and each of them proceeds to another branch. The value of the current in each branch depends on the total impedance in that branch. If the impedance is smaller, the current is higher and vice versa.

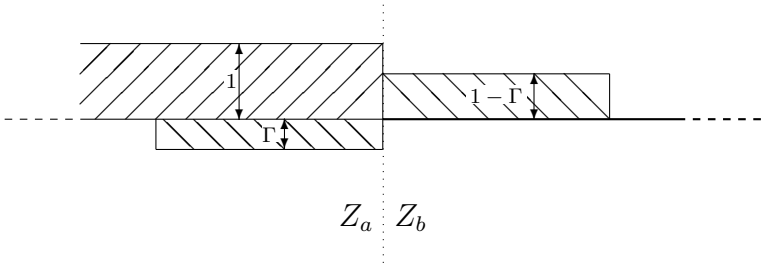

Figure 2.3: Reflection and refraction phenomena of waves in a one dimensional medium.

Figure 2.3 shows a unit step function reflected and refracted at a change in surge impedance of a distributed-constant line. For a simple discontinuity of this sort, the reflection coefficient (Γ) is given by:

$$\Gamma = \frac{Z_b - Z_a}{Z_a + Z_b} \tag{2.3}$$

When Z_a and Z_b are the impedance of the medium a and b. The behavior of the traveling wave in a transmission line will be discussed in more detail in chapter 3.

Traveling wave based fault location methods are based on the velocity of the traveling wave, assuming is constant for each transmission line, and can be calculate by $v_t = \frac{1}{\sqrt{LC}}$. Since the time it takes the wavefront to propagate from the fault point to the terminals may be measured, and the travel speed is known, then is possible to calculate how much distance the wavefront has traveled.

Two different methods can be used to calculate the travel distance: reflectometry and interferometry. Both methods are widely used in the optics field.

The reflectometry method is based on the phenomenon of reflection of the wave. i.e., the change in direction of the wavefront at an interface between two different media so a part of the wavefront returns to the medium from which it originated until the fault point. This process is repeated continuously as shown in Figure 2.4. Then, the fault distance from a measurement point can be calculate by equation (2.4).

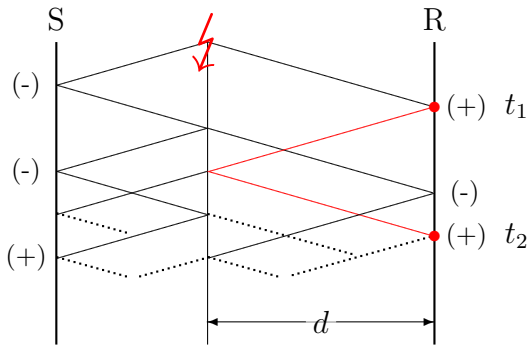

$$d = \frac{1}{2}(t_2 - t_1)(\frac{1}{\sqrt{LC}}) \qquad (2.4)$$

Figure 2.4: Reflectometry Lattice diagram.

Where d is the distance between the measurement point and the fault point, t_1 and t_2 are the first two consecutive wavefront arrival times measured, and L and C are the inductance and capacitance of the line by length unit, respectively.

Interferometry makes use of the principle of superposition to combine waves in a way that will cause the result of their combination to have some meaningful property that is a diagnosis of the original state of the waves. This works because when two waves with the same frequency are combined, the resulting pattern is determined by the phase difference between the two waves that are in phase will undergo constructive interference while waves that are out of phase will undergo destructive interference. Therefore, when a fault starts, two traveling waves are generated, one to each line end. The waves leave the fault point with the same phase, but they arrive at the line ends with a phase difference because of the difference of the distance between each line end and the fault point, as shown in Figure 2.5. By combining these waves is possible to calculate the difference. Then, the fault distance from a measurement point can be calculate by equation (2.5).

Where d is the distance between the fault point and the point where t_1 was measured, t_1 and t_2 are the wavefront arrival times measured at both measurement points, l is the total length of the line, and L and C are the inductance and capacitance

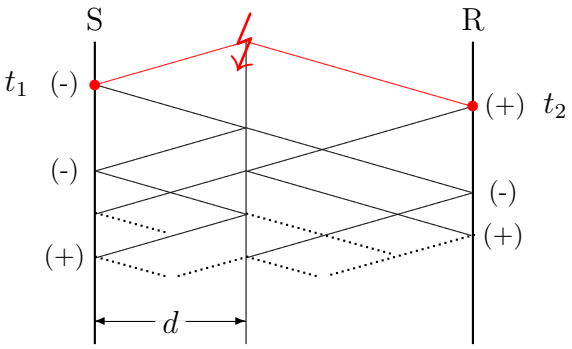

$$d = \frac{1}{2}[l + (t_1 - t_2)(\frac{1}{\sqrt{LC}})] \qquad (2.5)$$

Figure 2.5: Interferometry Lattice diagram.

of the line by length unit, respectively.

2.3.2 One-end and Two-ends Methods

The traveling wave based fault location was first proposed by Röhrig in 1931 [6]. Its use was implemented initially in the middle of the 20th century by Stevens and Lewis [7, 8] but they were gradually abandoned in the 1970s because of their high cost, poor reliability, and maintenance problems.

In the middle of the 1980s, the interest for traveling wave-based methods was renewed by SEL Inc., and other research articles were published to employ this technique for fault location [9-11]. A technique for locating faults using information from only one end of the line is developed in [9, 10]. This method uses successive reflections generated by faults (reflectometry technique). In many cases, there are large impedance mismatches when a fault starts, this generates transient waves that travel through the line and are reflected between the fault and the line ends. From measurements of the first two consecutive transient arrival times, the fault location can be calculated. Because the method only uses information from one line end, the key is the observation of the relative polarity of the two wavefronts generated by the fault and propagated towards each line end. So is possible to differentiate the wavefront originating from one line end and those reflected from the opposite end.

On the other hand, in [11] is developed a technique by Dewe et al. for location using information from both ends of the line. By having information available at both ends, the analysis is facilitated. In this method, the analysis is based on the time difference in the arrival of the fault-generated wave at each end of the line (interferometry technique). The simultaneous processing of information from both ends is achieved by a very accurate data acquisition technique with the time reference signals provided by a global positioning system receiver.

Since then, others traveling wave-based methods were developed, where the traveling wave-based method and other known methods were combined to facilitate the detections and fault analysis. Like the method proposed by Magnago et al. in [12], that uses the wavelet transform to improve the wavefront detection, because it allows time localization of different frequency components of a given signal.

After the 1990s, with the developments of communication systems and digital signal processing techniques, the traveling wave-based fault location techniques got more and more applications in different AC transmission systems. But these methods are mostly used for HVDC lines than for AC systems. In fact, fault location methods implemented on HVDC lines are all based on traveling wave without exception. Some examples of these are [13–15]. In [13] is proposed by Murthy et al. a method for fault location in HVDC lines using wavelet transforms. The ability of the wavelet transform to locate both time and frequency makes it possible to simultaneously determine the sharp transitions of signals and the location of their occurrence.

Other method is proposed by Ping et al. in [14], combining the single-end and two-ends methods. With this combination, the aim is to complement the results of both methods. This will reduce the amount of cases where each separate method is not enough or has problems in locating the fault. And in [15] is proposed by Young-Jin et al. a combination between a traveling wave with cross correlation methods for locations on HVDC cable lines. To detect the wavefront, it's used the cross correlation method, based on the similarity between the first wavefront (used as the template signal) and a subsequent wavefront, both measured at the same line end. If two signals have the same shape, the correlation result would be maximum.

All these traveling wave-based methods have a fast response and high accuracy. However, they are also facing some insurmountable technical problems:

- The detection of the wavefront is the key to traveling wave fault location. If the wavefront cannot be captured successfully, or the wavefront does not exist at all at the occurrence of a fault, the fault location will fail. For instance, when the line is grounded through a large resistance, the transient traveling wave signals are too weak to be detected, disabling the fault location under these circumstances. Moreover, if a fault is caused by a gradual change in the transition resistance, the traveling wave may also be too weak to be discovered, resulting in the failure of the fault location [9–12, 14–16].

- In these methods, is measured the time it takes the wavefront to arrive at the point where the device is installed, and the fault distance is the product of the time and the wave speed. Therefore, the accuracy of the fault location is dependent, to a great extent, on the wave speed, and since the wave speed is $v_t = 1/\sqrt{LC}$ (where L is the inductance and C is the capacitance of the propagation medium) these methods also depend on the line parameters [14–16].

- Accuracy in fault location depends upon sampling frequency. Since the speed at which the wave travels over transmission lines is slightly lower than light speed, in order to achieve higher accuracy, a very high sampling frequency has to be used in traveling wave fault location methods. Therefore, more expensive and complex equipments are required [11, 16].

- The wavefront must be identified to locate the fault, which is often carried

out by experienced professionals and cannot be implemented automatically by computers [1].

- Since the traveling wave fault location uses the signal high frequency components for the analysis, is vulnerable to interference of external signals [11, 14].
- If the fault occurs near a line end, is very difficult to identify the wavefront with information of this line end due to the high speed of the traveling wave [12, 13, 15, 16].
- Another difficulty arises for faults near the buses or for those faults occurring at near zero voltage inception angle because, if the voltage is zero when the fault starts, there is not an abrupt change of the line continuity and a wavefront is not produced [12, 13, 15, 16].

Table 2.1 shows a summary of all the fault location methods discussed here.

Table 2.1: Traveling wave-based fault location methods summary.

Reference	One-end	Two-ends	Synchronized	Unsynchronized	Long line application	Short line application	Communication needed
[7]	●			●	●		
[8]	●			●	●		
[9]	●			●	●	●	
[10]	●			●	●	●	
[11]		●	●		●		●
[12]		●	●		●		●
[13]	●			●	●		
[14]		●	●		●		●
[15]	●		●		●		●

2.3.3 Comparative Analysis

Most of the literature indicates the need for high sampling rate of fault records as one of the main disadvantages of traveling wave methods, but do not show quantitative results to support it.

In order to evaluate this statement, this section presents a sensitivity analysis, comparing the results of two methods. For the test, two of the most widely accepted methods were used. First, a one-end method based on spectrum estimation [17], and then a two-ends method based on wavelet [12].

The test consists in analyzing a fault repeatedly but using records with different sampling rate. The records sampling rate varies from 2 kHz to 5 MHz. The test was performed for both selected methods in order to compare the results.

Simulated faults were used for the analysis in order to study the sensitivity of these methods to variations in the frequency of sampling fault records. For this analysis, actual faults records could not be used, since different records of the same fault are required and also obtained in a wide frequency range. Likewise, is not enough to simulate changes in the records sampling rate by deleting samples, because the results would always be multiples of the original record and would not allow the integral study of all possible frequencies.

The fault was simulated using MatLab®. The power system was based on two parallel 735 kV 60 Hz transmission lines with 500 km length and two different equivalents systems, one at each line end. The resistance and reactance of each equivalent system was respectively 5.3754 Ω and 53.754 Ω for the equivalent system S and 2.6877 Ω and 26.877 Ω for the equivalent system R. Both lines were modeled using the distributed parameter line model. Table 2.2 shows the transmission system data used in the line models.

Table 2.2: Transmission line parameters.

	735 kV Line	
Parameter	Seq +, -	Seq 0
Resistance (Ω/km)	0.01165	0.2676
Inductance (H/km)	0.8679e-3	3.008e-3
Capacitance (F/km)	13.41e-9	8.57e-9

The analyzed event was a monophasic solid fault at 200 km from bus S as is shown on Figure 2.6. The fault begins at 0.031 sec. after the simulation starts and the line is opened at 0.05 sec. after that. Both line ends are opened simultaneously.

In order to make comparisons between records, the results are not shown in distance values (km), but referred to as percentage errors based on the total distances of the lines (%) as indicated in [18].

The fault distance was chosen to ensure that the incident and reflected wavefront don't coincide when arriving at each line end and, therefore, they can be clearly distinguishable at the analysis, as shown in the Lattice diagram of Figure 2.7.

In three-phase transmission lines, the traveling waves are coupled and a single wave velocity does not exist. In order to implement these methods in three-phase systems,

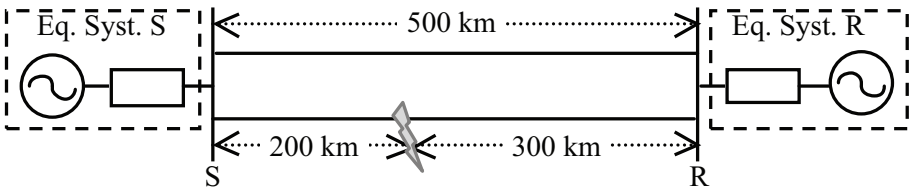

Figure 2.6: Simulated power system model.

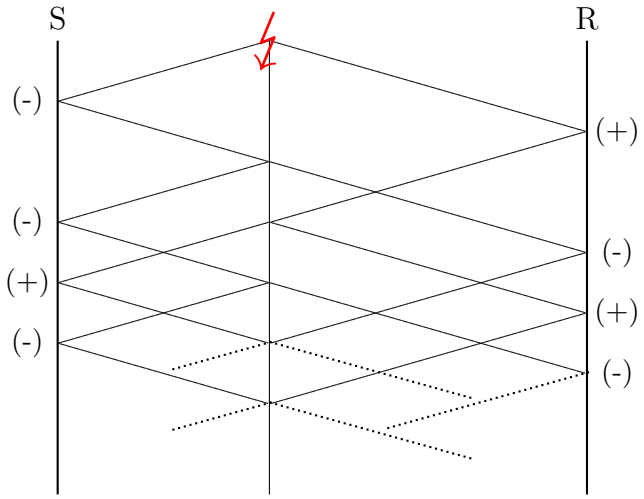

Figure 2.7: Simulated fault Lattice diagram.

the phase domain signals are first decomposed into their modal components [12]. In this study, all line models are assumed to be fully transposed, and therefore the well known Clarke's constant and real transformation matrix is used:

$$S_{mode} = \frac{1}{3}\begin{bmatrix} 1 & 1 & 1 \\ 2 & -1 & -1 \\ 0 & \sqrt{3} & -\sqrt{3} \end{bmatrix} S_{phase} \tag{2.6}$$

Where S_{phase} and S_{mode} are the phase signal and mode signal components, respectively.

Simulated records phase signals are first transformed into their modal components and the mode 2 is taken for analysis. The second mode (mode 2), also known as the aerial mode, is the most common mode used in this type of analysis since is present for any kind of fault.

In order to illustrate the tests, Figure 2.8 and Figure 2.9 show the voltages and currents records for both line ends during the fault. As records show, the fault begins intentionally far from the wave peak and zero crossing, in order to achieve a higher break in the continuity of the medium as possible. Also, is possible to see how traveling waves appear in the phases without fault due to mutual coupling effect between phases.

Currents from the S line-end were used for the analysis with spectrum estimation

method, and currents from both line ends were used for the analysis with wavelet method. Both methods are based on decomposing the fault records into the frequency components that exist in the signal. For this, the Fourier transform was used in the first method, and wavelet transform in the second method.

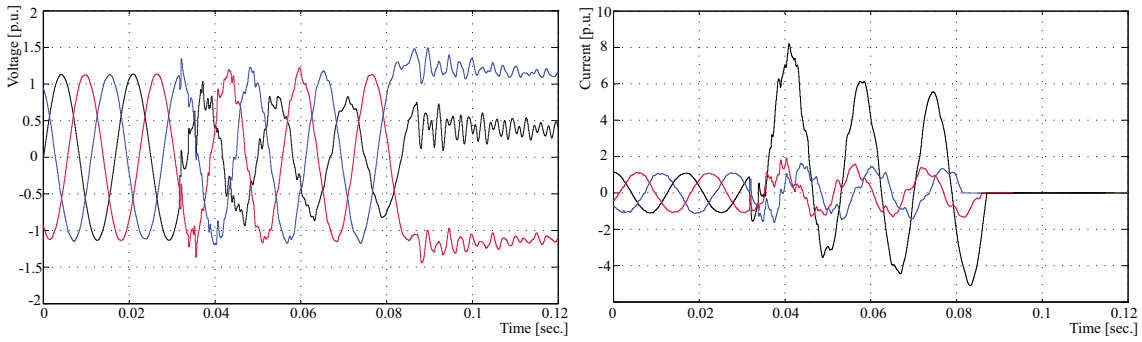

Figure 2.8: Voltages and currents signal for the S line-end.

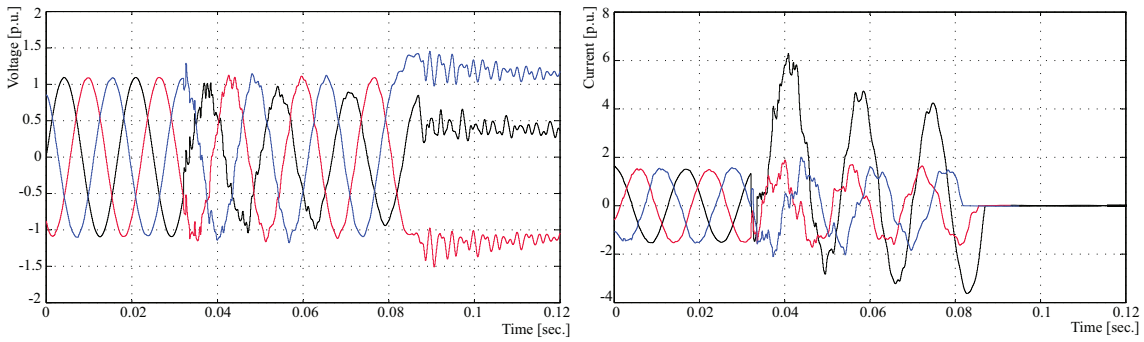

Figure 2.9: Voltages and currents signal for the R line-end.

With the Fourier transform is possible to see the different frequencies that compose the signal. Knowing which is the predominant frequency in the signal (besides the fundamental frequency), the time that takes the wavefront to travel from the line end to the fault point can be calculated and then the fault location is known.

With the wavelet transform, is possible to know not only the signal frequency components but also at what time they appear. Comparing these times with those of the opposite extreme, is easy to know the fault location.

Figure 2.10 and Figure 2.11 show two typical results obtained with each method for the same fault. These methods are applied repeatedly on the same fault, but using records with different sampling rate. The sensitivity analysis results of the methods against these variations are shown on the next section.

Figure 2.12 shows the test results obtained with variations of the records sampling rate for the spectrum estimation and wavelet methods, and also shows the minimum theoretical error. All results are presented using the distance from the S line end as reference.

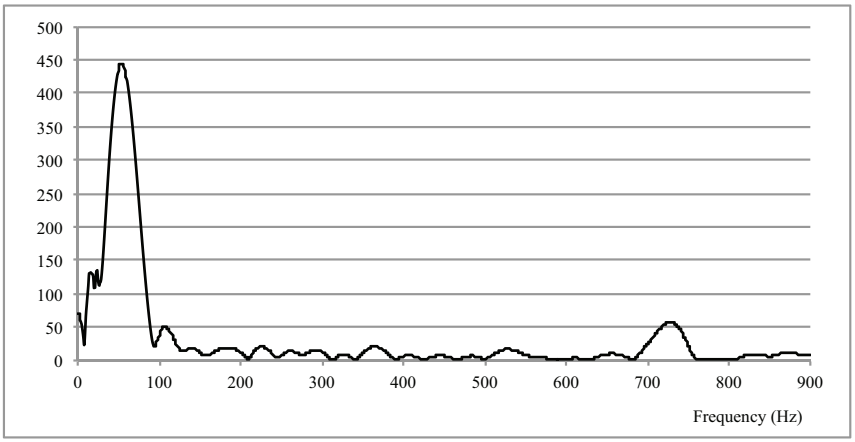

Figure 2.10: Fourier transform example for fault records.

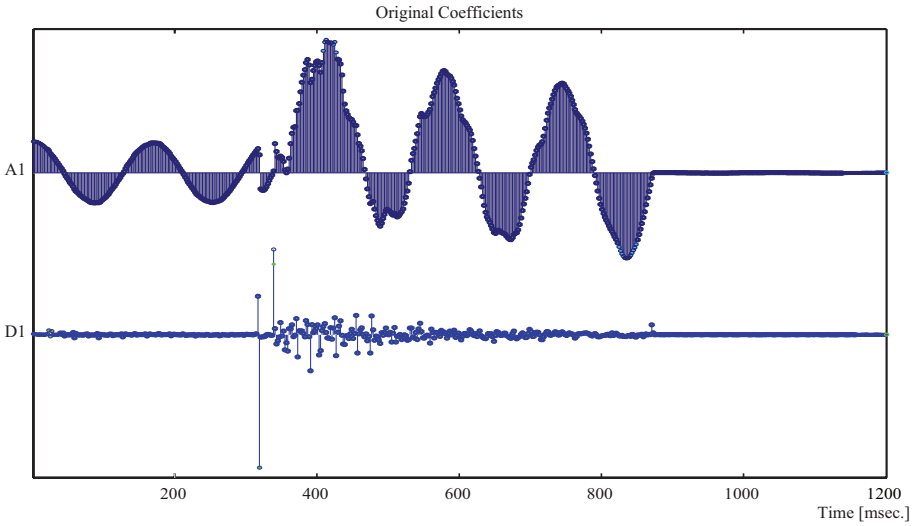

Figure 2.11: Wavelet transform example for fault records.

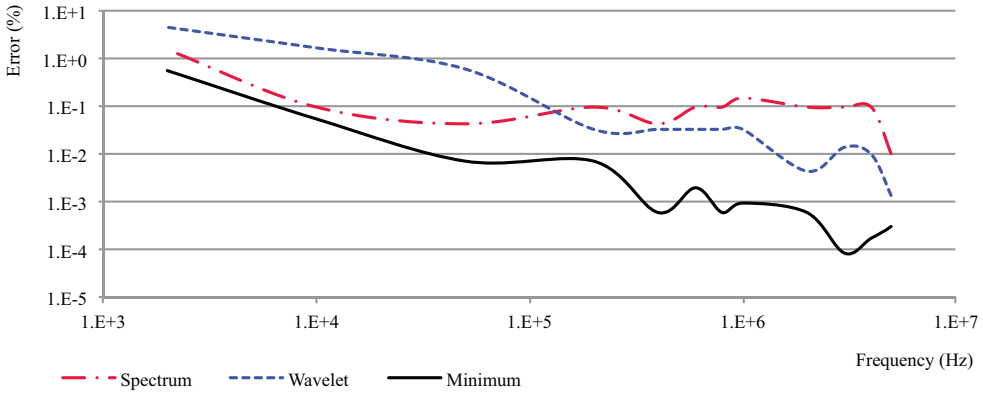

Figure 2.12: Records sampling rate variation test results.

The minimum theoretical value for the errors was calculated for this specific fault, based on the fault's start time, the distance to S line end, the traveling wave speed, and the different records sampling rate. On this basis, results beyond expectations are given such as the minimum error possible with 5 MHz (the biggest frequency tested) is greater than with 3 MHz (the smallest error point in the line) because the wavefront reaches to S line end just between two samplings, in the case of 5 MHz. In the case of 3 MHz, the arrival of the wavefront coincides precisely with a sample, so the precision in the analysis increases.

Many factors avoid that errors as low as theoretically expected may be obtained. Among the main factors are the signal analysis windows for frequency and time. Since the signal transforms are a function of both time and frequency, the exact time-frequency representation of a signal can't be known, i.e., is not possible to know what spectral components exist at what instances of times, but to know the time intervals in which certain band of frequencies exist, which is a resolution problem. This fact is known as the Heisenberg Uncertainty Principle.

Regarding the analyzed methods, is possible to observe that the spectrum estimation method is less sensitive to sample rate variations than the wavelet method. To low sample rate tests, the lower errors were obtained with the spectrum estimation method. While for high sample rate tests, the lower errors were obtained with the wavelet method. The results are in line with the main statement, because in general the errors are bigger as the records sample rate decreases.

2.4 Impedance-Based Fault Location

The impedance-based methods constitute the class most commonly used, due to its simplicity and low cost. In general, these methods are based on the fundamental components of voltage and current signals, to calculate the impedance of the loop created by the fault through the line, and extending from the measuring point to ground, like shown in Figure 2.13. In this figure, F is the fault point, l is the total line length, d is the distance from S line-end to the fault, and Z represents the line parameters per unit length (R, L, C and G). Since the line parameters are a distributed property, if the line impedance is known and is compared with the fault

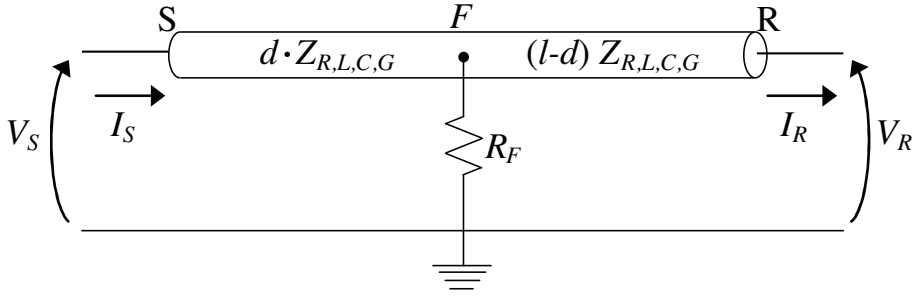

Figure 2.13: Simplified line fault diagram.

analysis results, then is possible to know the fault location.

The first uses of impedance measurements for fault detection was in distance protection in 1923 [19], but the main difference between protection and fault location is that fault location is used for pinpointing the fault position accurately, while protection systems only indicate the general area where a fault occurred (defined by a protective zone), which is the case for protective relays.

Some standards for the applications of fault locations were made, like [18] that gives a general guideline for fault location applications and some recommendations for adapting the different methods to specific user needs. The impedance-based methods are also classified into two main categories considering the measurements they use: one-end and two-ends measurement methods.

2.4.1 Principles of Operation

Impedance-based fault locators calculate the fault location from the apparent impedance found looking into the line. To locate all fault types, the phase-to-ground voltages and currents in each phase must be measured. If the fault resistance is assumed to be zero, is possible to use one of the impedance calculations in Table 2.3 to estimate fault location.

Table 2.3: Simple impedance equations.

Fault Type	Positive-sequence impedance equation ($dZ_l^+ =$)
a-g	$V_a/(I_a + kI_{Re})$
b-g	$V_b/(I_b + kI_{Re})$
c-g	$V_c/(I_c + kI_{Re})$
a-b	V_{ab}/I_{ab}
b-c	V_{bc}/I_{bc}
c-a	V_{ca}/I_{ca}
a-b-c	Any of: V_{ab}/I_{ab}, V_{bc}/I_{bc}, V_{ca}/I_{ca}

Where k is $(Z_l^0 - Z_l^+)/3Z_l^+$; Z_l^0 is the zero-sequence line impedance; d is the per unit distance to fault, and I_{Re} is the residual current. Voltage and current data are used to determine the impedance to the fault location, as shown in Table 2.3. By knowing the line impedance per unit, the distance to the fault per unit can be determined. A correct fault location estimate, unfortunately, is affected by many factors not represented by these equations:

- The combined effect of the load current and fault resistance (reactance effect).

The value of the fault resistance may be particularly high for ground faults, which represent the majority of the faults on overhead lines.

- Influence of zero-sequence mutual effects on the components.
- Uncertainty about the line parameters, particularly zero-sequence impedance.
- Presence of shunt reactors and capacitors.
- Load flow unbalance.

To improve the fault location estimate, it is important to eliminate or reduce errors caused by inadequate assumptions or inaccurate data applied to fault location algorithms. The algorithms will be more accurate if more information about the system is available. Depending on the circuit data available, different fault location methods may be implemented. The widest used method is the simple reactance method.

With the simple reactance method, the device measures the apparent impedance, then determines the ratio of the measured reactance to the reactance of the entire line. This ratio is proportional to the distance to the fault. The method assumes that the current through the fault resistance is in phase with the current at the measurement point, and there is no load prior to the fault.

The reactance algorithm is one of the earliest algorithms that compensates for the fault resistance by measuring only the imaginary part of the apparent line impedance during the fault Z_F. Per unit distance to the fault is shown in equation (2.7):

$$d = \Im(\frac{V_F/I_F}{Z_l}) \tag{2.7}$$

Where V_F and I_F are the voltage and current measured during the fault, and Z_l is the line impedance per unit distance. For example, for the line-to-ground fault (a-g), the calculation would be as shown in equation (2.8):

$$d = \Im[\frac{V_{Fa}/(I_{Fa} + kI_{Re})}{Z_l^+}] \tag{2.8}$$

Where the residual current $I_{Re} = 3I^0$. The error is zero if the fault resistance is zero or if I_a and I_F are in phase.

Present communications technology allows the use of data from both ends of the transmission line. The calculation of fault location using data from two ends is fundamentally similar to the single-ended methods, except now exists a means to determine and minimize or eliminate the effect of fault resistance and other similar factors that tend to throw off the accuracy of the estimate. These factors, such as non-transpositions, strong or weak sources, loading, and others, have been discussed earlier.

The two-ends location methods are more accurate than one-end methods and are able to minimize or eliminate the effects of fault resistance, loading, and charging

current. Fault type does not need to be calculated. Therefore, positive-sequence components are used rather than zero-sequence, thus eliminating adverse effects of zero-sequence components. The main drawback is the fact that data from both ends must be gathered at one location to be analyzed, whereas the one-end location can be done at the line terminal by the relay or other device collecting the data. Effective two-ends fault location requires an efficient means of collecting oscilographic or phasor data from electronic devices at each end of a line following a fault, and processing that data automatically, to simplify the procedure of providing the utility personnel with the proper information at the proper location.

The following sections, further explain the one-end and two-ends impedance fault location methods.

2.4.2 One-end Measurement Methods

One-end algorithms using local voltages and currents are proposed in [20–22], which have no requirements for communication channels to transmit the data from the remote end to the local end. The method [20, 21] proposes the equation of the fault resistance (arc resistance) based on the voltage and current phasors at the point of measurement. Then, the fault resistance is expressed in an imaginary equation and is a function of the distance between the fault and point of measurement. Since the arc resistance is a real number, the imaginary part of the arc equation can be equated to zero, and the distance can be found. This method is very simple and can be applied to any type of fault. However, is extremely dependent of the line parameters which may bring errors to the results.

The method in [22] is based at the same principles that [20, 21] but with a compensation for the fault resistance drop, eliminating the errors inherent in conventional reactance-type measurements, which bring more accuracy. However, such techniques require the use of mathematical assumptions in order to eliminate the effect of the pre-fault network conditions, which can result in fault location errors if the assumed conditions are not verified.

Other approaches were developed in this area, like the approach presented in [23] that uses pre-fault and fault current phasors at one-end of the line for estimating the fault location, assuming the source impedances to be available. However, the values of source impedance are not practically available for all situations.

Most commercial types of fault location systems are built based on one-end algorithms [24–27] due to its simplicity and low cost, but the results are highly dependent on the knowledge about the operation system's conditions and the actual line parameters. In counterpart, the other impedance-based fault locator group, i.e. the two-ends measured methods, provide more precise results without a thorough knowledge of the line or system conditions, but they need more sophisticated and expensive measurement and analysis equipment.

2.4.3 Two-ends Measurement Methods

The two-ends measurement methods compensate the errors from the line models and the conditions of the system with information of both terminals. In general, these methods try to describe the behavior of line voltages and currents viewed from both ends, using the fundamental component of input signals at each terminal. The point where the results from each end are equal must be the fault location. At the same time, these methods can be classified into two groups according to the type of data used: synchronized and unsynchronized data.

The methods that use synchronized data are [28–31]. Reference [28] was one of the first to describe a two-ends fault locator, which proposes a solution based on the comparison between the line behavior viewed from both ends. To ensure that the comparison is made between data obtained simultaneously at both ends, is performed artificial synchronization of data, i.e. a record synchronization after the event, where, to relate such data to that measured at the receiving end, the pre-fault voltages and currents data at the sending end can be used to provide a common phasor reference. This approach avoids the need for data synchronization via a communication link.

Another artificial synchronization form is proposed in [29], where the equations that describe the line's behavior are expanded, and the angle between both ends' voltage (called synchronization angle) is considered as unknown. Then, the fault location is obtained through an iterative process, evaluating at the same time between a possible range for the fault point and for the voltage angle. The same principle is proposed in [30], but using a short line model to simplify the calculations and a compensation for long lines is made after that. Also, the same approach for signals artificial synchronization is used in [31], where the method is based on a different model for the line, which follows the principles of superposition of three different balanced systems.

The methods that use synchronized measurements require more expensive equipments, because communication systems between both line-ends are needed [32–35]. One of the first to propose the use of synchronized measurement was [32] which aims to determine the voltages and currents along the entire line during the fault, from data recorded at each end. By ensuring that the analysis is done with data obtained simultaneously at both ends, is proposed an external reference provided by GPS to know the time of each measurement. This improves the accuracy of the method, since it is not based on any assumption of the system to synchronize the data, but in obtaining the time-stamps at which the measurements were actually made.

A GPS time-stamp data is also used in [33], where an adaptive method to improve the accuracy of measurement is proposed. This method continuously estimates the line parameters using data from times when there is no fault; in order to adjust the models as much as possible to actual system conditions.

Other method is proposed in [34]. This method uses synchronized data from both line-ends, but only voltage data is needed. The method begins to search what the voltage would be at the fault point viewed from both ends in terms of the line parameters and the distance to the fault. Because the line parameters are known

and the results of the fault's voltage viewed from both ends should be equal, then the equations are matched and the distance to the fault can be searched.

Moreover, in the last years a new methodology for fault location has been developed. This new methodology is also based on analysis of the fundamental voltage and current signals at both line ends and also uses data synchronized by GPS, but without using information about the line impedance. In [35] an algorithm based on this principle is shown. This is achieved by analyzing the symmetrical components networks for a fault (either symmetric or asymmetric faults) using a model for short lines. Using the short line model, the equations are greatly simplified and as all input line signals are known, it is possible to organize the equations in order to cancel the terms of the line's impedances. This algorithm is fast, simple, and eliminates any possible error given by the line parameters. But is inaccurate in cases that involve long lines. In addition, the method becomes iterative in the case of three-phase faults, because the algorithm depends of the fault's resistance.

2.4.4 Other Considerations

Until now, many of the currently available methods to locate faults through impedance computing have been analyzed. In general, its basic principles and the differences between them have been shown. But until now, all have been proposed for a generic line form, i.e. a single line with only two terminals.

In the literature, there are many other methods that use the algorithms shown here, and adapt them in order to take into account certain specific conditions that might exist in the different types of lines that compose an electric system.

There are methods that take into account other factors like changes due to parallel lines [36, 37], as well as line configurations like three-terminal lines [38], or multi-terminals lines [39, 40]. Some algorithms consider if the line is transposed or not [41, 42] or any special equipment that are in the line itself, like series compensation [43, 44] or FACTs [45]. Other algorithms try to minimize errors given by the measurement equipment itself, such as the current transformer saturation [46].

All these algorithms bring improvements in fault location for different types of line, but in the end, do not add innovation to the principles of fault location itself. The added value of these works is the adaptation of existing principles of location, whether adapted to more complex line models that take into account the different types of lines, as well as by the use of more complex decision-making algorithms that help to determine the best result.

Table 2.4 shows a summary of all the fault location methods discussed here.

2.4.5 Comparative Analysis

Most of the literature indicates the low sensitivity to errors in the parameters of the line model as one of the main advantages of the two-ends methods over the one-end methods. But do not show quantitative results to support it.

Table 2.4: Impedance-based fault location methods summary.

Reference	One-end	Two-ends	Synchronized	Unsynchronized	Long line application	Short line application	Communication needed
[20]	●				●	●	
[21]	●				●	●	
[22]	●				●	●	
[23]	●				●	●	
[28]		●		●	●	●	
[29]		●		●	●	●	
[30]		●		●		●	
[31]		●		●	●	●	
[32]		●	●		●	●	●
[33]		●	●		●	●	●
[34]		●	●		●	●	●
[35]		●	●			●	●

In order to evaluate this statement, a comparison of the results of two methods is presented. For the test, two of the most widely accepted methods were used, the one-end method [20], and the two-ends method [28].

In the analysis of asymmetrical faults where the sequence networks are used, the most common errors in transmission lines models are found in the ground conductivity (which are reflected in the zero-sequence network), and in differences in the conductors arrangement along the line (which are reflected in the positive and negative sequence networks). To be able to study the sensitivity to these kinds of errors, two different faults were analyzed. First, a monophasic fault, where the zero-sequence parameters were varied, and then a biphasic fault, where the positive and negative sequence parameters were varied.

The records used for the tests come from actual faults occurred in two overhead transmission lines, the monophasic fault record comes from a 765 kV line with 225 km, and the biphasic fault record comes from a 69 kV line with 11 km. In order to make comparisons between them, the results are not shown in distance values (km), but referred to percentage errors based on the total distances of the lines (%) as indicated

in [18]. To facilitate the comparison, faults with some common characteristics were required: in both cases the fault was cleared quickly (between 3 and 4 cycles), also, in both cases the fault was located near the "sender" end (the "sender" and "receiver" ends were determined with the pre-fault conditions of the line), the monophasic fault was located at 16.41% of the total length of the line and the biphasic one was at 14.91% of the total line length.

The variations were made individually and over all parameters (resistance, inductance, and capacitance), for both the zero-sequence test and the positive and negative sequence test. In this test, the conductances of the lines were neglected. The variations were from -100% to 100% of the real values, i.e. each parameter varies from zero to twice the real value.

In order to illustrate the tests made, Figure 2.14 and Figure 2.15 show the triphasic currents records for both ends of each fault.

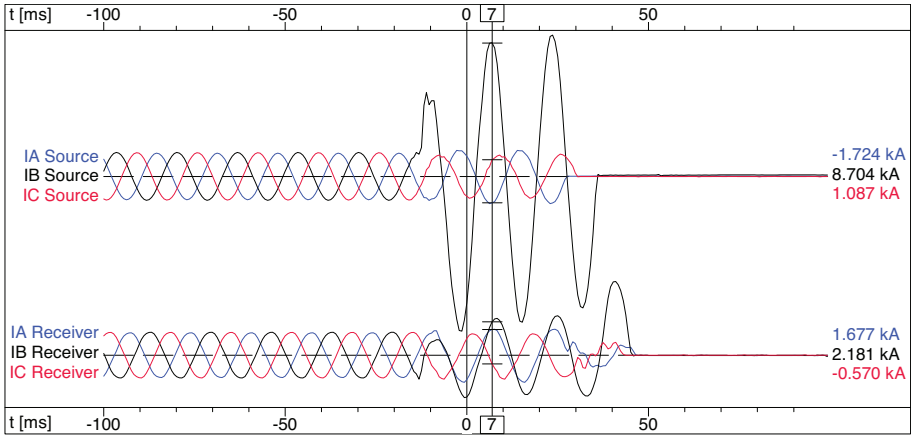

Figure 2.14: Triphasic currents for the monophasic fault.

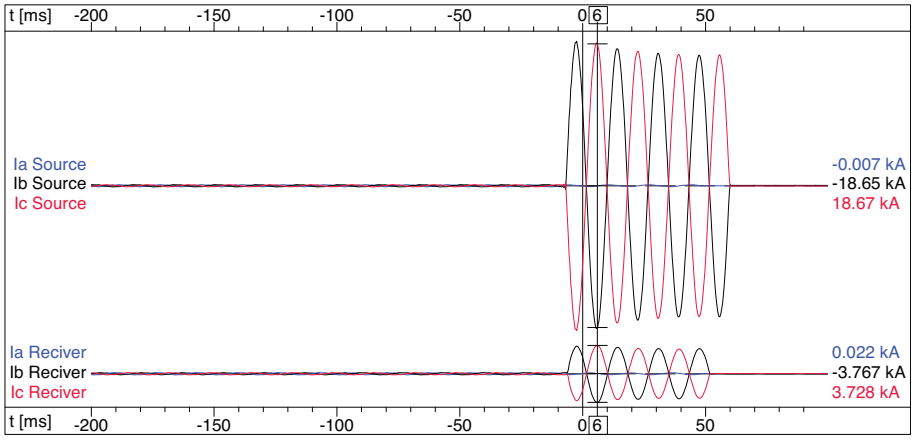

Figure 2.15: Triphasic currents for the biphasic fault.

Figure 2.16a and Figure 2.16b show the test results obtained with variations of the zero-sequence parameters (monophasic fault), and positive and negative sequences

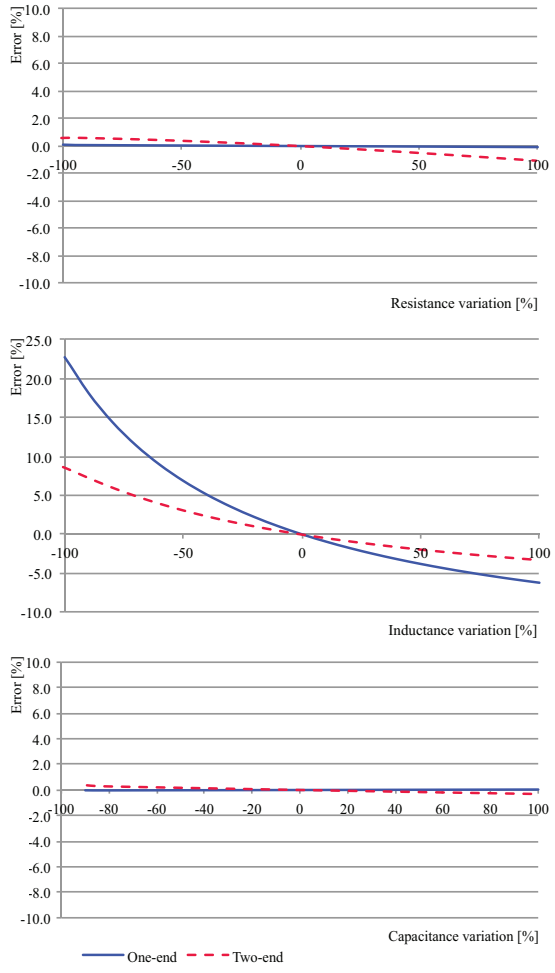

(a) Zero-sequence variation for the monophasic fault.

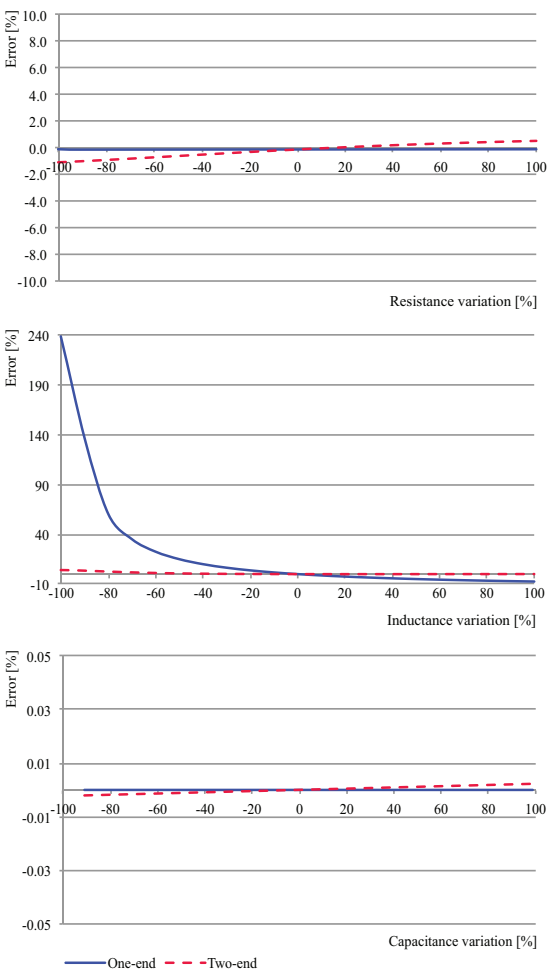

(b) Positive and negative sequence variation for the biphasic fault.

Figure 2.16: Parameters variation test results.

parameters (biphasic fault). All distances results are presented using the source end of each line as reference.

In the first approach, is possible to observe that the one-end method has higher sensitivity to variations in positive and negative sequence parameters, while the two-ends method is more sensitive to changes in zero-sequence parameters.

Table 2.5 shows in more detail the range achieved by the errors of each method and in every sensitivity test.

The results of the inductance variations are completely in line with the main statement, because the two-ends method proved to be less sensitive to the parameters variations of all sequence networks than the one-end method.

In the case of resistance variations, the results do not confirm that statement, since the two-ends method proved to be more sensitive to the parameters variations of all sequence networks than the one-end method. This could be because, as mentioned

Table 2.5: Results range for the sensibility tests.

Test \ Results		One-end		Two-ends	
		Max	Min	Max	Min
Seq. 0	Res.	0.077	-0.078	0.623	-1.070
	Ind.	22.84	-6.216	8.687	-3.293
	Cap.	0.038	-0.034	0.315	-0.315
Seq. +,-	Res.	0.015	-0.015	0.645	-0.963
	Ind.	238.97	-7.462	4.270	-0.049
	Cap.	0.00	0.00	0.002	-0.002

above, the method described in [20] uses only the imaginary part of the equations that describe the fault's resistance, whereas the method described in [28] uses the entire model line in the final resolution. For this reason, is expected that the two-ends method is more sensitive to changes in the real components of the line model. In any case, these results are not alarming since errors obtained varying the resistances are always very small compared with those obtained varying the inductances.

In the case of capacitance variations, the errors obtained were very small compared to the other two tests. Therefore, is noted that these methods do not have any sensitivity to changes in these parameters and this type of lines. But these results could be different if underground lines era analyzed, where the capacitance is more significant.

2.5 Final Remarks

This chapter presents the different methods that exist for fault location, as well as different types of tests are performed using these methods.

A comparative analysis is done between two of the traveling wave based methods. The analysis is based on the statement that the methods that use information from both line-ends are more robust than methods that use information from only one line-end. Although in general, this statement is well founded, this analysis showed that is not absolutely correct since the two-ends method proved to be more sensitive to the variations that the one-end method. In any case, these results are not alarming since differences between errors are very small, and also the two-ends methods have better results at higher sample rates which are the most common used samples for the traveling wave fault location methods.

Also a comparative analysis is done between two of the impedance-based methods in order to prove the general behavior of these type of methods, and the statement that the two-ends methods are more robust than the one-end methods because they

are less sensitive to errors in the line parameters. Although in general this statement is well founded, this analysis showed that is not absolutely correct and in some cases needs to be clarified in order to avoid confusions.

The objective of these tests is to deepen the understanding of the different methods by conducting comparisons between their performances, so as to observe their behavior and test the strengths and weaknesses of each method. The highlight of these tests is to show the importance of really knowing the different fault location methods in order to select the one that best suits the available resources.

As section 1.7 explained, the chapters of this work don't follow a linear order because the research of different fields of knowledge was required for its development. After the review of the different fault location methods, the next chapter will address the problem of transmission lines modeling. The transmission line models are an integral part in fault location methods based on impedance measurement. The line models are the framework used for calculating the line's impedance, from the voltage and current measurements obtained at the line-ends addressed in section 2.4.

Bibliography Chapter 2

[1] P. Gale, J. Stokoe, and P. Crossley, "Practical experience with travelling wave fault locators on scottish power's 275 & 400 kV transmission system," in *Sixth International Conference on Developments in Power System Protection*, pp. 192–196, 1997.

[2] L. de Andrade and R. Guanipa, "Costs reduction in attention to transmission lines faults using faults location equipment," *I Congreso Venezolano de Redes y Energía Eléctrica*, 2007.

[3] H. L. Clark, *An Elementary Treatise on Electrical Measurement.* London: E. & F. N. Spon, 1868.

[4] J. R. Carson, "Theory of the transient oscillations of electrical networks and transmission systems," *Transactions of the American Institute of Electrical Engineers*, vol. XXXVIII, no. 1, pp. 345–427, 1919.

[5] J. R. Carson, "Wave propagation in overhead wires with ground return," *Bell System Technical Journal*, vol. 5, no. 4, pp. 539–554, 1926.

[6] J. Röhrig, "Location of faulty places by measuring with cathode ray oscillographs," *Elektrotech. Zeits.*, vol. 8, pp. 241–242, 1931.

[7] R. Stevens and T. Stringfield, "A transmission line fault locator using fault-generated surges," *Transactions of the American Institute of Electrical Engineers*, vol. 67, no. 2, pp. 1168–1179, 1948.

[8] L. Lewis, "Traveling wave relations applicable to power-system fault locators," *Transactions of the American Institute of Electrical Engineers*, vol. 70, no. 2, pp. 1671–1680, 1951.

[9] M. Ando, E. O. Schweitzer, and R. A. Baker, "Development and field-data evaluation of single-end fault locator for two-thermal HVDC transmission lines part 1: Data collection system and field data," *IEEE Transactions on Power Apparatus and Systems*, vol. PAS-104, no. 12, pp. 3524–3530, 1985.

[10] M. Ando, E. O. Schweitzer, and R. A. Baker, "Development and field-data evaluation of single-end fault locator for two-terminal HVDC transmission lines-part 2 : Algorithm and evaluation," *IEEE Transactions on Power Apparatus and Systems*, vol. PAS-104, no. 12, pp. 3531–3537, 1985.

[11] M. Dewe, S. Sankar, and J. Arrillaga, "The application of satellite time references to HVDC fault location," *IEEE Transactions on Power Delivery*, vol. 8, no. 3, pp. 1295–1302, 1993.

[12] F. Magnago and A. Abur, "Fault location using wavelets," *IEEE Transactions on Power Delivery*, vol. 13, no. 4, pp. 1475–1480, 1998.

[13] P. Murthy, J. Amarnath, S. Kamakshiah, and B. Singh, "Wavelet transform approach for detection and location of faults in hvdc system," in *IEEE Region 10 and the Third international Conference on Industrial and Information Systems*, pp. 1–6, 2008.

[14] C. Ping, X. Bingyin, and L. Jing, "A traveling wave based fault locating system for HVDC transmission lines," in *International Conference on Power System Technology*, pp. 1–4, 2006.

[15] K. Young-Jin, K. Sang-Hee, L. Dong-Gyu, and K. Hyung-Kyu, "Fault location algorithm based on cross correlation method for HVDC cable lines," in *IET 9th International Conference on Developments in Power System Protection*, pp. 360–364, 2008.

[16] T. Kawady and J. Stenzel, "Investigation of practical problems for digital fault location algorithms based on EMTP simulation," in *IEEE/PES Transmission and Distribution Conference and Exhibition*, vol. 1, pp. 118–123 vol.1, 2002.

[17] E. Styvaktakis, M. Bollen, and I. Gu, "A fault location technique using high frequency fault clearing transients," *IEEE Power Engineering Review*, vol. 19, no. 5, pp. 58–60, 1999.

[18] IEEE, "IEEE guide for determining fault location on AC transmission and distribution lines," *IEEE Std C37.114-2004*, pp. 1–36, June 2005.

[19] L. Crichton, "The distance relay for automatically sectionalizing electrical net works," *Transactions of the American Institute of Electrical Engineers*, vol. XLII, pp. 527–537, 1923.

[20] T. Takagi, Y. Yamakoshi, J. Baba, K. Uemura, and T. Sakaguchi, "A new algorithm of an accurate fault location for EHV/UHV transmission lines: Part I - Fourier transformation method," *IEEE Transactions on Power Apparatus and Systems*, vol. PAS-100, no. 3, p. 8, 1981.

[21] T. Takagi, Y. Yamakoshi, J. Baba, K. Uemura, and T. Sakaguchi, "A new algorithm of an accurate fault location for EHV/UHV transmission lines: Part II - Laplace transform method," *IEEE Transactions on Power Apparatus and Systems,*, vol. PAS-101, no. 3, pp. 564–573, 1982.

[22] L. Eriksson, M. Saha, and G. Rockefeller, "An accurate fault locator with compensation for apparent reactance in the fault resistance resulting from remore-end infeed," *IEEE Transactions on Power Apparatus and Systems*, vol. PAS-104, no. 2, pp. 423–436, 1985.

[23] M. Djuric, Z. Radojevic, and V. Terzija, "Distance protection and fault location utilizing only phase current phasors," *IEEE Transactions on Power Delivery*, vol. 13, no. 4, pp. 1020–1026, 1998.

[24] GE Multilin, "DDFR distributed digital fault recorder instruction manual," 2011.

[25] SEL Inc., "SEL-734 advanced metering system instruction manual," tech. rep., Schweitzer Engineering Laboratories, Inc., 2010.

[26] ABB Inc., *REL 512 Line Protection and Breaker Control Terminal Instruction Booklet*, vol. V. 2.31. PA, USA: Substation Automation and Protection Division, 2003.

[27] Siemens, "SIMEAS R. digital fault and power quality recorder manual," tech. rep., Siemens AG, 2011.

[28] A. Johns and S. Jamali, "Accurate fault location technique for power transmission lines," *IEEE Proceedings Generation, Transmission and Distribution*, vol. 137, no. 6, pp. 395–402, 1990.

[29] A. Girgis, D. Hart, and W. Peterson, "A new fault location technique for two- and three-terminal lines," *IEEE Transactions on Power Delivery*, vol. 7, no. 1, pp. 98–107, 1992.

[30] D. Novosel, D. Hart, E. Udren, and J. Garitty, "Unsynchronized two-terminal fault location estimation," *IEEE Transactions on Power Delivery*, vol. 11, no. 1, pp. 130–138, 1996.

[31] J. Izykowski, E. Rosolowski, P. Balcerek, M. Fulczyk, and M. Saha, "Accurate noniterative fault location algorithm utilizing two-end unsynchronized measurements," *IEEE Transactions on Power Delivery*, vol. 25, no. 1, pp. 72–80, 2010.

[32] M. Kezunovic and B. Perunicic, "Automated transmission line fault analysis using synchronized sampling at two ends," *IEEE Transactions on Power Systems*, vol. 11, no. 1, pp. 441–447, 1996.

[33] J. Joe-Air, Y. Jun-Zhe, L. Ying-Hong, L. Chih-Wen, and M. Jih-Chen, "An adaptive PMU based fault detection/location technique for transmission lines. I. theory and algorithms," *IEEE Transactions on Power Delivery*, vol. 15, no. 2, pp. 486–493, 2000.

[34] S. Brahma and A. Girgis, "Fault location on a transmission line using synchronized voltage measurements," *IEEE Transactions on Power Delivery*, vol. 19, no. 4, pp. 1619–1622, 2004.

[35] G. Preston, Z. Radojevic, C. Kim, and V. Terzija, "New settings-free fault location algorithm based on synchronised sampling," *IET Generation, Transmission & Distribution*, vol. 5, no. 3, pp. 376–383, 2011.

[36] M. Saha, K. Wikstrom, J. Izykowski, and E. Rosolowski, "New accurate fault location algorithm for parallel lines," in *Seventh International Conference on Developments in Power System Protection*, pp. 407–410, 1999.

[37] H. Jung, Y. Park, M. Han, C. Lee, H. Park, and M. Shin, "Novel technique for fault location estimation on parallel transmission lines using wavelet," *International Journal of Electrical Power & Energy Systems*, vol. 29, no. 1, pp. 76–82, 2007.

[38] J. Izykowski and E. Rosolowski, "Accurate non-iterative fault location algorithm for three-terminal line," in *International Conference on Electrical and Electronics Engineering*, pp. I–154–I–158, 2009.

[39] L. de Andrade and E. Sorrentino, "Fault locator for parallel multi-terminal transmission lines with sources only at two terminals," *II Congreso Venezolano de Redes y Energía Eléctrica*, p. 7, 2009.

[40] G. Manassero, E. Senger, R. Nakagomi, E. Pellini, and E. Rodrigues, "Fault-location system for multiterminal transmission lines," *IEEE Transactions on Power Delivery*, vol. 25, no. 3, pp. 1418–1426, 2010.

[41] K. Sang-Hee, A. Yong-Jin, K. Yong-Cheol, and N. Soon-Ryul, "A fault location algorithm based on circuit analysis for untransposed parallel transmission lines," *IEEE Transactions on Power Delivery*, vol. 24, no. 4, pp. 1850–1856, 2009.

[42] C. Apostolopoulos and G. Korres, "A novel algorithm for locating faults on transposed/untransposed transmission lines without utilizing line parameters," *IEEE Transactions on Power Delivery*, vol. 25, no. 4, pp. 2328–2338, 2010.

[43] M. Saha, J. Izykowski, E. Rosolowski, and B. Kasztenny, "A new accurate fault locating algorithm for series compensated lines," *IEEE Transactions on Power Delivery*, vol. 14, no. 3, pp. 789–797, 1999.

[44] G. Preston, Z. Radojevic, and V. Terzija, "Novel parameter-free fault location algorithm for transmission lines with series compensation," in *10th IET International Conference on Developments in Power System Protection. Managing the Change.*, pp. 1–5, 2010.

[45] G. Mahdi and S. Javad, "An accurate and noniterative fault location algorithm for transmission lines in the presence of shunt connected FACTS devices," *IEEE Transactions on Power Delivery*, 2011.

[46] L. Yuan and M. Kezunovic, "Optimal estimate of transmission line fault location considering measurement errors," *IEEE Transactions on Power Delivery*, vol. 22, no. 3, pp. 1335–1341, 2007.

Chapter 3

Transmission Line Model

No general model for arbitrary wave shapes or combinations of line parameters is known. Exact models have been produced for only a few special cases. In other cases, approximate solution procedures have been proposed. Consequently, there are many ways of obtaining a solution available [1]. Each has its own advantages and disadvantages relative to the others depending on the particular transmission system being analyzed and the nature of the signals being considered. A survey of these techniques, together with their advantages and disadvantages, will assist in appreciating how a particular transmission problem might be solved best. In general, transmission line models can be classified according to Figure 3.1.

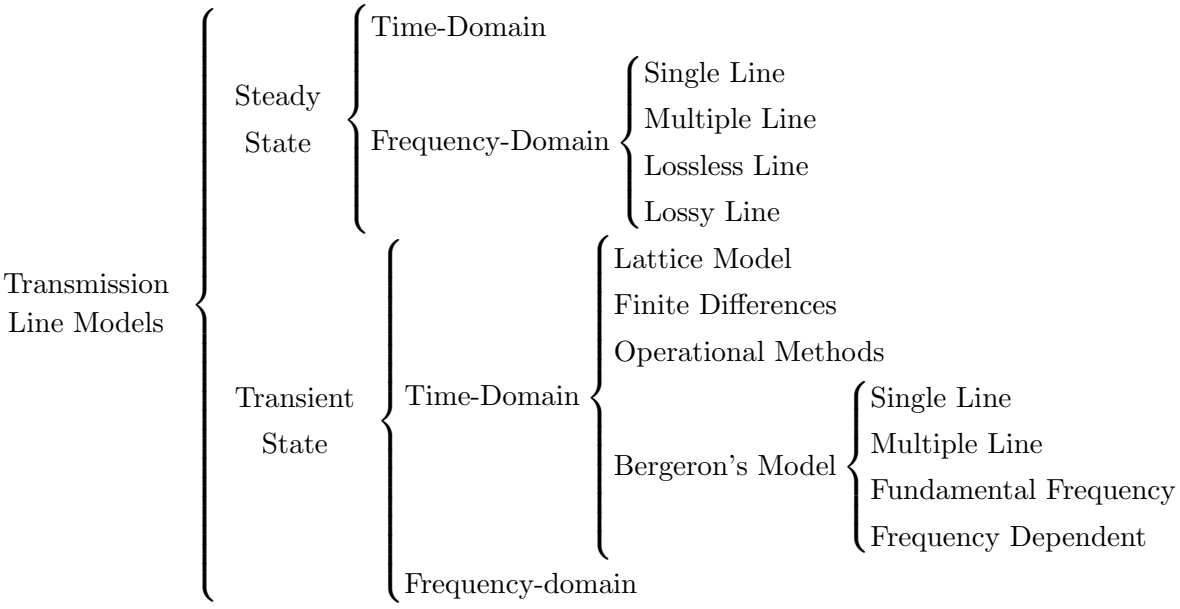

Figure 3.1: Classification of transmission line models

It will be seen that solution techniques have been classified into two types. Frequency-domain and time-domain. Frequency-domain solutions are those in which time is removed as an independent variable from both the network equations and the initial

conditions while the equations are being solved. Time-domain solutions refer to those solutions during which no intermediate process removes time as an independent variable. These solutions start with initial conditions expressed in time. Often these don't need to be predetermined, only instantaneous values at discrete points in time are required.

For a steady state sinusoidal signal, the only method of solution that would normally be applied is solution in the frequency-domain. Time-domain techniques can also be applied to the steady-state but have little to offer when compared with the frequency-domain alternative.

Frequency-domain models for transient state become considerably more complex than for the case of a steady state. It is necessary to analyze the signal being applied into its frequency components. For linear systems this is usually easily achieved. The network equations are then solved for each component frequency using the analysis of a steady-state sinusoidal signal.

The time-domain transmission lines models are of great importance in the electromagnetic transient simulation of power systems. Currently, time-domain line models are based on simplifications of distributed parameters, or on lumped models. Models based directly on distributed parameters are most commonly used in frequency-domain, because the distributed parameters property of transmission lines are descibed by differential equations, and frequency-domain facilitates the manipulation of such equations.

Operational methods of solution that produce exact solutions as functions of time, have been classified as time-domain methods. Those methods that produce operational expressions (in the frequency-domain) requiring further processing by numerical inversion have been classified as frequency-domain methods.

3.1 Line Model Differential Equations

The power transmission lines are formed by two or more isolated conductors, in order to allow the power flow only in the longitudinal direction of the line (here called X direction) with minimal losses, and to prevent the flow in other directions as much as possible. For simplicity, the model will be deduced for a single line, but could also be deduced for multi-conductor lines.

Transmission lines have four primary parameters, which are a series resistance R, a series inductance L, a parallel capacitance C, and a parallel conductance G. These parameters are distributed along the entire line and are used to model the behavior of the voltage (V) and current (I) signals as they travel through the line, as represented in Figure 3.2. For simplicity, the model will be deduced for the fundamental frequency parameters, but the model could also be expanded in order to incorporate parameters at other frequencies.

The differential equations of a transmission line are obtained focusing attention on an infinitesimal section of Δx line length, which is located at the coordinate X on

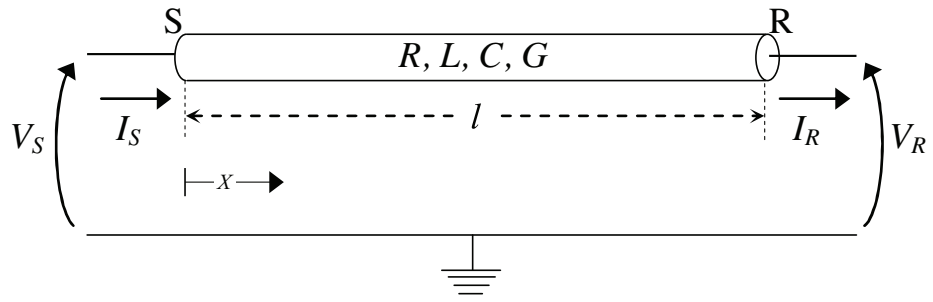

Figure 3.2: General line representation.

the line, and far from the line ends. This line section has a total resistance $R\Delta x$, a total inductance $L\Delta x$, a total capacitance $C\Delta x$, and a total conductance $G\Delta x$. Its equivalent circuit in a quadrupole form can be represented incorporating these circuit elements in many ways. One of these is shown in Figure 3.3.

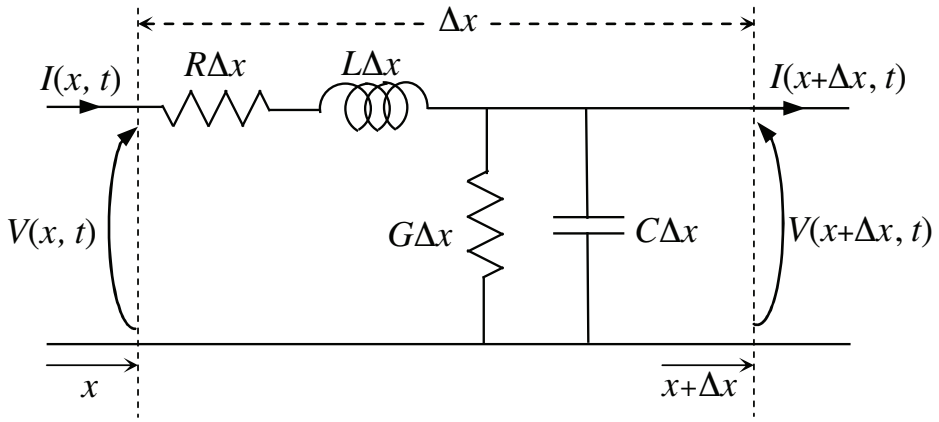

Figure 3.3: Line section of Δx length.

Using the instantaneous quantities of Figure 3.3, these relations can be expressed by the following equations, applying the Kirchhoff laws:

$$V(x+\Delta x,t)-V(x,t)=\Delta V(x,t)=-R\Delta x I(x,t)-L\Delta x\frac{\partial I(x,t)}{\partial t} \tag{3.1}$$

$$I(x+\Delta x,t)-I(x,t)=\Delta I(x,t)=-G\Delta x V(x,t)-C\Delta x\frac{\partial V(x,t)}{\partial t} \tag{3.2}$$

Both V and I, are function of the distance x and the time t. Then, dividing by Δx, and making Δx tend to zero, leads to the following partial differential equations:

$$\frac{\partial V(x,t)}{\partial x}=-RI(x,t)-L\frac{\partial I(x,t)}{\partial t} \tag{3.3}$$

$$\frac{\partial I(x,t)}{\partial x}=-GV(x,t)-C\frac{\partial V(x,t)}{\partial t} \tag{3.4}$$

Voltage $V(x,t)$ and current $I(x,t)$ will be denoted only as V and I respectively, but knowing that they are always functions of x and t.

Equations (3.3) and (3.4) describe the general behavior of a transmission line. These equations were first proposed by Lord Kelvin in 1855 [2] for the first trans-Atlantic submarine telegraph cable project (for this reason, they are also known as telegraph equations). The deduction of this equations has not used special assumptions, so they are complete descriptions of the possible interrelationships of voltage, current, and its derivatives. To find an accurate solution to these equations is the main problem of transmission line modeling.

Equations (3.3) and (3.4) are the telegraph equations of a single circuit transmission line. For multiple circuit transmission lines, the variables $V(x,t)$ and $I(x,t)$ become vectors of variables, and the coefficients become matrices of coefficients.

It is observed that $V(x,t)$, $I(x,t)$, $\partial V(x,t)/\partial x$, and $\partial I(x,t)/\partial x$ must be continuous with respect to x. This still allows waves with sharp corners, hence it's necessary to consider the limit exists. For practical purposes, $I(x,t)$ will be finite but may not be differentiable with respect to t everywhere.

Therefore, it is possible that there will be a number of points on the line where the equations will not apply. Existing theorems related to partial differential equations indicate that characteristic positions exist where there is no solution. These positions are curves in the (x,t) plane, where discontinuities can be propagated.

This is the basis of the method of characteristics, a technique of solving differential equations which will be dealt with in detail later in section 3.3.1 of this analysis.

3.2 Frequency-Domain Model

In order of present the different models developed from equations (3.3) and (3.4), this section shows the deductions for line models in frequency-domain, and expressions for voltage and current along the distributed lines are obtained. Propagation constant and characteristic impedance are defined, and it's demonstrated that the electrical power is being transmitted over the lines at approximately the speed of light. The model used to calculate voltages and currents depends on the length of the line. For a long line, the effects of all line parameters are significant so they must be considered in order to find an accurate solution. But for a short line, some approximations can be done in order to simplify the model and still maintain a reasonable accuracy.

3.2.1 Long Line Model

The frequency-domain long line model was first proposed by O. Heaviside in 1885 [3], who adapted complex numbers to the study of electrical circuits, and invented mathematical techniques to the solution of differential equations (later found to be equivalent to Laplace transforms). Using this transform, equations (3.3) and (3.4)

can be written as first order differential equations, facilitating their resolution:

$$dV = RIdx + L\omega jIdx = zIdx \tag{3.5}$$

$$dI = GVdx + C\omega jVbx = yVdx \tag{3.6}$$

Where ω is the signal's frequency, z is the series impedance of the line per unit length, and y is the parallel admittance of the line per unit length. Differentiating (3.6) and substituting from (3.5):

$$\frac{d^2I}{dx^2} = z\frac{dI}{dx} = zyI \tag{3.7}$$

From this second-order differential equation it will result a solution with the form:

$$I = K_1 e^{\sqrt{zy}x} + K_2 e^{-\sqrt{zy}x} \tag{3.8}$$

Then, from (3.6), the voltage is:

$$V = \frac{1}{y}\frac{dI}{dx} = \sqrt{\frac{z}{y}}(K_1 e^{\sqrt{zy}x} - K_2 e^{-\sqrt{zy}x}) \tag{3.9}$$

Also let $\gamma = \sqrt{zy}$ and $Z_o = \sqrt{\frac{z}{y}}$. Where γ is known as the propagation constant and Z_o is known as the characteristic impedance. Then, (3.8) and (3.9) can be written as:

$$I = K_1 e^{\gamma x} + K_2 e^{-\gamma x} \tag{3.10}$$

$$V = Z_o(K_1 e^{\gamma x} - K_2 e^{-\gamma x}) \tag{3.11}$$

The constants K_1 and K_2 can be found fixing the border conditions, that is, when $x = 0$, $V = V_S$, and $I = I_S$. Then, equation (3.10) and (3.11) become:

$$\begin{cases} I = K_1 + K_2 \\ V = Z_o(K_1 - K_2) \end{cases} \tag{3.12}$$

And constants are found to be:

$$\begin{cases} K_1 = \frac{1}{2}(I_R + \frac{V_S}{Z_o}) \\ K_2 = \frac{1}{2}(I_R - \frac{V_S}{Z_o}) \end{cases} \tag{3.13}$$

Upon substitution in (3.10) and (3.11), the general expressions for voltage and current along a long transmission line becomes:

$$V = \frac{V_S + Z_o I_S}{2} e^{\gamma x} + \frac{V_S - Z_o I_S}{2} e^{-\gamma x} \tag{3.14}$$

$$I = \frac{I_S + \frac{V_S}{Z_o}}{2} e^{\gamma x} + \frac{I_S - \frac{V_S}{Z_o}}{2} e^{-\gamma x} \tag{3.15}$$

The equations for voltage and current can be rearranged as follow:

$$V = \frac{e^{\gamma x} + e^{-\gamma x}}{2} V_S + Z_o \frac{e^{\gamma x} - e^{-\gamma x}}{2} I_S \tag{3.16}$$

$$I = \frac{1}{Z_o} \frac{e^{\gamma x} - e^{-\gamma x}}{2} V_S + \frac{e^{\gamma x} + e^{-\gamma x}}{2} I_S \tag{3.17}$$

Recognizing the hyperbolic functions $\sinh(\beta) = \frac{e^{\beta} - e^{-\beta}}{2}$, and $\cosh(\beta) = \frac{e^{\beta} + e^{-\beta}}{2}$, the above equations are written as follows:

$$V = \cosh(\gamma x) V_S + Z_o \sinh(\gamma x) I_S \tag{3.18}$$

$$I = \frac{1}{Z_o} \sinh(\gamma x) V_S + \cosh(\gamma x) I_S \tag{3.19}$$

Rewriting the above equations in matrix form:

$$\begin{bmatrix} V \\ I \end{bmatrix} = \begin{bmatrix} A & B \\ C & D \end{bmatrix} \begin{bmatrix} V_S \\ I_S \end{bmatrix} \tag{3.20}$$

Where A, B, C, and D are:

$$\begin{aligned} A &= \cosh(\gamma x) \\ B &= Z_o \sinh(\gamma x) \\ C &= \frac{\sinh(\gamma x)}{Z_o} \\ D &= \cosh(\gamma x) \end{aligned}$$

Note that $A = D$ and $AD - BC = 1$.

The line's behavior depends on the propagation constant and the characteristic impedance. Since γ is a complex quantity, to the real part is called attenuation constant (α), and is measured in nepers per length unit , and the imaginary part is called phase constant (β), and is measured in radians per length unit. α is related to the change in amplitude of the wave as it moves through the line, while β is related to the phase shifting of the wave as it travels:

$$\gamma = \alpha + j\beta = \sqrt{zy} = \sqrt{(R + j\omega L)(G + j\omega C)} \tag{3.21}$$

For the lossless line case, $R = 0$ and $G = 0$, therefore α which results from the loss, is zero. Then $\beta = \omega\sqrt{LC}$ and the velocity of propagation would be the product

of the length traveled by the wave during one period, and the time it takes to cross it (which is inverse to the frequency):

$$v = \frac{2\pi f}{\beta} = \frac{1}{\sqrt{LC}} \approx \frac{1}{\sqrt{\mu_o \epsilon_o}} \tag{3.22}$$

Since $\mu_o = 4\pi \times 10^{-7}$ and $\epsilon_o = 8.85 \times 10^{-12}$, the velocity of the wave in a lossless line is approximately 3×10^8 m/sec., i.e., the velocity of light (c). In real conditions, the velocity of the wave does not reach the velocity of light but it is always a value close to this.

3.2.2 Short Line Model

As the length of the line decreases, the distance traveled by the wave during one cycle (wavelength), approaches to the total line length, and the time that takes to the wavefront to travel the entire line is reduced. Under these conditions, the line parameters can be treated as lumped parameters, while still maintaining a reasonable accuracy. The series resistance and inductance may be considered as lumped between each line end, and half of the shunt capacitance may be considered to be lumped at each line end. This is referred to as the π model and is shown in Figure 3.4. Z is the total series impedance of the line ($Z = Rl + j\omega Ll$), and Y is the total shunt admittance of the line ($Y = Gl + j\omega Cl$).

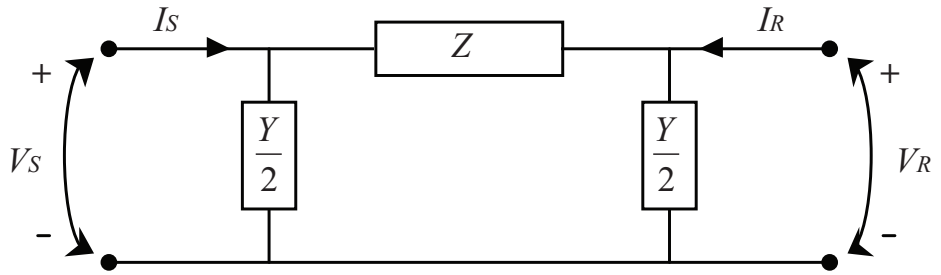

Figure 3.4: π Model for short length lines.

From Figure 3.4 can be found the equations for V_S and I_S as function of V_R and I_R:

$$V_R = (1 + \frac{ZY}{2})V_S + ZI_S \tag{3.23}$$

$$I_R = Y(1 + \frac{ZY}{4})V_S + (1 + \frac{ZY}{2})I_S \tag{3.24}$$

Rewriting the above equations in matrix form, the $ABCD$ constants for the π model are given by:

$$
\begin{aligned}
A &= 1 + \tfrac{ZY}{2} \\
B &= Z \\
C &= Y(1 + \tfrac{ZY}{4}) \\
D &= 1 + \tfrac{ZY}{2}
\end{aligned}
$$

Note that here is also true that $A = D$ and $AD - BC = 1$.

3.3 Time-Domain Model

This section describes general solution methods for finding the time responses of electromagnetic transients in arbitrary single or multiphase networks with lumped and distributed parameters.

The time-domain model most widely used for transient analysis was proposed by Dommel in 1969 [4], and is based in solving equations (3.3) and (3.4) by neglecting the losses and using the method of characteristics.

3.3.1 Bergeron's Model

The method of characteristics is a mathematical method for solving hyperbolic partial differential equations and was originally given by Allievi in 1902 [5], and later developed by Schnyder in 1929[6], Angus in 1935 [7], and Bergeron in 1928 [8], where it was used as a graphical method of calculating transients in penstocks. Bergeron developed a particular proficiency with the graphical method and published a number of articles in the 1930's. His applications range over a wide variety of topics including the propagation of surges on electrical transmission lines. An English translation of his work was published in 1961, and for this reason the model is called the Bergeron's model, but it found application in a power system transients program by Dommel.

It has generally been assumed that the method has application only for lossless transmission systems, this being stated as late as 1967 [9]. All the examples cited above have concerned lossless transmission systems. But Dommel used the method for a losses line, first using a lossless transmission line, and then giving a representation of a lumped losses element in the model.

Equations (3.3) and (3.4) are not directly integrable. Therefore, losses will be neglected at this stage, i.e., $R = 0$ and $G = 0$. Consider a lossless line with inductance L and capacitance C per length unit, then at a point x along the line, voltage and current are related by:

$$\frac{\partial V(x,t)}{\partial x} = -L\frac{\partial I(x,t)}{\partial t} \tag{3.25}$$

$$\frac{\partial I(x,t)}{\partial x} = -C\frac{\partial V(x,t)}{\partial t} \tag{3.26}$$

The method of characteristics to solve these equations is based on a transformation in the $x-t$ plane which accomplishes the conversion of (3.25) and (3.26) into a pair of ordinary differential equations. Each of these two ordinary differential equations holds true along a different family of characteristic curves in the $x-t$ plane, one family corresponds to the forward or incident wave, and the other to the backward or reflected wave. Then, the general solution, first given by d'Alembert[10] is:

$$V(x,t) = Z_o(f_1(x-vt) - f_2(x+vt)) \tag{3.27}$$

$$I(x,t) = f_1(x-vt) + f_2(x+vt) \tag{3.28}$$

with $f_1(x-vt)$ and $f_2(x+vt)$ being arbitrary functions of the variables $(x-vt)$ and $(x+vt)$. The physical interpretation of $f_1(x-vt)$ is a wave traveling at velocity v in a forward direction, and of $f_2(x+vt)$ is a wave traveling in a backward direction. Z_o in (3.27) is the surge impedance ($Z_o = \sqrt{\frac{L}{C}}$), v is the wave's velocity ($v = \frac{1}{\sqrt{LC}}$).

Multiplying (3.28) by Z_o, and adding it to or subtracting it from (3.27) gives:

$$V(x,t) + Z_o I(x,t) = 2Z_o f_1(x-vt) \tag{3.29}$$

$$V(x,t) - Z_o I(x,t) = -2Z_o f_2(x+vt) \tag{3.30}$$

Note that in (3.29) the expression $(V(x,t) + Z_o I(x,t))$ is constant when $(x-vt)$ is constant, and in (3.30) $(V(x,t) - Z_o I(x,t))$ is constant when $(x+vt)$ is constant. The expressions $(x-vt)$=constant and $(x+vt)$=constant are called the characteristics of the differential equations. The significance of (4) may be visualized in the following way: let a fictitious observer travel along the line in a forward direction at velocity v, then $(x-vt)$ and, consequently, $(V(x,t)+Z_o I(x,t))$ along the line will be constant for him. If the travel time to get from one end of the line to the other is $\tau = l/v = l\sqrt{LC}$ (l is the line's length), then the expression $(V(x,t) + Z_o I(x,t))$ encountered by the observer when he leaves node S at time $t-\tau$ must still be the same when he arrives at node R at time t, that is:

$$V_R(t-\tau) + Z_o I_{R,S}(t-\tau) = V_S(t) + Z_o(-I_{S,R}(t)) \tag{3.31}$$

From this equation follows the simple two-port equation for $I_{S,R}$

$$\begin{aligned} I_{S,R}(t) &= \frac{1}{Z_o} V_S(t) + I_S(t-\tau) \\ I_{R,S}(t) &= \frac{1}{Z_o} V_R(t) + I_R(t-\tau) \end{aligned} \tag{3.32}$$

With equivalent current sources I_S and I_R, which are known at state t from the past state at time $t-\tau$,

$$I_S(t-\tau) = -\frac{1}{Z_o}V_R(t-\tau) - I_{R,S}(t-\tau)$$
$$I_R(t-\tau) = -\frac{1}{Z_o}V_S(t-\tau) - I_{S,R}(t-\tau) \tag{3.33}$$

Figure 3.5 shows the corresponding equivalent impedance network, which fully describes the lossless line at its terminals. Topologically, the terminals are not connected; the conditions at the other end are only seen indirectly and with a time delay τ through the equivalent current sources I.

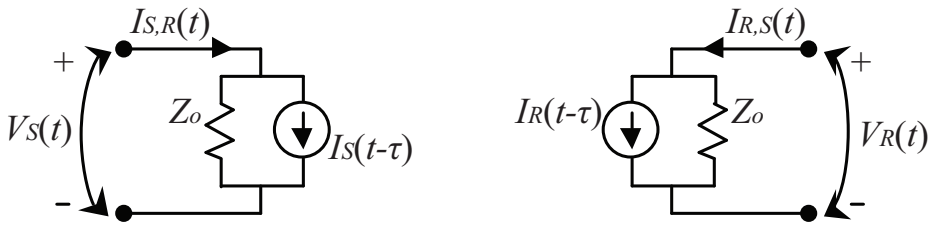

Figure 3.5: Equivalent impedance network for a lossless line.

The simplicity of the method of characteristics rests on the fact that losses are neglected. This simplicity also holds true for the line without distortion, where $R/L = G/C$; the only difference is in computing I_S (and analogous I_R):

$$I_S(t-\tau) = e^{-(\frac{R}{L})\tau}(-\frac{1}{Z_o}V_R(t-\tau) - I_{R,S}(t-\tau)) \tag{3.34}$$

Unfortunately, power lines are not distortionless, since G is usually negligible (or a very complicated function of voltage if the corona effect is to be taken into account).

The distributed series resistance with $G = 0$ can easily be approximated by treating the line as lossless, and adding lumped resistances at both ends. Such lumped resistances can be inserted in many places along the line when the total length is divided into many line sections. In its present form, resistance was lumped as $R_T/4$ at both ends, and $R_T/2$ at the middle of the line (R_T is the total series resistance); under these assumptions the equivalent impedance network of Figure 3.5 is still valid and only the values change (I_S analogous to I_R):

$$I_S(t-\tau) = (\frac{1+h}{2})(-\frac{1}{Z_o}V_R(t-\tau) - I_{R,S}(t-\tau)) + (\frac{1+h}{2})(-\frac{1}{Z_o}V_S(t-\tau) - I_{S,R}(t-\tau)) \tag{3.35}$$

With $h = (Z_o - \frac{R_T}{4})/(Z_o + \frac{R_T}{4})$

From equations 3.34 and 3.35 is possible to find a general solution for current at any point of the line (x), and at any time (t), but remembering that τ is not for the entire line, i.e., $\tau = x/v$, and also that $e^{-(\frac{R}{L})\tau} \approx 1 - \frac{Rx}{Z_o} + \frac{1}{2}(\frac{Rx}{Z_o})^2$, then the current is:

$$I(x,t) = (Z_o + \frac{Rx}{4})(V_S(t - x/v) + (Z_o + \frac{Rx}{4})I_S(t - x/v)) - (Z_o - \frac{Rx}{4}) \cdot (V_S(t + x/v) - (Z_o - \frac{Rx}{4})I_S(t + x/v)) + \frac{Rx}{2(1 + \frac{Rx}{4Z_o})^2}(V_S(t) - \frac{Rx}{4}I_S(t)) \tag{3.36}$$

The same deduction can be applied to find an equation for the voltage at any point of the line (x), and at any time (t):

$$\begin{aligned} V(x,t) = & \frac{1}{2}(\frac{Z_o - \frac{Rx}{4}}{Z_o})^2(V_S(t - x/v) + (Z_o - \frac{Rx}{4})I_S(t - x/v)) \\ & + \frac{1}{2}(\frac{Z_o + \frac{Rx}{4}}{Z_o})^2(V_S(t + x/v) - (Z_o + \frac{Rx}{4})I_S(t + x/v)) \\ & - (\frac{Rx}{4Z_o})^2 V_S(t) - \frac{Rx}{4}(\frac{Z_o + \frac{Rx}{4}}{Z_o})(\frac{Z_o - \frac{Rx}{4}}{Z_o})I_S(t) \end{aligned} \tag{3.37}$$

which reduces the equations for the case of a lossless line, where $R = 0$ and $G = 0$, thus the equation can be integrated directly. Then lumped resistance is added in order to compensate the attenuation effect produced by losses.

3.3.2 Other Approximations

Directly in time-domain some solutions have been developed, reducing the generality of the specifications, i.e., assuming that some parameters R, L, G, and C are small enough to be negligible. This simplifies (3.3) and (3.4), and solutions for certain border conditions can be found. These reductions represent specific applications of the transmission line.

One of these approximations is $L = 0$ and $G = 0$ to describe underground cables. This type of approach is widely used to model systems of low frequency or DC [11]. Another solution is given in [9] which reduces the equations for the case of a lossless line, where $R = 0$ and $G = 0$, thus the equation can be integrated directly. The solution provides a useful model in time-domain, but is limited to short lines or short segments of long lines that can be approximated to models with small loss. Other solution is based on starting with the frequency-domain model to see the effect that different frequencies have in the line parameters and transfer it to time-domain doing some approximations [12, 13]. This approach results in a time-domain model equivalent to [9] but that can be used for studies that require frequencies other than the fundamental to be represented.

Works for transmission line modeling in time-domain that do not apply simplifications to (3.3) and (3.4) have also been proposed, in order to find a direct solution to the problem. These works propose the use of different numerical methods for

solving the differential equation. Like using π-circuits [14], the modal method [15], the finite difference method (FDTD) [16], the finite element method [17], the time-step integration method [18] and others. All these works bring useful transmission lines models, but all these resolution methods require, in a greater or lesser extent, numerical approximations for solving the differential equation. This compromises in one way or another, the ability of models to accurately describe the transmission lines behavior.

Other methods for transmission lines modeling based on traveling wave theory have been proposed, as in [19] who describes a model which is an extension of the Lattice diagram solution widely used for graphical solution of simple distributed-constant networks. In this method, the voltage and current signals are calculated as the sum of the different incident and reflected waves in each point of the line, and which are obtained with the wave's velocity (v_t) and the reflection's coefficient (Γ).

Finite difference approximations to derivatives or integrals lead to formulas from which accurate solutions are possible, but from which exact solutions can never be obtained. Consequently, for this case they have little to offer in comparison with the three previous solution techniques. They are however finding application in the general lossy transmission line case, particularly for multiple circuit transmission lines.

Multiple circuit transmission lines can be handled as for steady state sinusoidal frequencies. Modal components are mostly used. For each frequency is carried out the transformation to modal components, the component solutions, and the inverse transformation . Unfortunately the transformation to modal components is usually frequency dependent. Consequently, a different transformation must be found for each component's frequency. A few combinations of line parameters enable transformations to be found that are frequency invariant.

3.4 Final Remarks

One feature revealed by this section is the abundance of simple and exact techniques available for solution of the lossless transmission problem. Another feature revealed by this section is the lack of any simple technique to handle the general lossy transmission problem. For this problem, solution in the frequency-domain requires numerical inverse transformation and sometimes numerical forward transformation. Solution in the time-domain requires calculation at many points. Both frequency and time-domain solutions can require the storage of large amounts of information and neither yield an exact solution. Thus, it's common to use a lossless transmission line representation to reduce to workable proportions the complexity of problems involving traveling waves in power systems. Since power system transmission lines belong to the general lossy category, this represents a fairly rough approximation, and as power system voltage levels has increased, a need for more accurate representation has become apparent.

Typically transient, like power system's faults, involves non-linear circuit elements, changing system topology, and discontinuous signals. These are inherently more easily

handled by time-domain formulations. Frequency-domain methods are more suited to the solution of linear problems. Problems where non-linearities can be considered to be composed of discontinuous linear segments can be solved using frequency-domain methods, but at the expense of increased computational effort.

Time-domain methods of solution fall into two categories. In the first, voltage and current increments are propagated throughout the system, these are the superposition-based techniques (Lattice method). In the second, actual system voltages and currents are used directly (Bergeron's model).

The Bergeron's Model is the most simple time-domain model and is used as a foundation for the most widely used models in power systems simulations. For more than 40 years, Bergeron's Model has provided a widely accepted solution for line modeling. But in the last 40 years, electrical systems have changed greatly. The markets aperture and the introduction of renewable energy, have led systems to operate at the limit of safety. Under these conditions, it is increasingly important the accurate prediction of the system's behavior. This justifies the search of more accurate line models. This approach will be further investigated in Chapter 4, in an attempt to find a accurate representation of a lossy transmission line in order to implement it in a impedance-based fault location method.

Bibliography Chapter 3

[1] A. Ametani, "The history of transient analysis and the recent trend," *IEEJ Transactions on Electrical and Electronic Engineering*, vol. 2, no. 5, pp. 497–503, 2007.

[2] W. Thomson (Lord Kelvin), "On the theory of the electric telegraph," *Mathematical and Physical Papers, Cambridge Unv. Press*, vol. 2, pp. 61–76, 1884.

[3] O. Heaviside, "General solution of maxwell's electromagnetic equations in a homogeneous isotropic medium, especially in regard to the derivation of special solutions and the formulae for plane waves," *Philosophical Magazine and Journal of Science*, vol. 27, no. 164, p. 20, 1889.

[4] H. W. Dommel, "Digital computer solution of electromagnetic transients in single-and multiphase networks," *IEEE Transactions on Power Apparatus and Systems*, vol. PAS-88, no. 4, pp. 388–399, 1969.

[5] Allievi, "Teoria generale del moto perturbato dell acqua nei tubi in pressione," *Annali della Societá degli Ingegneri ed Architette Italiani*, 1902.

[6] S. Schelkunoff, "Druckstösse in pumpensteigleitungen," *Schweiz Bauzig*, vol. 94, pp. 271–273 and 283–286, 1929.

[7] W. Angus, "Simple graphical solution for pressure risc in pipes and pump discharge lines," *Journal of Eng. Institute of Canada*, vol. 18, pp. 72–81, 1935.

[8] L. Bergeron, *Water Hammer in Hydraulics and Wave Surges in Electricity*. New York: Wiley, 1961.

[9] F. J. Branin, "Transient analysis of lossless transmission lines," *Proceedings of the IEEE*, vol. 55, no. 11, pp. 2012–2013, 1967.

[10] J. d'Alembert, "Recherches sur la courbe que forme une corde tenduë mise en vibration," *Histoire de l'académie royale des sciences et belles lettres de Berlin*, vol. 3, pp. 214–249, 1747.

[11] A. Heaton and A. Issa, "Transient response of crossbonded cable systems," *Proceedings of the Institution of Electrical Engineers*, vol. 117, no. 3, pp. 578–586, 1970.

[12] J. Marti, "Accuarte modelling of frequency-dependent transmission lines in electromagnetic transient simulations," *IEEE Transactions on Power Apparatus and Systems*, vol. PAS-101, no. 1, pp. 147–157, 1982.

[13] J. Marti, L. Marti, and H. W. Dommel, "Transmission line models for steady-state and transients analysis," in *Joint International Power Conference Athens Power Tech*, vol. 2, pp. 744–750, 1993.

[14] H. W. Dommel, *EMTP Theory Book*. Vancouver, Canada: Microtran Power System Analysis Corporation, 2th ed., 1992.

[15] J. Faria, "A new generalized modal analysis theory for nonuniform multiconductor transmission lines," *IEEE Transactions on Power Systems*, vol. 19, no. 2, pp. 926–933, 2004.

[16] P. Trakadas and C. Capsalis, "Validation of a modified FDTD method on nonuniform transmission lines," *Progress In Electromagnetics Research*, no. PIER 31, pp. 311–329, 2001.

[17] R. Lucic, I. Juric-Grgic, and V. Jovic, "FEM analysis of electromagnetic transients in linear networks," *European Transactions on Electrical Power*, vol. 19, no. 6, pp. 890–897, 2009.

[18] M. Tang and J. Mao, "Transient analysis of lossy nonuniform transmission lines using a time-step integration method," *Progress In Electromagnetics Research*, vol. 69, pp. 257–266, 2007.

[19] L. Barthold and G. Carter, "Digital traveling-wave solutions i-single-phase equivalents," *Power Apparatus and Systems, Part III. Transactions of the American Institute of Electrical Engineers*, vol. 80, no. 3, pp. 812–818, 1961.

Chapter 4

Proposal for Impedance-Based Fault Location for HVDC

All currently available commercial equipment to locate faults in HVDC lines use methods based on traveling wave[1]. In general, these methods are based on calculating the time that takes an electromagnetic pulse to travel through the line under investigation.

Most accurate methods use special equipment installed on one end of the line and send an electromagnetic pulse. This pulse travels without interruption throughout the line until it reaches the location where the fault is reflected, and then returns to the starting point. Knowing the time that takes the pulse to make the entire route and its speed, is easy to calculate the distance traveled finding the location of the fault. These methods require that the line is de-energized and only apply to permanent failures, and they require personnel and equipment in the field.

Other methods of easier application, use for the analysis the data obtained during the occurrence of the fault. When a fault starts, it generates pulses that travel throughout the line, these pulses are recorded by measuring devices located on both ends of the line. The CT's and VT's of a HVDC system are usually installed behind an harmonic filtering circuit and their outputs can't be used to detect traveling waves from the line. The transient voltage must be acquired by measuring the transient current through the earth wire of the surge using a coupling capacitor and an external transformer.

The records can be decomposed into its waves with different frequencies to find the high frequency wave generated by the fault. With this information, and knowing the velocity of the wave, it's possible to calculate the fault's location[2]. These methods are faster and simpler to implement than those that require personnel and special equipment in the field. It can also be used with the line energized and in the analysis of transitory faults. But the great weakness of these methods is that not all faults produce pulses easily identifiable in the records. If the pulse produced by the fault

[1]The main manufacturers of these equipments are Manitoba HVDC Centre (https://hvdc.ca/), and ABB (www.abb.com/)

[2]This issue was addressed in more detail in Section 2.3

cannot be identified, then is not possible to perform the location.

The impedance-based fault location methods constitute the class most commonly used for AC systems due to its simplicity and low cost. Although designed for AC lines, these methods can also be applied to locate faults on DC lines, since there is no essential difference in line primary parameters between AC and DC lines. But AC lines models used in these methods are function of the system's frequency, so they cannot be applied directly as HVDC lines models because DC lines don't have a fundamental frequency. The main problem in this formulation is to find a model that fulfills the functions of the traditional frequency-domain line models, but in the time-domain, in order to adapt it to an impedance-based fault locator.

The few available literature about its application in HVDC lines shows it has not been sufficiently studied because of difficulties in the implementation of the DC line models that are necessary for this methodology. Although there is not a commercially available HVDC impedance-based fault locator, one work has been done to adapt this technology to use in HVDC [1]. Nevertheless, this work is based on the Bergeron's time-domain model, which is a simple fundamental-frequency model that uses lumped parameters and its accuracy decreases as the line's length increases[3].

This work proposes the implementation of an impedance-based method for locating faults in two-terminal HVDC for both overhead line and underground cables. This method aims to bring improvements in this area in three main aspects: accuracy, location of high impedance faults, and faults in shorts HVDC.

As mentioned before, traveling wave-based methods have problems detecting high impedance faults since it doesn't generate a large wavefront. But impedance-based methods are not affected by this problem. These types of faults are more common in overhead lines. On the other hand, almost 50% of the world's HVDC cables have a length of 100 km or less[2], making difficult the use of traveling wave-based methods. Since the line model can be applied to both overhead and cables, they could also be used in fault location in short HVDC cables.

The fault location method developed in here is based on analysis of voltage and current signals from fault records viewed from both line-ends. To ensure that the comparison is made between data obtained simultaneously at both ends, synchronized data is used. The signal synchronization may be done by GPS. Since the fault location is an after fault analysis, a dedicated communication channel is not required.

In order to describe the line's behavior with accuracy, a time-domain line model is required.

[3]This model was addressed in more detail in Section 3.3.1

4.1 Time-Domain Distributed Parameters Transmission Line Model

The classical approach to transmission line analysis considers the transmission phenomena to be completely determined by the self and mutual series impedances, and the self and mutual shunt admittances of the conductors. As a consequence, the phenomena are completely specified in terms of the propagation constants and the corresponding characteristic impedances of the possible modes of propagation.

Although simple and of great value, the above approach is not exact. To obtain an accurate solution it would be necessary to begin with Maxwell's equations, and take into account such things as electromagnetic radiation, proximity effects, terminal conditions, and skin effects. However, an analysis of the approximations involved done by Carson [3] shows that although the complete specification of a transmission system in terms of its self and mutual impedances is rigorously valid, only for the case of perfect conductors embedded in a perfect dielectric, the errors introduced are of small practical significance provided that the resistivity of the conductors is much smaller than that of their surrounding dielectric, and the distances between the conductors is large compared to their radio. Most systems that could be used for the efficient transmission of electrical energy would satisfy these requirements. In such cases, it is possible to specify the system of conductors in terms of its self and mutual line parameters to a high degree of approximation.

The partial differential equations resulting from the above considerations were presented in Chapter 3, and are known as the telegraph equations.

$$\frac{\partial V(x,t)}{\partial x} = -RI(x,t) - L\frac{\partial I(x,t)}{\partial t} \tag{4.1}$$

$$\frac{\partial I(x,t)}{\partial x} = -GV(x,t) - C\frac{\partial V(x,t)}{\partial t} \tag{4.2}$$

The telegraph equations have been the object of much study in the past, and continue to be so. They will be used as the starting point of, and will form the basis of, the linear transmission line analysis that follows [4].

4.1.1 Line Model Deduction

Usually, the first step to try to solve these equation systems is by removing one variable. To solve (4.1), and (4.2), is required to apply partial differential, with respect to t on (4.1), and with respect to x on (4.2):

$$\frac{\partial^2 V}{\partial t \partial x} = -R\frac{\partial I}{\partial t} - L\frac{\partial^2 I}{\partial t^2} \tag{4.3}$$

$$\frac{\partial^2 I}{\partial x^2} = -G\frac{\partial V}{\partial x} - C\frac{\partial^2 V}{\partial t \partial x} \tag{4.4}$$

and substituting (4.1) and (4.3) in (4.4), a differential equation for I is obtained.

$$LC\frac{\partial^2 I}{\partial t^2} + (RC + LG)\frac{\partial I}{\partial t} + RGI - \frac{\partial^2 I}{\partial x^2} = 0 \tag{4.5}$$

In the same manner, a differential equation for V is obtained.

These equations are a complete description of the possible interrelationships between voltage and current, and its derivatives at any time (t) and at any point in the line(x).

Equation (4.5) is a second order linear partial differential equation with a coordinate of space and other of time, making it difficult to obtain a complete solution for them in terms of V and I as functions of x and t. To find an accurate solution to this equation is the main problem of transmission line modeling.

The presented solution begins by dividing the partial differential equation of (4.5) into two equations: one in time-domain, and the other in space-domain. Then, the general solutions of each one compensate each other, in order to describe the complete behavior of the line. Therefore, the general solution for (4.5) is given by the general solutions of its components in time and space, as shown in the auxiliary equations:

Time-domain:

$$LCS_t^2 + (RC + LG)S_t = 0 \begin{cases} S_{t1} = 0 \\ S_{t2} = -(\frac{R}{L} + \frac{G}{C}) \end{cases} \tag{4.6}$$

Space domain:

$$-S_x^2 + RG = 0 \begin{cases} S_{x1} = \sqrt{RG} \\ S_{x2} = -\sqrt{RG} \end{cases} \tag{4.7}$$

The general solution of the entire equation is:

$$I = K_a e^{-\left[(\frac{R}{L}+\frac{G}{C})t+\sqrt{RG}x\right]} + K_b e^{-\left[(\frac{R}{L}+\frac{G}{C})t-\sqrt{RG}x\right]} + K_c e^{\sqrt{RG}x} + K_d e^{-\sqrt{RG}x} \tag{4.8}$$

This deduction does not use approximations to solve the differential equations, instead a different approach is used where a relative weight of importance is given to t and x in the partial derivatives, then each variable is solved separately as a first-order differential equation.

Now, (4.8) is differentiated with respect to t in order to obtain the general solution for V, and substituting in (4.1), is obtained a differential equation for V as function of x and t :

$$\begin{aligned} \frac{\partial V}{\partial x} = \; & \tfrac{LG}{C} K_a e^{-\left[(\frac{R}{L}+\frac{G}{C})t+\sqrt{RG}x\right]} + \tfrac{LG}{C} K_b e^{-\left[(\frac{R}{L}+\frac{G}{C})t-\sqrt{RG}x\right]} \\ & -RK_c e^{\sqrt{RG}x} - RK_d e^{-\sqrt{RG}x} \end{aligned} \tag{4.9}$$

If (4.9) is integrated to find the expression for V. Then, the general solution for V is obtained:

$$\begin{aligned} V = \; & -\tfrac{L}{C}\sqrt{\tfrac{G}{R}}K_a e^{-\left[(\frac{R}{L}+\frac{G}{C})t+\sqrt{RG}x\right]} + \tfrac{L}{C}\sqrt{\tfrac{G}{R}}K_b e^{-\left[(\frac{R}{L}+\frac{G}{C})t-\sqrt{RG}x\right]} \\ & -\sqrt{\tfrac{R}{G}}K_c e^{\sqrt{RG}x} + \sqrt{\tfrac{R}{G}}K_d e^{-\sqrt{RG}x} \end{aligned} \tag{4.10}$$

4.1.1.1 Boundary Conditions

Values for K_a, K_b, K_c and K_d can be determined, establishing boundary conditions at one line end, e.g., the voltage V_1 and current I_1 when $x = 0$ and $t = t_1$, and V_2 and I_2 when $x = 0$ and $t = t_2$.

$$\begin{aligned} I_1 &= (K_a + K_b)e^{-(\frac{R}{L}+\frac{G}{C})t_1} + K_c + K_d \\ V_1 &= \frac{L}{C}\sqrt{\frac{G}{R}}(-K_a + K_b)e^{-(\frac{R}{L}+\frac{G}{C})t_1} + \sqrt{\frac{R}{G}}(-K_c + K_d) \\ I_2 &= (K_a + K_b)e^{-(\frac{R}{L}+\frac{G}{C})t_2} + K_c + K_d \\ V_2 &= \frac{L}{C}\sqrt{\frac{G}{R}}(-K_a + K_b)e^{-(\frac{R}{L}+\frac{G}{C})t_2} + \sqrt{\frac{R}{G}}(-K_c + K_d) \end{aligned} \tag{4.11}$$

With this four equations system, the expressions for K_a, K_b, K_c, and K_d are obtained:

$$\begin{aligned} K_a = \; & \tfrac{1}{2}\left[(I_2 - I_1) - \tfrac{(V_2-V_1)}{\frac{L}{C}\sqrt{\frac{G}{R}}}\right]\tfrac{1}{e^{-(\frac{R}{L}+\frac{G}{C})t_2} - e^{-(\frac{R}{L}+\frac{G}{C})t_1}} \\ K_b = \; & \tfrac{1}{2}\left[(I_2 - I_1) + \tfrac{(V_2-V_1)}{\frac{L}{C}\sqrt{\frac{G}{R}}}\right]\tfrac{1}{e^{-(\frac{R}{L}+\frac{G}{C})t_2} - e^{-(\frac{R}{L}+\frac{G}{C})t_1}} \\ K_c = \; & \tfrac{1}{2}\left[I_2 e^{-(\frac{R}{L}+\frac{G}{C})t_1} - I_1 e^{-(\frac{R}{L}+\frac{G}{C})t_2}\right. \\ & \left. - \tfrac{V_2 e^{-(\frac{R}{L}+\frac{G}{C})t_1} - V_1 e^{-(\frac{R}{L}+\frac{G}{C})t_2}}{\sqrt{\frac{R}{G}}}\right]\tfrac{1}{e^{-(\frac{R}{L}+\frac{G}{C})t_2} - e^{-(\frac{R}{L}+\frac{G}{C})t_1}} \\ K_d = \; & \tfrac{1}{2}\left[I_2 e^{-(\frac{R}{L}+\frac{G}{C})t_1} - I_1 e^{-(\frac{R}{L}+\frac{G}{C})t_2} + \right. \\ & \left. + \tfrac{V_2 e^{-(\frac{R}{L}+\frac{G}{C})t_1} - V_1 e^{-(\frac{R}{L}+\frac{G}{C})t_2}}{\sqrt{\frac{R}{G}}}\right]\tfrac{1}{e^{-(\frac{R}{L}+\frac{G}{C})t_2} - e^{-(\frac{R}{L}+\frac{G}{C})t_1}} \end{aligned} \tag{4.12}$$

Substituting these values in (4.8) and (4.10), the expressions for current I and voltage V at any time t and place x of the line are obtained.

$$
\begin{aligned}
V = \quad & V_2 \left[\frac{e^{-(\frac{R}{L}+\frac{G}{C})t} - e^{-(\frac{R}{L}+\frac{G}{C})t_1}}{e^{-(\frac{R}{L}+\frac{G}{C})t_2} - e^{-(\frac{R}{L}+\frac{G}{C})t_1}} \frac{e^{\sqrt{RG}x} + e^{-\sqrt{RG}x}}{2} \right] \\
& - V_1 \left[\frac{e^{-(\frac{R}{L}+\frac{G}{C})t} - e^{-(\frac{R}{L}+\frac{G}{C})t_2}}{e^{-(\frac{R}{L}+\frac{G}{C})t_2} - e^{-(\frac{R}{L}+\frac{G}{C})t_1}} \frac{e^{\sqrt{RG}x} + e^{-\sqrt{RG}x}}{2} \right] \\
& + I_2 \sqrt{\frac{R}{G}} \left[\frac{\frac{LG}{RC} e^{-(\frac{R}{L}+\frac{G}{C})t} + e^{-(\frac{R}{L}+\frac{G}{C})t_1}}{e^{-(\frac{R}{L}+\frac{G}{C})t_2} - e^{-(\frac{R}{L}+\frac{G}{C})t_1}} \frac{e^{\sqrt{RG}x} - e^{-\sqrt{RG}x}}{2} \right] \\
& - I_1 \sqrt{\frac{R}{G}} \left[\frac{\frac{LG}{RC} e^{-(\frac{R}{L}+\frac{G}{C})t} + e^{-(\frac{R}{L}+\frac{G}{C})t_2}}{e^{-(\frac{R}{L}+\frac{G}{C})t_2} - e^{-(\frac{R}{L}+\frac{G}{C})t_1}} \frac{e^{\sqrt{RG}x} - e^{-\sqrt{RG}x}}{2} \right]
\end{aligned} \tag{4.13}
$$

$$
\begin{aligned}
I = \quad & \frac{V_2}{\sqrt{\frac{R}{G}}} \left[\frac{\frac{RC}{LG} e^{-(\frac{R}{L}+\frac{G}{C})t} + e^{-(\frac{R}{L}+\frac{G}{C})t_1}}{e^{-(\frac{R}{L}+\frac{G}{C})t_2} - e^{-(\frac{R}{L}+\frac{G}{C})t_1}} \frac{e^{\sqrt{RG}x} - e^{-\sqrt{RG}x}}{2} \right] \\
& - \frac{V_1}{\sqrt{\frac{R}{G}}} \left[\frac{\frac{RC}{LG} e^{-(\frac{R}{L}+\frac{G}{C})t} - e^{-(\frac{R}{L}+\frac{G}{C})t_2}}{e^{-(\frac{R}{L}+\frac{G}{C})t_2} - e^{-(\frac{R}{L}+\frac{G}{C})t_1}} \frac{e^{\sqrt{RG}x} - e^{-\sqrt{RG}x}}{2} \right] \\
& + I_2 \left[\frac{e^{-(\frac{R}{L}+\frac{G}{C})t} - e^{-(\frac{R}{L}+\frac{G}{C})t_1}}{e^{-(\frac{R}{L}+\frac{G}{C})t_2} - e^{-(\frac{R}{L}+\frac{G}{C})t_1}} \frac{e^{\sqrt{RG}x} + e^{-\sqrt{RG}x}}{2} \right] \\
& - I_1 \left[\frac{e^{-(\frac{R}{L}+\frac{G}{C})t} - e^{-(\frac{R}{L}+\frac{G}{C})t_2}}{e^{-(\frac{R}{L}+\frac{G}{C})t_2} - e^{-(\frac{R}{L}+\frac{G}{C})t_1}} \frac{e^{\sqrt{RG}x} + e^{-\sqrt{RG}x}}{2} \right]
\end{aligned} \tag{4.14}
$$

From $\sinh(\beta) = \frac{e^{\beta} - e^{-\beta}}{2}$ and $\cosh(\beta) = \frac{e^{\beta} + e^{-\beta}}{2}$. And also, taking a similar definition to propagation coefficient (γ) and characteristic impedance (Z_0) from the frequency-domain model [5, 6]: $\gamma_{RG} = \sqrt{RG}$, $Z_{RG} = \sqrt{\frac{R}{G}}$ and $Z_{LC} = \sqrt{\frac{L}{C}}$, where RG and LC denote the line's parameters that compose them. Then, if the values at the line origins are known, the values for voltage and current at any point of the line are expressed by:

$$
\begin{aligned}
V = \quad & V_1 \frac{e^{-(\frac{R}{L}+\frac{G}{C})t_2} - e^{-(\frac{R}{L}+\frac{G}{C})t}}{e^{-(\frac{R}{L}+\frac{G}{C})t_2} - e^{-(\frac{R}{L}+\frac{G}{C})t_1}} \cosh(x\gamma_{RG}) \\
& - I_1 \frac{e^{-(\frac{R}{L}+\frac{G}{C})t_2} + \frac{LG}{RC} e^{-(\frac{R}{L}+\frac{G}{C})t}}{e^{-(\frac{R}{L}+\frac{G}{C})t_2} - e^{-(\frac{R}{L}+\frac{G}{C})t_1}} Z_{RG} \sinh(x\gamma_{RG}) \\
& - V_2 \frac{e^{-(\frac{R}{L}+\frac{G}{C})t_1} - e^{-(\frac{R}{L}+\frac{G}{C})t}}{e^{-(\frac{R}{L}+\frac{G}{C})t_2} - e^{-(\frac{R}{L}+\frac{G}{C})t_1}} \cosh(x\gamma_{RG}) \\
& + I_2 \frac{e^{-(\frac{R}{L}+\frac{G}{C})t_1} + \frac{LG}{RC} e^{-(\frac{R}{L}+\frac{G}{C})t}}{e^{-(\frac{R}{L}+\frac{G}{C})t_2} - e^{-(\frac{R}{L}+\frac{G}{C})t_1}} Z_{RG} \sinh(x\gamma_{RG})
\end{aligned} \tag{4.15}
$$

$$
\begin{aligned}
I = \quad & -V_1 \frac{e^{-(\frac{R}{L}+\frac{G}{C})t_2} + \frac{RC}{LG} e^{-(\frac{R}{L}+\frac{G}{C})t}}{e^{-(\frac{R}{L}+\frac{G}{C})t_2} - e^{-(\frac{R}{L}+\frac{G}{C})t_1}} \frac{\sinh(x\gamma_{RG})}{Z_{RG}} \\
& + I_1 \frac{e^{-(\frac{R}{L}+\frac{G}{C})t_2} - e^{-(\frac{R}{L}+\frac{G}{C})t}}{e^{-(\frac{R}{L}+\frac{G}{C})t_2} - e^{-(\frac{R}{L}+\frac{G}{C})t_1}} \cosh(x\gamma_{RG}) \\
& + V_2 \frac{e^{-(\frac{R}{L}+\frac{G}{C})t_1} + \frac{RC}{LG} e^{-(\frac{R}{L}+\frac{G}{C})t}}{e^{-(\frac{R}{L}+\frac{G}{C})t_2} - e^{-(\frac{R}{L}+\frac{G}{C})t_1}} \frac{\sinh(x\gamma_{RG})}{Z_{RG}} \\
& - I_2 \frac{e^{-(\frac{R}{L}+\frac{G}{C})t_1} - e^{-(\frac{R}{L}+\frac{G}{C})t}}{e^{-(\frac{R}{L}+\frac{G}{C})t_2} - e^{-(\frac{R}{L}+\frac{G}{C})t_1}} \cosh(x\gamma_{RG})
\end{aligned} \tag{4.16}
$$

The signals V and I in a time t at any point x of the line, are formed by the sum of a series of traveling waves. In this deduction, V_1 and I_1 are the signals measured at time t_1 and V_2, and I_2 are the signals measured at time t_2. t_1 and t_2 are two arbitrary values, but because the model follows the form proposed by d'Alembert [7], the results are actually more precise if $t - t_1 = t_2 - t$, where t is the time where the values of V and I want to be found. The choice of t_1 and t_2 is also related to the distance between the point of measurement, and the point where V and I want to be found. For example, if the values of V and I want to be known in point x of the line shown in Figure 4.1, the result will be more precise if the condition $t - t_1 = t_2 - t = x/v_t$ is met, where v_t is the wave velocity and is $v_t = 1/\sqrt{LC}$.

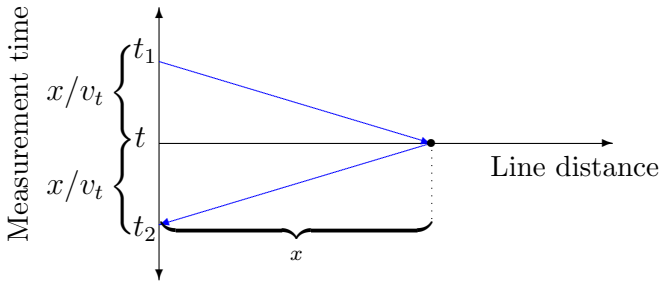

Figure 4.1: Criteria by which t_1 and t_2 were chosen that provide greater accuracy.

The time that is taken by both waves to travel between the sender terminal and the point x are equal, and are expressed by x/v_t. Therefore, the times t_1 and t_2 measured at the sender terminal are related to the travel time, and with t by $t_1 = t - x\sqrt{LC}$, and $t_2 = t + x\sqrt{LC}$. So, substituting these expressions of t_1 and t_2 into (4.15) and (4.16), are obtained:

$$
\begin{aligned}
V = \quad & V_1 \frac{e^{-(\frac{R}{L}+\frac{G}{C})t}(e^{-(\frac{R}{L}+\frac{G}{C})x\sqrt{LC}} - 1)}{e^{-(\frac{R}{L}+\frac{G}{C})t}(e^{-(\frac{R}{L}+\frac{G}{C})x\sqrt{LC}} - e^{(\frac{R}{L}+\frac{G}{C})x\sqrt{LC}})} \cosh(x\gamma_{RG}) \\
& - I_1 \frac{e^{-(\frac{R}{L}+\frac{G}{C})t}(e^{-(\frac{R}{L}+\frac{G}{C})x\sqrt{LC}} + \frac{LG}{RC})}{e^{-(\frac{R}{L}+\frac{G}{C})t}(e^{-(\frac{R}{L}+\frac{G}{C})x\sqrt{LC}} - e^{(\frac{R}{L}+\frac{G}{C})x\sqrt{LC}})} Z_{RG} \sinh(x\gamma_{RG}) \\
& - V_2 \frac{e^{-(\frac{R}{L}+\frac{G}{C})t}(e^{(\frac{R}{L}+\frac{G}{C})x\sqrt{LC}} - 1)}{e^{-(\frac{R}{L}+\frac{G}{C})t}(e^{-(\frac{R}{L}+\frac{G}{C})x\sqrt{LC}} - e^{(\frac{R}{L}+\frac{G}{C})x\sqrt{LC}})} \cosh(x\gamma_{RG}) \\
& + I_2 \frac{e^{-(\frac{R}{L}+\frac{G}{C})t}(e^{(\frac{R}{L}+\frac{G}{C})x\sqrt{LC}} + \frac{LG}{RC})}{e^{-(\frac{R}{L}+\frac{G}{C})t}(e^{-(\frac{R}{L}+\frac{G}{C})x\sqrt{LC}} - e^{(\frac{R}{L}+\frac{G}{C})x\sqrt{LC}})} Z_{RG} \sinh(x\gamma_{RG})
\end{aligned} \tag{4.17}
$$

$$
\begin{aligned}
I = \quad & -V_1 \frac{e^{-(\frac{R}{L}+\frac{G}{C})t}(e^{-(\frac{R}{L}+\frac{G}{C})x\sqrt{LC}}+\frac{RC}{LG})}{e^{-(\frac{R}{L}+\frac{G}{C})t}(e^{-(\frac{R}{L}+\frac{G}{C})x\sqrt{LC}}-e^{(\frac{R}{L}+\frac{G}{C})x\sqrt{LC}})} \frac{\sinh(x\gamma_{RG})}{Z_{RG}} \\
& +I_1 \frac{e^{-(\frac{R}{L}+\frac{G}{C})t}(e^{-(\frac{R}{L}+\frac{G}{C})x\sqrt{LC}}-1)}{e^{-(\frac{R}{L}+\frac{G}{C})t}(e^{-(\frac{R}{L}+\frac{G}{C})x\sqrt{LC}}-e^{(\frac{R}{L}+\frac{G}{C})x\sqrt{LC}})} \cosh(x\gamma_{RG}) \\
& +V_2 \frac{e^{-(\frac{R}{L}+\frac{G}{C})t}(e^{(\frac{R}{L}+\frac{G}{C})x\sqrt{LC}}+\frac{RC}{LG})}{e^{-(\frac{R}{L}+\frac{G}{C})t}(e^{-(\frac{R}{L}+\frac{G}{C})x\sqrt{LC}}-e^{(\frac{R}{L}+\frac{G}{C})x\sqrt{LC}})} \frac{\sinh(x\gamma_{RG})}{Z_{RG}} \\
& -I_2 \frac{e^{-(\frac{R}{L}+\frac{G}{C})t}(e^{(\frac{R}{L}+\frac{G}{C})x\sqrt{LC}}-1)}{e^{-(\frac{R}{L}+\frac{G}{C})t}(e^{-(\frac{R}{L}+\frac{G}{C})x\sqrt{LC}}-e^{(\frac{R}{L}+\frac{G}{C})x\sqrt{LC}})} \cosh(x\gamma_{RG})
\end{aligned} \tag{4.18}
$$

The expression $e^{-(\frac{R}{L}+\frac{G}{C})t}$ is canceled, and the equation's dividend can be expressed as follows:

$$
e^{-(\frac{R}{L}+\frac{G}{C})x\sqrt{LC}} - e^{(\frac{R}{L}+\frac{G}{C})x\sqrt{LC}} = -2\sinh((\frac{R}{Z_{LC}} + GZ_{LC})x)
$$

So, (4.17) and (4.18) are simplified as follows:

$$
\begin{aligned}
V = \quad & -V_1 \frac{e^{-(\frac{R}{Z_{LC}}+GZ_{LC})x}-1}{2\sinh((\frac{R}{Z_{LC}}+GZ_{LC})x)} \cosh(x\gamma_{RG}) \\
& +I_1 \frac{e^{-(\frac{R}{Z_{LC}}+GZ_{LC})x}+\frac{LG}{RC}}{2\sinh((\frac{R}{Z_{LC}}+GZ_{LC})x)} Z_{RG}\sinh(x\gamma_{RG}) \\
& +V_2 \frac{e^{(\frac{R}{Z_{LC}}+GZ_{LC})x}-1}{2\sinh((\frac{R}{Z_{LC}}+GZ_{LC})x)} \cosh(x\gamma_{RG}) \\
& -I_2 \frac{e^{(\frac{R}{Z_{LC}}+GZ_{LC})x}+\frac{LG}{RC}}{2\sinh((\frac{R}{Z_{LC}}+GZ_{LC})x)} Z_{RG}\sinh(x\gamma_{RG})
\end{aligned} \tag{4.19}
$$

$$
\begin{aligned}
I = \quad & V_1 \frac{e^{-(\frac{R}{Z_{LC}}+GZ_{LC})x}+\frac{RC}{LG}}{2\sinh((\frac{R}{Z_{LC}}+GZ_{LC})x)} \frac{\sinh(x\gamma_{RG})}{Z_{RG}} \\
& -I_1 \frac{e^{-(\frac{R}{Z_{LC}}+GZ_{LC})x}-1}{2\sinh((\frac{R}{Z_{LC}}+GZ_{LC})x)} \cosh(x\gamma_{RG}) \\
& -V_2 \frac{e^{(\frac{R}{Z_{LC}}+GZ_{LC})x}+\frac{RC}{LG}}{2\sinh((\frac{R}{Z_{LC}}+GZ_{LC})x)} \frac{\sinh(x\gamma_{RG})}{Z_{RG}} \\
& +I_2 \frac{e^{(\frac{R}{Z_{LC}}+GZ_{LC})x}-1}{2\sinh((\frac{R}{Z_{LC}}+GZ_{LC})x)} \cosh(x\gamma_{RG})
\end{aligned} \tag{4.20}
$$

Finally, the solutions in (4.19) and (4.20) can be expressed in matrix form:

$$
\begin{bmatrix} V \\ I \end{bmatrix} = \left[\begin{array}{cc:cc} A_1 & B_1 & A_2 & B_2 \\ C_1 & D_1 & C_2 & D_2 \end{array}\right] \begin{bmatrix} V_1 \\ I_1 \\ V_2 \\ I_2 \end{bmatrix} \tag{4.21}
$$

Where A_1, B_1, C_1, D_1, A_2, B_2, C_2, and D_2 are:

$$A_1 = -\frac{e^{-(\frac{R}{Z_{LC}}+GZ_{LC})x}-1}{2\sinh((\frac{R}{Z_{LC}}+GZ_{LC})x)}\cosh(x\gamma_{RG})$$

$$B_1 = \frac{e^{-(\frac{R}{Z_{LC}}+GZ_{LC})x}+\frac{LG}{RC}}{2\sinh((\frac{R}{Z_{LC}}+GZ_{LC})x)}Z_{RG}\sinh(x\gamma_{RG})$$

$$C_1 = \frac{e^{-(\frac{R}{Z_{LC}}+GZ_{LC})x}+\frac{RC}{LG}}{2\sinh((\frac{R}{Z_{LC}}+GZ_{LC})x)}\frac{\sinh(x\gamma_{RG})}{Z_{RG}}$$

$$D_1 = -\frac{e^{-(\frac{R}{Z_{LC}}+GZ_{LC})x}-1}{2\sinh((\frac{R}{Z_{LC}}+GZ_{LC})x)}\cosh(x\gamma_{RG})$$

$$A_2 = \frac{e^{(\frac{R}{Z_{LC}}+GZ_{LC})x}-1}{2\sinh((\frac{R}{Z_{LC}}+GZ_{LC})x)}\cosh(x\gamma_{RG})$$

$$B_2 = -\frac{e^{(\frac{R}{Z_{LC}}+GZ_{LC})x}+\frac{LG}{RC}}{2\sinh((\frac{R}{Z_{LC}}+GZ_{LC})x)}Z_{RG}\sinh(x\gamma_{RG})$$

$$C_2 = -\frac{e^{(\frac{R}{Z_{LC}}+GZ_{LC})x}+\frac{RC}{LG}}{2\sinh((\frac{R}{Z_{LC}}+GZ_{LC})x)}\frac{\sinh(x\gamma_{RG})}{Z_{RG}}$$

$$D_2 = \frac{e^{(\frac{R}{Z_{LC}}+GZ_{LC})x}-1}{2\sinh((\frac{R}{Z_{LC}}+GZ_{LC})x)}\cosh(x\gamma_{RG})$$

4.1.1.2 Model Analysis

As (4.21) shows, the results for (4.1) and (4.2) have the form $f(x,t) = f_1(x,t_1) + f_2(x,t_2)$ which are exactly the results predicted by d'Alembert's method [7], who first provides a solution to the wave propagation, and then was applied for transient phenomena transmission line analysis [8–11].

At first glance, it seems that the elements A_1, B_1, C_1, D_1, A_2, B_2, C_2, and D_2 are not time-dependent because of the canceling of $e^{-(\frac{R}{L}+\frac{G}{C})t}$ in (4.17), and (4.18). But is necessary to remember that $x\sqrt{LC}$ is a time measurement and describes the time that takes the waves to travel from one terminal to the point x throughout the line.

The model deduced here has a structure similar to other well known time-domain models, such as the Bergeron's model, but in a more complex way that provides greater accuracy. This is because approximations are not used to solve differential equations.

In this model there are also factors similar to the propagation coefficient and characteristic impedance that are equivalent terms to the model in the frequency-domain [5, 6]. In the frequency-domain exists only one expression for the characteristic impedance because the frequency-domain provides the way to encompass the various

line parameters as one impedance or admittance. But in this time-domain model are two characteristic impedances because the primary parameters come from different physical properties of the line. Since R and G describe the energy dissipation or line losses, they are included in a characteristic impedance, while L and C describe the storage of energy in the fields around the line, they are encompassed by a second characteristic impedance.

Other line models entirely deduced from time-domain, have also one of these two characteristic impedances, but no previous model has both terms. The presence of one or other characteristic impedance depends on the type of simplification used in the deduction of each different model. This model is able to take into account the full range of characteristic impedances and propagation coefficient, since Z_{LC}, Z_{RG}, and γ_{RG} are not approximated values of characteristic impedances and propagation coefficient in frequency-domain, instead, they are time-domain decoupled representations of the characteristic impedances and propagation coefficient in frequency-domain.

In order to illustrate the previous idea, the particular case of DC systems can be analyzed using (4.21). Thus, the terms where Z_{LC} appears tend to decrease for long time intervals since it exists a limit to the energy stored in the fields of the line. Also, as the line losses are always present, the terms where Z_{RG} appears do not decrease over time. This condition would be maintained as long as the voltages and currents do not vary. When variations occur in the system, the energy stored in the fields also changes, and the terms related to Z_{LC} reappear, until the system is stabilized again in another operational point. Thus, the terms where Z_{LC} appears can be associated with states where there are variations of voltage and current, while the terms where Z_{RG} appears can be associated with the states where the voltage and current are constant. Take as example the case of a steady-state line:

If steady-state phenomena are analyzed, some simplifications can be applied to the model, that is, when $t \to \infty$, then $V_1 \approx V_2$, and $I_1 \approx I_2$, therefore the matrix factors of (4.21) become:

$$A_1 + A_2 = \cosh(x\gamma_{RG}); \quad B_1 + B_2 = -Z_{RG}\sinh(x\gamma_{RG});$$
$$C_1 + C_2 = -\frac{\sinh(x\gamma_{RG})}{Z_{RG}}; \qquad D_1 + D_2 = \cosh(x\gamma_{RG})$$

And (4.21) is simplified to:

$$\begin{bmatrix} V \\ I \end{bmatrix} = \begin{bmatrix} \cosh(x\gamma_{RG}) & -Z_{RG}\sinh(x\gamma_{RG}) \\ -\frac{\sinh(x\gamma_{RG})}{Z_{RG}} & \cosh(x\gamma_{RG}) \end{bmatrix} \begin{bmatrix} V_1 \\ I_1 \end{bmatrix} \tag{4.22}$$

Which is the typical transmission line model with distributed parameters presented in section 3.2.1 [5, 6]. Note that for this particular case, $\gamma_{RG} = \sqrt{RG}$ and $Z_{RG} = \sqrt{R/G}$, so the frequency system is $\omega = 0$ which is an analysis for DC lines, and is consistent with the statement of section 4.1.1.2 concerning to the model's application in low frequency conditions. It's important to take into account that the term "steady-state", with conditions $V_1 \approx V_2$, and $I_1 \approx I_2$ applies only to DC systems; for AC

systems the instantaneous values of voltages and currents are not equal over time. In AC systems "steady-state" refers to the voltage and current phasors when they are stable over time, and not their instantaneous values.

Also, if this steady-state approximation is applied to the Bergeron's model derived in [8, 10], the result is:

$$\begin{bmatrix} V \\ I \end{bmatrix} = \begin{bmatrix} 1 & -xR \\ 0 & 1 \end{bmatrix} \begin{bmatrix} V_1 \\ I_1 \end{bmatrix} \tag{4.23}$$

Which is a simple model for short DC lines for steady-state approximation, but that is not used for long transmission lines.

The following sections will be dedicated to a more detailed analysis of the model in order to validate its behavior.

4.1.2 Illustrative Examples

In this section, actual transient-state records in COMTRADE format of different transmission lines will be analyzed with the model deduced here in order to validate the model's behavior. The results will be compared to the Bergeron's model which is the line model most widely used. Tests with records of AC and DC systems were carried out in order to show that the model is applicable to different types of lines.

The tests consist in taking the voltage and current from transient event records of the sender line-end, and with this information, try to predict the events at the receiver end. This is done with the model deduced here and with the Bergeron's model. Then, the results are compared with actual records of the receiver end in order to show which of the two models can predict more accurately the actual behavior of the lines.

4.1.2.1 AC Line Tests

In order to use actual transient event records in COMTRADE format, two faults in AC lines were selected for this test. One fault in a long 765 kV line with 153 km, and another fault in a short 230 kV line with 44 km. The faults are single-phase and they occur outside the lines analyzed, i.e., faults occurred on the receiver end of parallel lines, so they are not fault records but contribution records to an external fault. The reason for selecting these records is to avoid the change in power flow that occurs in the receiver end. If the fault was within the line, this flow change would prevent the calculation of receiver end signals during the fault, and could not observe the model's accuracy during different system conditions (pre-fault, fault, and post-fault). For AC systems testing, the signals instantaneous values were used.

There are some circumstances that have not been taken into account that could affect the model's accuracy during real faults analysis of an AC system. One is that the most common problems in real faults analysis are possible inaccuracies in the line's parameters. In this test, any problems of this type would affect in the same way

both models, and would not affect the final results because this test seeks to compare these results to each other.

On the other hand, the model deduced here is based on a single-phase line, while AC systems are triphasic, and there are mutual effects from other phases; this problem is corrected using decoupled parameters, in other words, in order to implement this model in three-phase systems, the phase domain signals are first decomposed into their modal components [12]. In this study, all line models are assumed to be fully transposed, so a transformation matrix is used accordingly.

$$S_{mode} = \frac{1}{3}\begin{bmatrix} 1 & 1 & 1 \\ 2 & -1 & -1 \\ 0 & \sqrt{3} & -\sqrt{3} \end{bmatrix} S_{phase} \tag{4.24}$$

Where S_{phase}, and S_{mode} are the phase signal and mode signal components, respectively. Simulated records phase signals are first transformed into their modal components and the mode 2 is taken for analysis. The second mode (mode 2), also known as the aerial mode, is the most common mode used in this type of analysis since is present for any kind of fault.

Tables 4.1 and 4.2 show the percentage of errors obtained when comparing the results of both models with actual measured values. These errors are in percentages (%) based on the nominal values of each line. They are an average of the instantaneous values of each stage that make up the records.

Table 4.1: Test average errors with 765 kV line records.

	Voltage Error (%)		Current Error (%)	
	BM	DM	BM	DM
Pre-fault	12.541	2.637	5.298	2.470
Fault	14.506	3.061	6.502	3.960
Post-fault	12.072	3.695	5.788	3.333

Table 4.2: Test average errors with 230 kV line records.

	Voltage Error (%)		Current Error (%)	
	BM	DM	BM	DM
Pre-fault	1.492	1.480	3.139	3.106
Fault	0.730	0.727	2.771	2.693
Post-fault	1.360	1.345	3.079	3.041

Also, in order to illustrate the tests, Figure 4.2 and 4.3 are the results of voltage and current in the faulted phase of the records analyzed, these graphics show the results obtained with both models superimposed on the receiver end of the actual records.

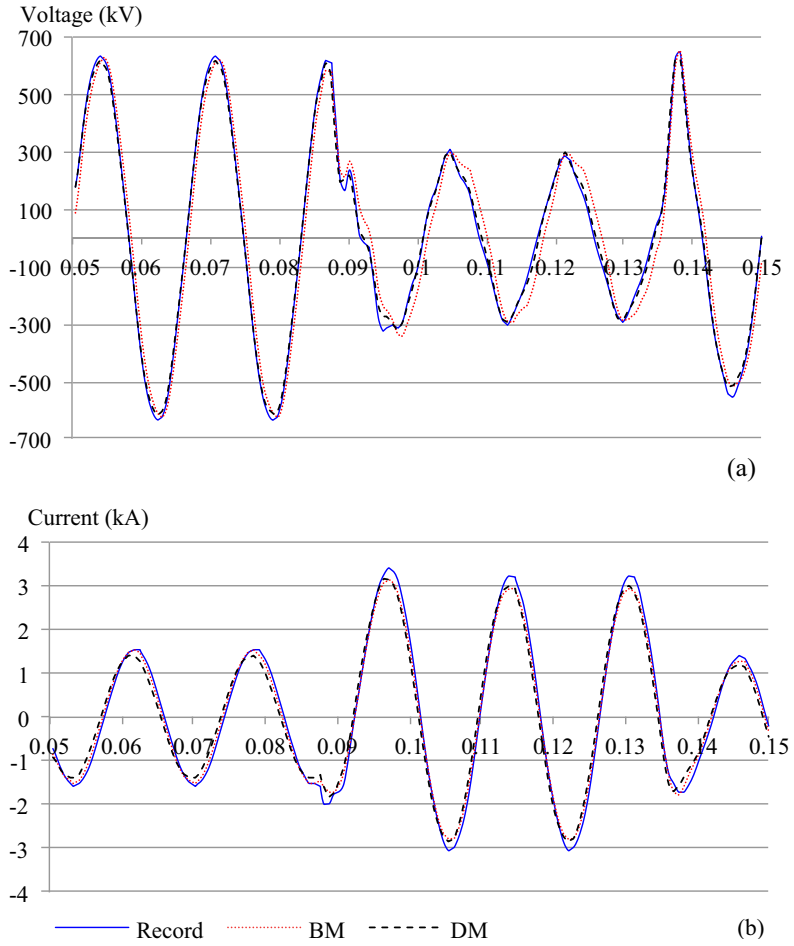

Figure 4.2: 765kV line real record compared with Bergeron's model (BM) and with the developed model (DM). (a) Voltage (b) Current.

The largest errors were obtained in long line tests using the Bergeron's model. In this test, the model presented here showed to be more accurate because it is better adapted for the modeling of long lines.

In the short line test, the results obtained with both models are similar and they are more precise than in the long line test. This is because the approximations used in Bergeron's model apply better to this type of line than with long lines. Even so, the model deduced here was slightly more accurate than Bergeron's model.

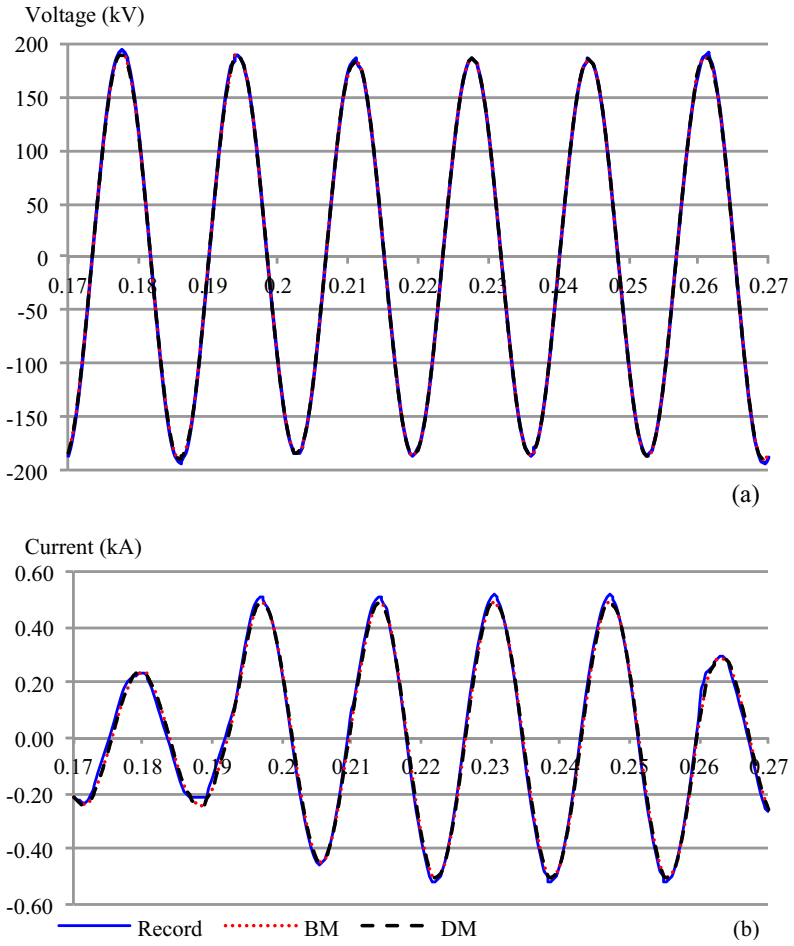

Figure 4.3: 230kV line real record compared with Bergeron's model (BM) and with the developed model (DM). (a) Voltage (b) Current.

4.1.2.2 DC Line Tests

In the following item, simulated records of different DC lines are analyzed with the deduced model. The results are compared with Bergeron's model. Like in the previous item, the tests consist in taking the voltage and current records of the line's sender-end, and with this information try to predict what is happening at the receiver-end. The results of both models are compared with the records produced to the receiver-end in order to see which model can predict more accurately the actual behavior of the line.

For this test, there were simulated transient events of two DC lines. A long line with 900 km and a short line with 150 km. The transient event used was the line being energized. The SimPowerSystem module of Simulink/MatLab®was used for the simulation with sample time steps of 0.5 ms. The resistance and inductance of each equivalent system were: 0.001 Ω, and 0.5 H respectively for the equivalent system S, and 30 Ω, and 0.5 H for the equivalent system R. Both lines were modeled using the

distributed parameter line model. Table 4.3 shows the transmission system data used in the line models.The energizing was simulated without any control so that the lines pass from zero to 1 p.u. (sender-end) in a natural way. This gives the opportunity to analyze two different system conditions: first, a transitional period when the line is energized, and then a steady-state period when the line reaches a value close to 1 p.u. (on the receiver end).

Table 4.3: Transmission line parameters.

	Long Line	Short Line
Length (km)	900	150
Resistance (Ω/km)	0.011	0.011
Inductance (mH/km)	0.832	0.832
Capacitance (pF/km)	13.41	13.41
Conductance (pS/km)	27.668	27.668

Tables 4.4 and 4.5 show the percentage of errors obtained when comparing the results of both models with the receiver end values. They are an average of the instantaneous values of each period that make up the records.

Table 4.4: Test average errors with the long line records.

	Voltage Error (%)		Current Error (%)	
	BM	DM	BM	DM
Transient	0.789	0.662	0.820	0.558
Steady-state	0.437	0.426	0.410	0.140

Table 4.5: Test average errors with the short line records.

	Voltage Error (%)		Current Error (%)	
	BM	DM	BM	DM
Transient	0.421	0.421	0.178	0.175
Steady-state	0.045	0.045	0.044	0.017

Also, in Figure 4.4 and 4.5 are presented the results for voltage and current for the lines energizing process, these graphics show the results obtained with both models superimposed on the receiver end records.

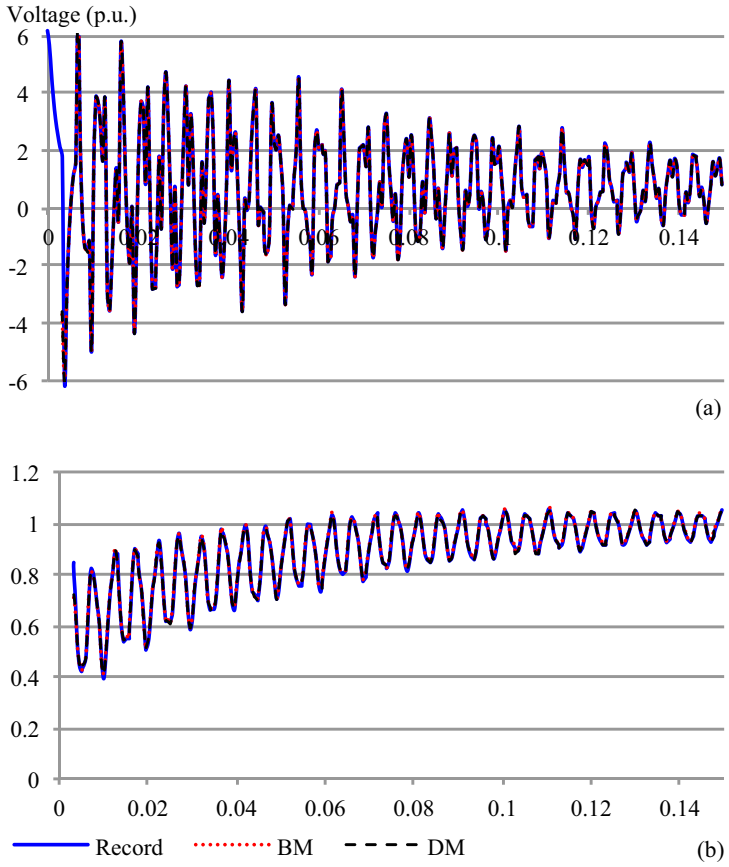

Figure 4.4: Long DC line record compared with Bergeron's model (BM) and with the developed model (DM). (a) Voltage (b) Current.

The errors shown in tables 4.4 and 4.5 are much smaller than those of tables 4.1 and 4.2, because the tests with simulated data have a better control of the accuracy of the line parameters.

In the long-line analysis (table 4.4), is possible to see that the model presented here is more accurate than Bergeron's model. While in the short-line analysis (table 4.5) the results of both models are virtually identical in most cases. Like in the other test, this is because the approximations used in Bergeron's model apply better to short lines than long lines.

4.1.3 Final Remarks of the Model

This section presented the basics of a general transmission line and the development of the time-domain model for a single-phase line. Also, some analysis are presented using this time-domain transmission line model. This analysis increases the credibility of the presented model. This section also proved that this model is more accurate in describing the behavior of different transmission lines than Bergeron's model. Since the most widely used models, like models with frequency-dependent parameters, use

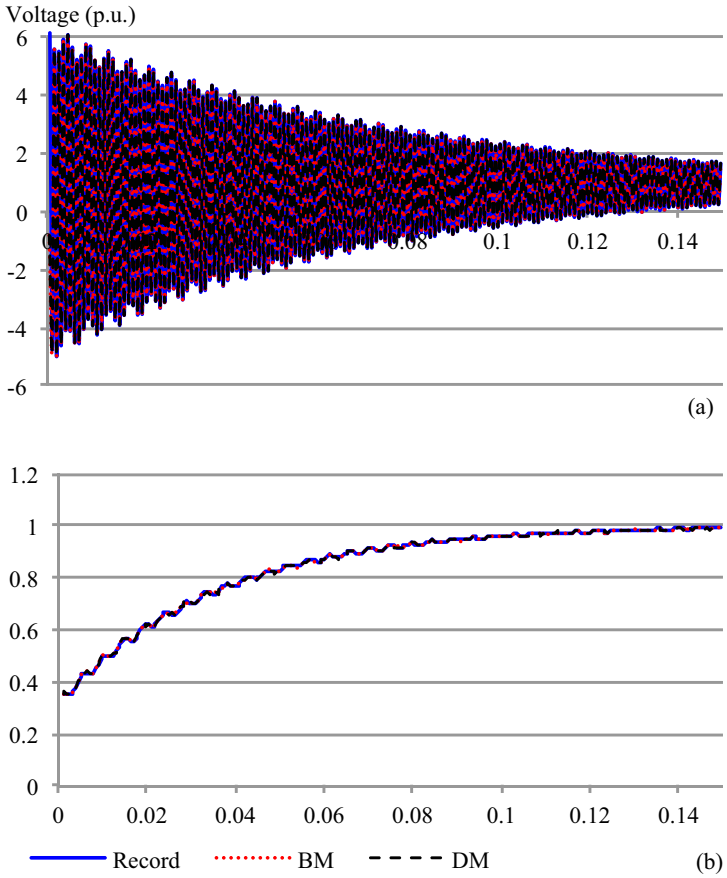

Figure 4.5: Short DC line record compared with Bergeron's model (BM) and with the developed model (DM). (a) Voltage (b) Current.

an approach which retains the basic idea behind Bergeron's model, this more detailed model could be used to improve other models.

The added value of this model is the adoption of the distributed characteristics of all line parameters, which allows a more accurate description of the transmission line's behavior in time-domain.

These are some initial tests that were performed to validate the model. The objective of these tests is to deepen the understanding of the different models making comparisons between their performances, so as to observe their behavior before using the model into the fault location method.

This section shows the deduction of a model for fundamental frequency parameters and single-phase, but the model can also be extended for cases with multi-conductor and frequency depended parameters. In this regard, the model has potential for improvements in areas such as electromagnetic transient simulation or any other analysis that requires a high accuracy in predicting the transmission lines behavior in time-domain.

4.1.3.1 Other Comments

Applying accepted approximations is possible to develop previously known models from the model proposed here. The fact that these models can be deduced from simplifications applied to the proposed model, despite to have different origins, increases the credibility of the proposed model.

Although these approximations are widely accepted, they are only valid to describe the behavior of a line in particular cases. These deductions are listed here as a way to illustrate that the model deduced here already contains several particular cases and has a more general range of application than other known models. Like in the case of short lines where some approximations in the hyperbolic functions are allowed:

$$\begin{aligned} \cosh(x\gamma_{RG}) &\approx 1 \\ Z_{RG}\sinh(x\gamma_{RG}) &\approx Rx \\ \frac{\sinh(x\gamma_{RG})}{Z_{RG}} &\approx Gx \approx 0 \\ \sinh((\frac{R}{Z_{LC}}+GZ_{LC})x) &\approx (\frac{R}{Z_{LC}}+GZ_{LC})x \end{aligned} \tag{4.25}$$

So, inserting (4.25) into the model of (4.21):

$$\begin{aligned} V = -V_1\frac{e^{-(\frac{R}{Z_{LC}}+GZ_{LC})x}-1}{2(\frac{R}{Z_{LC}}+GZ_{LC})x} + I_1\frac{(e^{-(\frac{R}{Z_{LC}}+GZ_{LC})x}+\frac{LG}{RC})Rx}{2(\frac{R}{Z_{LC}}+GZ_{LC})x} + \dots \\ V_2\frac{e^{(\frac{R}{Z_{LC}}+GZ_{LC})x}-1}{2(\frac{R}{Z_{LC}}+GZ_{LC})x} - I_2\frac{(e^{(\frac{R}{Z_{LC}}+GZ_{LC})x}+\frac{LG}{RC})Rx}{2(\frac{R}{Z_{LC}}+GZ_{LC})x} \end{aligned} \tag{4.26}$$

$$I = -I_1\frac{e^{-(\frac{R}{Z_{LC}}+GZ_{LC})x}-1}{2(\frac{R}{Z_{LC}}+GZ_{LC})x} + I_2\frac{e^{(\frac{R}{Z_{LC}}+GZ_{LC})x}-1}{2(\frac{R}{Z_{LC}}+GZ_{LC})x} \tag{4.27}$$

For short transmission lines, G is a very small number, therefore (4.26) and (4.27) can be simplified to:

$$\begin{aligned} V = -\frac{1}{2}\frac{Z_{LC}}{Rx}(e^{-\frac{Rx}{Z_{LC}}}-1)V_1 + \frac{1}{2}Z_{LC}e^{-\frac{Rx}{Z_{LC}}}I_1 + \dots \\ \frac{1}{2}\frac{Z_{LC}}{Rx}(e^{\frac{Rx}{Z_{LC}}}-1)V_2 - \frac{1}{2}Z_{LC}e^{\frac{Rx}{Z_{LC}}}I_2 \end{aligned} \tag{4.28}$$

$$I = -\frac{1}{2}\frac{Z_{LC}}{Rx}(e^{-\frac{Rx}{Z_{LC}}}-1)I_1 + \frac{1}{2}\frac{Z_{LC}}{Rx}(e^{\frac{Rx}{Z_{LC}}}-1)I_2 \tag{4.29}$$

Finally, others mathematical approximation typical for short lines can be used:

$$e^{-\frac{Rx}{Z_{LC}}} \approx 1 - \frac{Rx}{\sqrt{\frac{L}{C}}} + \frac{1}{2}(\frac{Rx}{\sqrt{\frac{L}{C}}})^2 \quad \text{and} \quad e^{\frac{Rx}{Z_{LC}}} \approx 1 + \frac{Rx}{\sqrt{\frac{L}{C}}} + \frac{1}{2}(\frac{Rx}{\sqrt{\frac{L}{C}}})^2$$

Therefore, replacing this in (4.28) and (4.29), expressions for V and I are simplified to:

$$\begin{aligned} V = \frac{1}{2}[(1 - \frac{Rx}{2\sqrt{\frac{L}{C}}})V_1 + \sqrt{\frac{L}{C}}(1 - \frac{Rx}{\sqrt{\frac{L}{C}}} + \frac{1}{2}(\frac{Rx}{\sqrt{\frac{L}{C}}})^2)I_1 + \dots \\ (1 + \frac{Rx}{2\sqrt{\frac{L}{C}}})V_2 - \sqrt{\frac{L}{C}}(1 + \frac{Rx}{\sqrt{\frac{L}{C}}} + \frac{1}{2}(\frac{Rx}{\sqrt{\frac{L}{C}}})^2)I_2] \end{aligned} \tag{4.30}$$

$$I = \frac{1}{2}[(1 - \frac{Rx}{2\sqrt{\frac{L}{C}}})I_1 + (1 + \frac{Rx}{2\sqrt{\frac{L}{C}}})I_2] \tag{4.31}$$

Equations (4.30) and (4.31) are Bergeron's model presented in section 3.3.1, and developed in [8–10], that compose the time-domain model more widely used and is based on a lossless line model with lumped resistance. This shows that there is great analogy between both models, because the most widely used model can be deducted from the proposed model.

4.2 Fault Location Method Scheme

The work developed here proposes the implementation of an impedance-based method for locating faults in two-terminal HVDC lines, using the time-domain line model in order to estimate the voltage profile over the line during the fault. To achieve the results, some processes must be fulfilled. Figure 4.6 shows the scheme for the fault location algorithm. As seen in Figure 4.6, the algorithm is simple and straight. The different stages of the algorithm are explained below.

- Data Collection: collects and organizes the data from fault records (in COMTRADE format) in a comprehensive way in order to be analyzed by the method.
- Fault Detection: fixed the point where the fault begins to be recorded from each line-end.
- Start Time of the Fault: sets the time where the fault started with the analysis of fault detection viewed from each line-end. With this data is possible to define the samples to be analyzed in the fault location process.

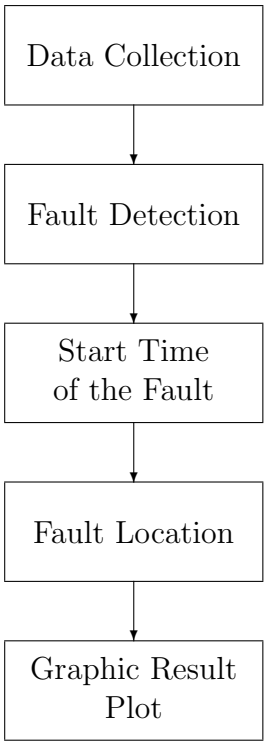

Figure 4.6: Fault location algorithm.

- Fault Location: is where the fault location process itself is done.
- Graphic Result Plot: shows the results analysis by plotting the voltage profiles of the line viewed from each end during the fault.

Next, the explanation of the two most important stages of the method is deepened.

4.2.1 Fault Detection

Fault detection are a group of methods that seek to detect any abnormal condition in the system (not necessarily faults), as quickly as possible. For fault location purposes, the fault detection marks the beginning of the analysis because it divides the conditions of fault and pre-fault from the records.

These methods are mainly used for protection systems where a number of approaches to fault detection are proposed in the literature [13, 14, 14, 15]. But, since the fault location is a post-hoc analysis, fault location may adopt slower and more precise methods. The faults could be detected by measuring different type of signals like the phase impedances, current, voltage, or zero-sequence current. Depending on a particular application, different activation criteria are combined in a different way. To speed up the fault detection, one may also apply derivatives of the relevant signals.

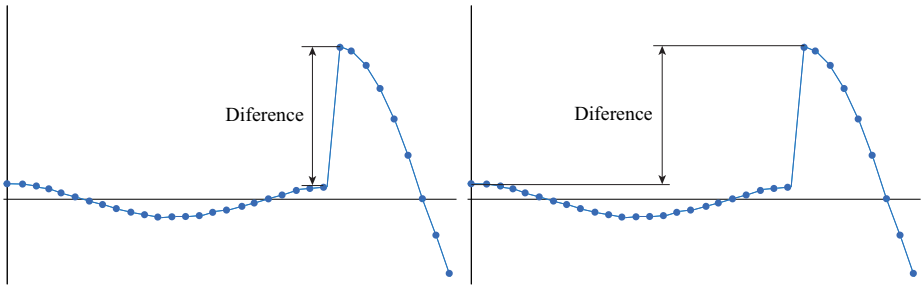

(a) Sample-by-sample. (b) Cycle-by-cycle.

Figure 4.7: Illustration of differentiation methods.

The easiest methods refer directly to samples of current or voltage waveforms. Disregarding a particular solution, two approaches are considered: a sample-by-sample method which compares the variation of individual samples of signals. And a cycle-by-cycle algorithm which compares a present sample with the sample one cycle back (Figure 4.7). If the variation exceeds a pre-set value a counter starts to count. The fault is detected when the counter reaches its highest value because that pre-set value is surpassed several times. The length of the data window may be either fixed or adaptable. On-line data window adjustment can be applied for improving the fault's detection.

When considering a fault-detection issue, it is worth listing traveling-wave approaches too [14]. Correct classification of all types of faults from the information available at the local bus appears difficult, therefore a communication channel is required. However, significant improvement has been made by utilizing some extra information present at the local bus and related to the subsequent wave reflections.

There are also several applications of artificial neural networks (ANN) to fault detection [16]. The most typical is aimed towards arcing fault detection.

The fault detection in DC is easier that in AC since the steady-state voltage and current signals in HVDC lines have no variation compared to those on AC lines. For this work, the sample-by-sample fault detection method was selected. In third case, the variation of the current signal is calculated. If this variation overruns a pre-set value, an auxiliary counter starts to count up. In DC lines this pre-set value may be small in order to improve sensitivity. This counter is incremented by the absolute value of the variation. When it reaches another pre-set threshold, the fault is confirmed. To improve safety of the method and avoid false detections due to irregularities in the records, each sample is not compared with the previous sample, but with a window of average values of samples, as shown in (4.32).

$$DEC = 1 - \frac{I_n * (n-1)}{\sum_{k=n-m}^{n-1} I_k} \tag{4.32}$$

Where DEC is the indicator, n is the number of the analyzed sample , m is the number of samples for the analysis window, and I is the current signal analyzed.

4.2.2 Impedance-Based Fault Location Method

The line model is used together with the voltage and current signals from the fault records in order to calculate the voltage at the fault point. The fault voltage obtained from the voltage distribution profiles viewed at each line-end, should be equal over time at the fault point (Figure 4.8).

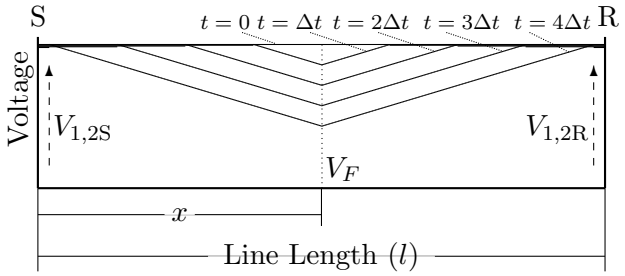

Figure 4.8: Fault voltage behavior over time.

Therefore, the voltage at the fault point (V_F) can be calculated using records from each line-end. Being then the voltage seen from the S line-end:

$$V_F = A_{1(x)}V_{1S} + B_{1(x)}I_{1S} + A_{2(x)}V_{2S} + B_{2(x)}I_{2S} \tag{4.33}$$

And from the R line-end:

$$V_F = A_{1(l-x)}V_{1R} + B_{1(l-x)}I_{1R} + A_{2(l-x)}V_{2R} + B_{2(l-x)}I_{2R} \tag{4.34}$$

Equations (4.33) and (4.34) form a system of two equations with two variables (V_F and x), so it is possible to calculate the distance to the fault.

As Figure 4.8 shows, the fault's effect is not measured instantaneously at the line-ends (that would only happen with an infinite speed of the traveling wave). Since speed of the traveling wave is $v_t = 1/\sqrt{LC}$, a nonzero time is required to measure the fault's effect on both line-ends. So this required to have more than one voltage and current sample from each line-end in order to calculate the voltage profiles along the line. For that reason, as the distance x increases, it also varies the sample time t required for the calculation of the voltage profile.

Most HVDC lines are two-wire (bipolar) systems, so they have self and mutual line parameters. Therefore, line parameters should be decoupled in order to use them in the line model. Unlike three-phase systems, in two-wire HVDC lines there are only one aerial mode and one ground mode, so a decoupling matrix [11] can be given as follows:

$$[T] = \frac{1}{\sqrt{2}} \begin{bmatrix} 1 & 1 \\ 1 & -1 \end{bmatrix} \tag{4.35}$$

Where the matrix inverse equals its transpose ($[T]^{-1} = [T]^t$).

For this fault location method, aerial model is used. The aerial mode is the most common mode used in this type of analysis since is present for any kind of fault.

Bibliography Chapter 4

[1] S. Jiale, G. Shuping, S. Guobing, J. Zaibin, and K. Xiaoning, "A novel fault-location method for HVDC transmission lines," *IEEE Transactions on Power Delivery*, vol. 25, no. 2, pp. 1203–1209, 2010.

[2] W. G. on HVDC and FACTS, "HVDC projects listing," *IEEE Transmission and Distribution Committee*, 2008.

[3] J. R. Carson, "The rigorous and approximate theories of electrical transmission along wires," *Bell System Technical Journal*, vol. 7, no. 1, pp. 11–25, 1928.

[4] L. de Andrade, H. Leite, and T. Ponce de Leão, "Time-domain distributed parameters transmission line model for transient analysis," *Progress In Electromagnetics Research B*, vol. 53, pp. 25–46, 2013.

[5] R. Chipman, *Theory and Problems of Transmission Lines*. Schaum's outline series, McGraw-Hill, 1968.

[6] P. Kundur, *Power System Stability and Control*. New York: McGraw Hill, 1993.

[7] J. d'Alembert, "Recherches sur la courbe que forme une corde tenduë mise en vibration," *Histoire de l'académie royale des sciences et belles lettres de Berlin*, vol. 3, pp. 214–249, 1747.

[8] F. J. Branin, "Transient analysis of lossless transmission lines," *Proceedings of the IEEE*, vol. 55, no. 11, pp. 2012–2013, 1967.

[9] H. W. Dommel, "Digital computer solution of electromagnetic transients in single-and multiphase networks," *IEEE Transactions on Power Apparatus and Systems*, vol. PAS-88, no. 4, pp. 388–399, 1969.

[10] J. Marti, L. Marti, and H. W. Dommel, "Transmission line models for steady-state and transients analysis," in *Joint International Power Conference Athens Power Tech*, vol. 2, pp. 744–750, 1993.

[11] H. W. Dommel, *EMTP Theory Book*. Vancouver, Canada: Microtran Power System Analysis Corporation, 2th ed., 1992.

[12] C. R. Paul, "A brief history of work in transmission lines for EMC applications," *IEEE Transactions on Electromagnetic Compatibility*, vol. 49, no. 2, pp. 237–252, 2007.

[13] D. Gilbert and I. Morrison, "A statistical method for detection of power system faults," in *Int. Conf. on Power System Transients*, (Lisbon), pp. 288–293, 1995.

[14] H. Zhengyou, F. Ling, L. Sheng, and B. Zhiqian, "Fault detection and classification in EHV transmission line based on wavelet singular entropy," *IEEE Transactions on Power Delivery*, vol. 25, no. 4, pp. 2156–2163, 2010.

[15] W. Kwon, G. Lee, Y. Park, M. Yoon, and M. Yoo, "High impedance fault detection utilizing incremental variance of normalized even order harmonic power," *IEEE Transactions on Power Delivery*, vol. 6, no. 2, pp. 557–564, 1991.

[16] Q. jin Guo, H.-B. Yu, and A. dong Xu, "Modified morlet wavelet neural networks for fault detection," in *International Conference on Control and Automation*, vol. 2, pp. 1209–1214, 2005.

Chapter 5

Working Examples

In this chapter, fault records of a HVDC line will be analyzed with the developed method in order to validate the method's performance. The results will be compared with two commercially available methods: a single-end, and a two-ends method [1].

As said in Chapter 4, there is not commercially available HVDC impedance-based fault locator, but one work has been done to adapt this technology for use in HVDC [2] that uses the Bergeron's model.The work developed here argues that the development of a specific line model for this method is advantageous because it increases the accuracy of the method, so the results of the method will also be compared to [2] to check the veracity of this argument.

Tests with records of actual and simulated faults were carried out in order to prove the method with the highest number of possible variations.

5.1 Furnas HVDC Line

The validation stage of the method developed in this work was carried out with assistance with the company Eletrobras Furnas. The company Eletrobras Furnas has a HVDC overhead line which was used as the basis for the tests shown in this chapter.

5.1.1 Furnas Transmission System

Eletrobras Furnas (Furnas - Centrais Elétricas SA) is a Brazilian regional power utility and a major subsidiary of Eletrobras. The company has 15 hydroelectric and two thermoelectric plants with a total capacity of 10,050 MW which corresponds to 10% of Brazil's electrical production. The company generates or transmits electricity to 51% of households in Brazil, and more than 40% of the nation's electricity passes through their grid.

The Eletrobras Furnas transmission system has 52 substations interconnected by 19.277,5 km of transmission lines with voltages of 138, 230, 345, 500, 750, and ±600 kV, which cross eight Brazilian states and the Federal District. Among the functions of

Eletrobras Furnas, stands out the operation and maintenance of Itaipu's transmission system, composed of five transmission lines that cross 800 km from the state of Paraná to São Paulo. This system consists of three 750 kV AC lines and two ±600 kV DC lines (see Figure 5.1[1]).

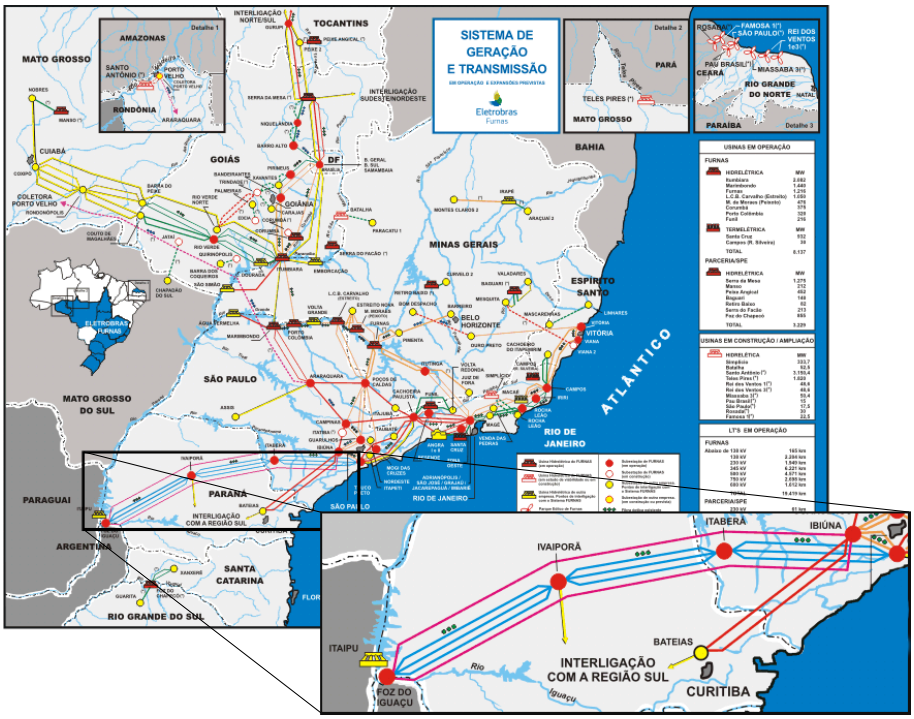

Figure 5.1: Eletrobras Furnas transmission system with focus in their HVDC lines.

The HVDC lines that are part of Itaipu's transmission system aim to solve the problem of differences in frequencies used by Brazil and Paraguay, to be able to connect the Brazilian transmission system with the Itaipu dam on the side that corresponds to Paraguay[2]. The HVDC system is composed of two dipole lines that go from the Foz do Iguaçu rectifier station (in Paraná State) to the Ibiúna inverter station (in São Paulo State) [3, 4]. The dipole 1 has a length of 792 km and the dipole 2 has a length of 816 km. The converters system are composed by thyristor bridge of 12-pulse. Each converter station comprises by two 300kV converters systems with 12 valves and 96 thyristors per valve. In Figure 5.2 is shown a top view of the Foz do Iguaçu substation[3], where its different components are emphasized.

5.1.2 The HVDC Fault Process

When a fault is detected by the DC line's fault protection, this protection orders the rectifier into inverter mode and this discharges the line effectively. This process is

[1]Photo source: Eletrobras Furnas' website
[2]This HVDC line is also mentioned in Sec. 1.2.1
[3]Photo source: Google Maps

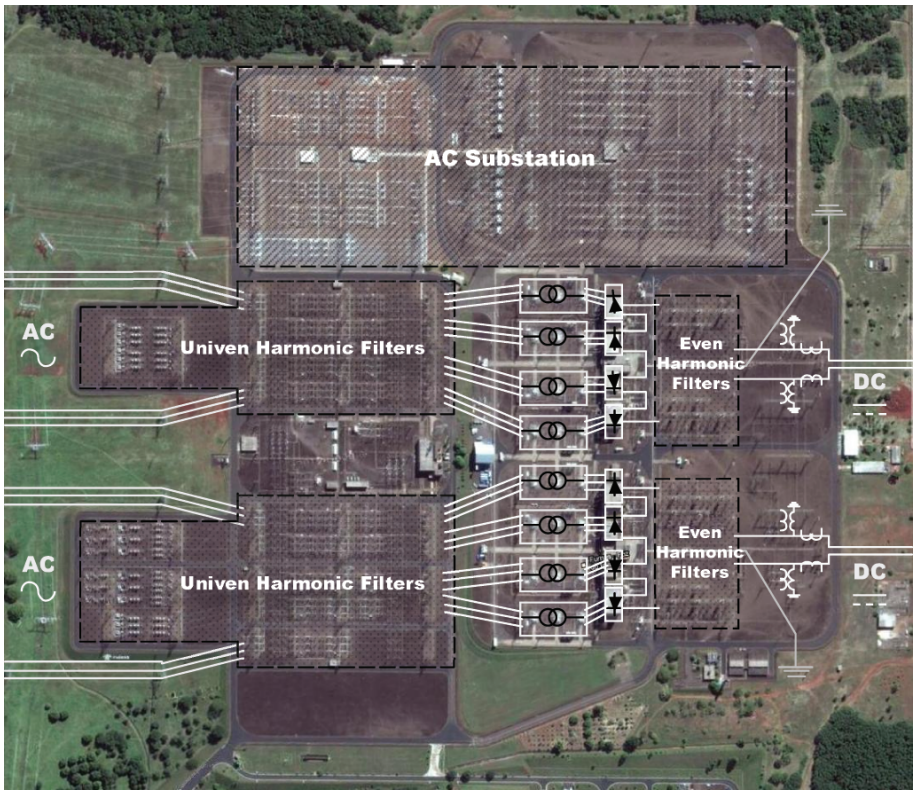

Figure 5.2: Foz do Iguaçu substation, 750 kV AC and ±600 kV DC.

done by placing the thyristor's trigger angle at values near to 180°, so the converter temporarily reverses the polarity of the line's voltage to extinguish the current and deionize the arc. The protection of the line is made at the converter level following two basic criteria: one by low level of DC voltage, and another by high-differential of DC voltage. The fault extinction is also achieved at the converters level, acting on the trips of the thyristors associated only to the faulted pole. In this way, is avoided the loss of the entire transmission capacity, and achieved only half of the loss.

After some 80 - 100 ms, the line is charged again by the rectifier. If the fault was intermittent, then normally the line can support the voltage and the power transmission continues. Full power is then resorted in about 200 ms after the fault. But if the fault was permanent, there is a risk that re-charging of the line will result in a second fault. The HVDC line was designed in order to have 3 more restart attempts, the last two attempts are made with reduced voltage (80% and 40% respectively). It should be pointed out that the DC line fault clearing does not involve any mechanical action, and is faster than for an AC line. The DC fault current is also lower (the load current) than the AC fault current, and therefore the dead time before the restart is shorter than for an AC line. The reduced voltage restart is also unique for HVDC.

For the fault location in the HVDC system, Furnas has a methodology based on traveling wave analysis that uses records taken directly from the fault. As previously mentioned (Sec. 2.3), these records can be decomposed into its waves with different frequencies to find the wave generated by the fault. This decomposition is made using

high-pass filters located in the converters at both ends, then the pulse is measured in the voltage signal of a capacitor located at the end of the filter.

5.1.3 The HVDC Fault Location Equipment

The fault location equipment was supplied by ABB and is based on traveling wave techniques. The Furnas HVDC line has had two fault location equipment: the first was commissioned with the line in 1986. This first equipment had timers on each line-end that were activated when a wavefront was recognized, and each line-end simultaneously sent an indication to the opposite line-end via communication channel. When indication sent from each line-end was received by the opposite line-end's equipment, the timer stopped. Figure 5.3 shows the operation of this equipment using a Lattice diagram. The fault distance can be calculated using equation 5.1.

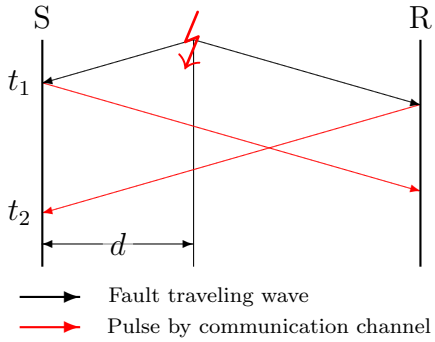

Figure 5.3: Lattice diagram.

$$d = \frac{1}{2}[l + (t_1 - t_2 + t_c) * k * c] \qquad (5.1)$$

Where d is the distance between the measurement point and the fault point, l is the total length, t_1 is the trig time at the line-end 1, t_2 is the trig time when the pulse signal is received on line-end 2 via communication channel, t_c is the entire communication channel time, k is a correction factor for surge front delay, and c is the speed of traveling wave.

Due to the expiration of its useful life, this equipment was removed in 2009 and replaced by one based on the same principles but with the support of modern technologies.

The newer fault location equipment was also supplied by ABB [5]. In this equipment, satellite-synchronized clocks (GPS) are used in each line-end of the monitored line for absolute time marking of the arrival of the first incoming wavefront when a fault occurs (as shown in Figure 2.5). Then, the fault distance can be calculated using equation 5.2

$$d = \frac{1}{2}[l + (t_1 - t_2 + offset) * k * c] \qquad (5.2)$$

Where d is the distance between the measurement point and the fault point, l is the total length, t_1 is the trig time at line-end 1, t_2 is the trig time at line-end 2, $offset$ is an offset constant for trig time difference, k is a correction factor for surge front delay and c is the speed of the traveling wave. The speed of the traveling wave

is ideally the same as the speed of light (c), however a correction (k) is introduced to compensate for surge front delay, and an offset to compensate for trig time differences.

The wavefront is measured trough two shunt capacitors, one at each line-end. The grounding conductor of the capacitors is equipped with a pulse transformer. The output of the pulse transformer is connected to a detector unit which will rectify the signal caused by the high derivative voltage drop. The detector generates a light pulse if a preset level of the line fault pulse is exceeded. The light pulse is received by a trigger unit in the control room. The pulse then triggers the GPS clock. Since the triggering circuit and the time registration of the wavefront arrival is common for both lines, information from the DC line protection is needed to identify the faulty line.

The automatic calculated fault location is presented as an event on a list. The event includes date, time, line, and the distance to the fault. The presentation is made on a computer in the main cubicle, and calculations are performed in both stations. In this case, also post fault calculations can be manually performed using the individually stored fault time in each station. The formula as used in the automatic calculations can, in this case, be fed into Excel for the case where telecommunication channels are faulty.

Figure 5.4 shows the HVDC fault location equipments. First the field equipments[4] (a pulse transformer and a detector card), and then the control room equipment[5] (a cabinet with GPS clock, computer for the analysis and data storage; and display unit). A set of these equipments is needed at each line-end. Is important to note that these equipment are to be used only with the fault location method and is estimated that manufacturing and installation costs is around 2.500.000 US$ for a dipole HVDC line[6] (four sets of equipment).

Figure 5.5[7] shows the dipole 1 output of the line at the rectifier end (Foz do Iguaçu substation). In this photo can be seen the field equipment used in the measurement and fault analysis: shows the capacitor that collects the wavefront used for the traveling wave-based fault location equipment, the CT for current measurement and fault recording; and the PT for voltage measurement, protection and fault recording. The voltage and current signals recorded by these devices are used as input data in the fault location methodology developed in this work.

5.2 Fault Location Test

The tests consist to estimate the fault location from the voltage and current fault's records. The fault location is calculated using each method. Then, the results are compared with the actual fault distance in order to show which of the four methods can predict more accurately the fault point.

[4]Photo source: ABB
[5]Photo source: own work
[6]Estimated costs source: ABB
[7]Photo source: own work

(a) Field equipments. (b) Control room equipments.

Figure 5.4: HVDC fault location equipments.

Figure 5.5: Dipole 1 output of the line at the rectifier end.

Actual fault records from the Itaipu HVDC line are used and also the Itaipu HVDC model was used in the fault simulations [6] in order to validate the method's performance. All fault location distances are referenced to the rectifier station's line-end. In order to make comparisons between results, they are not shown in distance values (km) but referred to percentage errors based on the total distances of the lines (%) as indicated in [7].

5.2.1 Method Performance to Actual Faults

In this part was assessed the performance of the developed method under real conditions. For this test, two records of faults occurred in the Itaipu HVDC line were used. One fault was located correctly by the equipment installed in the line, while in the other fault, equipment was unable to make the detection. Both faults were analyzed using the developed method. The sample time intervals were 0.173 ms. which is higher than those of simulated fault records but is a typical sample time under real conditions.

The first fault was near of the rectifier's line-end. Field crews that carried out the inspection, found the cause of the fault at 91 km (see Figure 5.6). For this fault, the traveling wave was detected for the fault locator, and the analysis' result was 92.0 km (0.1266 % of error). When the fault was analyzed by the developed method, the result was 91.26 km (0.0329 % of error). Then, the developed method was more accuracy than the traveling wave method for this fault.

Figure 5.6: Fault origin located to 91 km from the rectifier line-end.

In order to illustrate the fault analysis, Figure 5.7 shows the rectifier and inverter side records used by the developed method. The commercial equipment doesn't use this type of records, instead it uses a high frequency sensor in order to detect only the traveling wave.

The second fault was a high impedance fault occurred for unknown reasons. In this case, the equipment installed in the line was not able to calculate the location of the fault. The fault records were analyzed using the method developed and resulted in a distance of 513.28 km and a fault resistance of 384.02 Ω, which agrees with a high impedance fault. The location indicated by the analysis is an area of dense vegetation.

In order to illustrate the fault analysis, Figure 5.8 shows the graphic result analysis made by the developed method. This represents the voltage profiles when the fault starts. The lowest voltage peak marks the fault point.

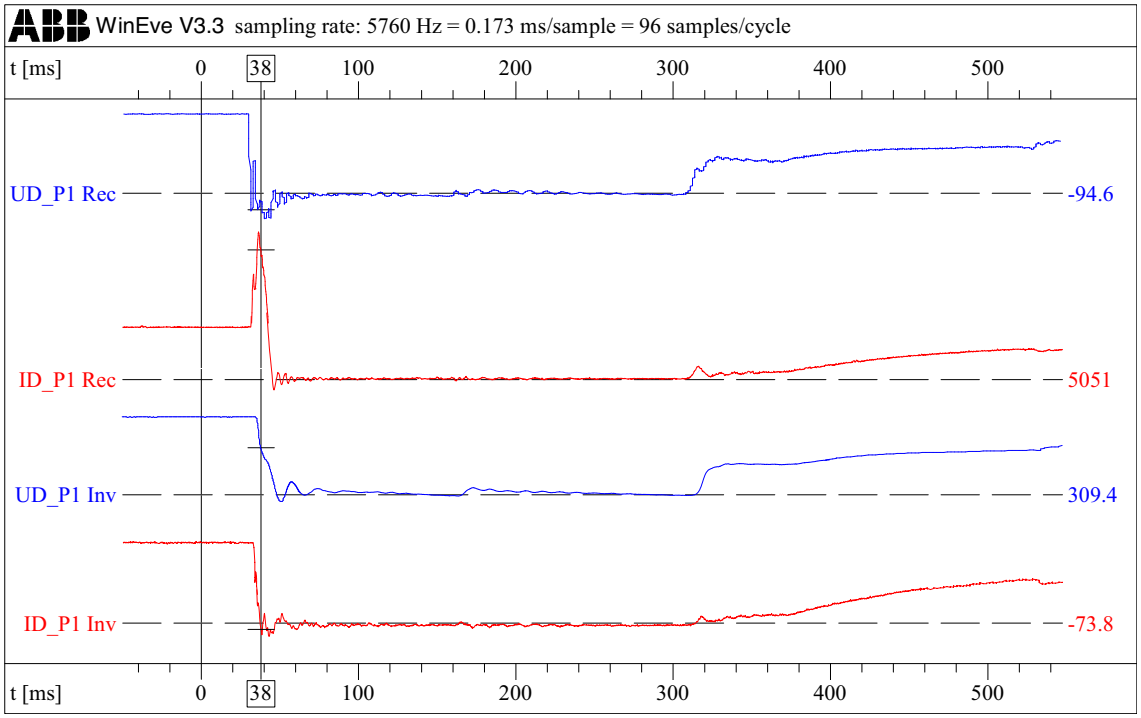

Figure 5.7: Fault record from both line-end.

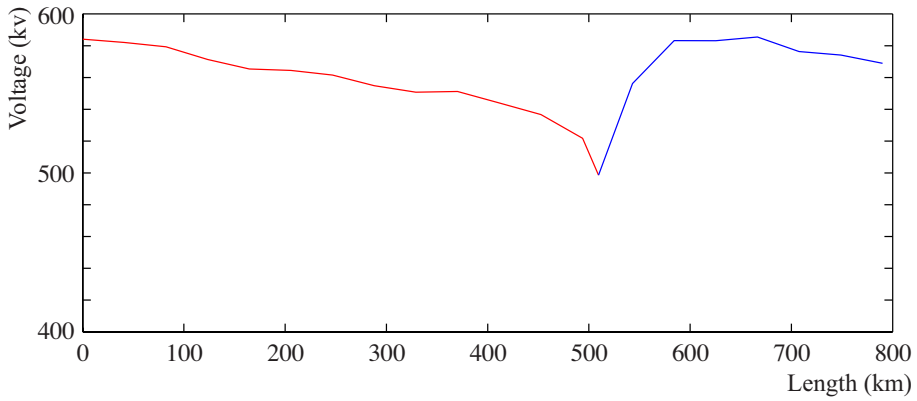

Figure 5.8: Fault record analisys result.

In order to illustrate the fault analysis, Figure 5.9 shows the rectifier and inverter side records used by the developed method. The commercial equipment doesn't use this type of records, instead it uses a high frequency sensor in order to detect only the traveling wave.

In this two real case, the developed method proved to have better performance than the traditional method. The result obtained in the first fault was more accurate, while in the second fault it had a more robust performance since it gave a result in a type of fault where the traditional method does not work. Figure 5.10 shows a

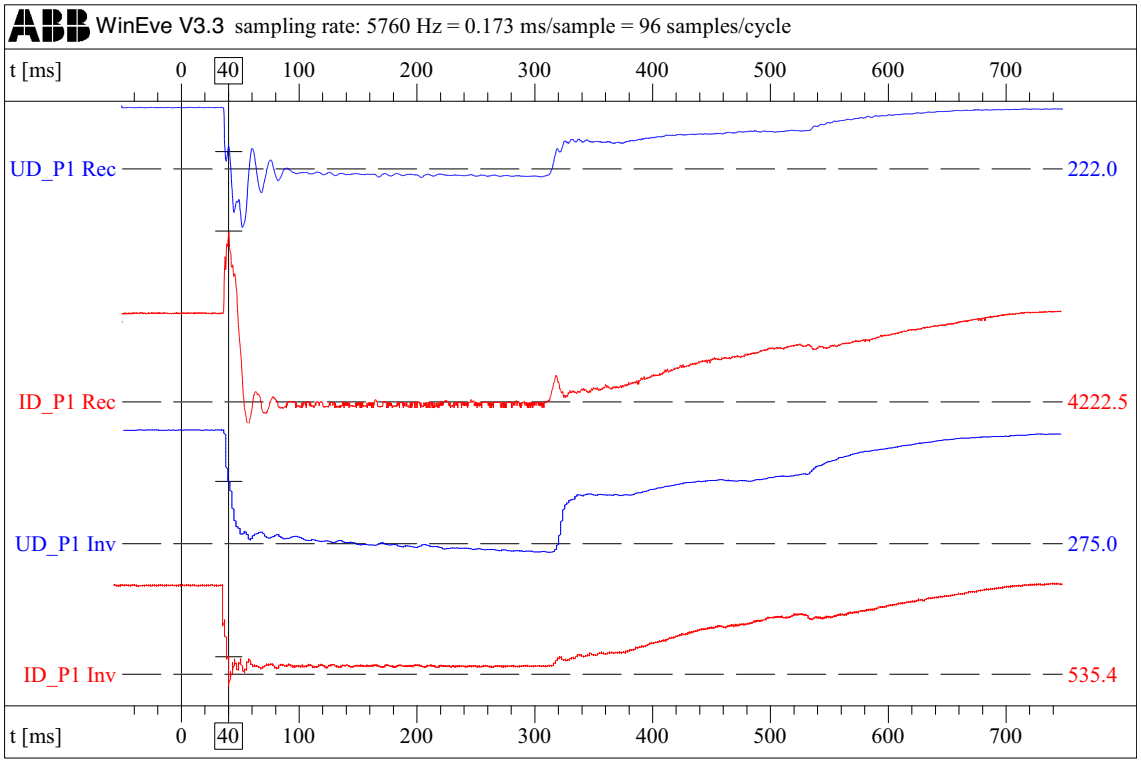

Figure 5.9: Fault record from both line-end.

summary of the faults analyzed and the actual location where they occurred[8].

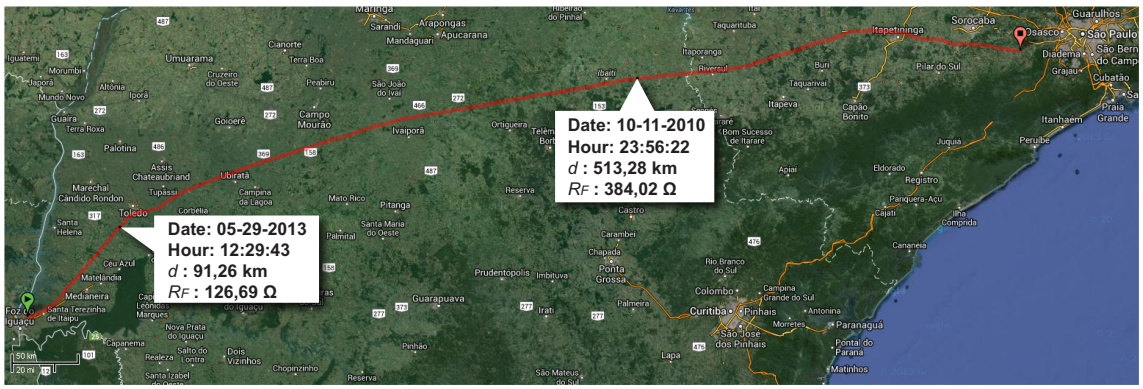

Figure 5.10: Indication of actual faults in the path of the line.

5.2.2 Accuracy Test Using Simulation Data

In order to extrapolate the above results to a more general behavior, the analysis of many faults is needed. But in order to have control over a large number of records,

[8]Map's photo source: Google Maps

simulated fault data is needed. In this section the accuracy of the developed method is evaluated using a comparative analysis with fault simulated data.

For this test, a solid bolted fault was simulated in the HVDC system at every 10 km. Then the faults were analyzed using each method and the results were compared. MatLab was used for all the analysis performed.

For the fault simulation, a dipole HVDC line was modeled, using the SimPowerSystem module of the Simulink/MatLab software. The modeling of the HVDC line is covered in depth in Appendix A. Figure 5.11 shows the HVDC system modeled for the fault simulations. The sample time intervals are of 50 μs. The system parameters are shown in Tables 5.1 and 5.2.

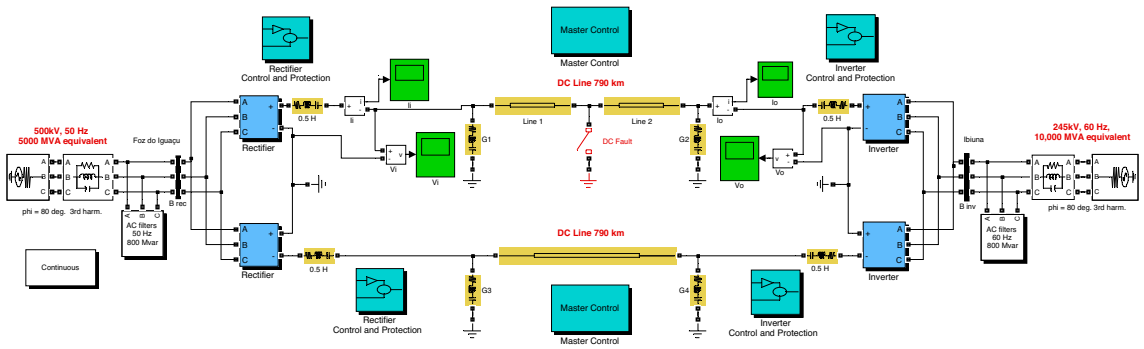

Figure 5.11: MatLab HVDC system model.

Table 5.1: HVDC Transmission line parameters.

	±600 kV Line
Parameter	790 km
Resistance (Ω/km)	0,04671
Inductance (H/km)	$1{,}3791{\cdot}10^{-3}$
Conductance (℧· km)	$0{,}2371{\cdot}10^{-6}$
Capacitance (F/km)	$12{,}91{\cdot}10^{-9}$

Table 5.2: Equivalent AC system data.

	Equivalent system	
Data	Rectifier	Inverter
Frequency (Hz)	50	60
Voltage (kV)	500	245
Power (MVA)	5000	10000
Resistance (Ω)	2160,6	24,81
Inductance (mH)	151	36,5

The fault begins at 100 ms after the simulation starts, the line's protections and controls act 10 ms after that, and the line's current turns to zero 25 ms after the protections acted. Both line-ends are opened simultaneously. Figure 5.12 shows the rectifier and the inverter side records for one simulated fault.

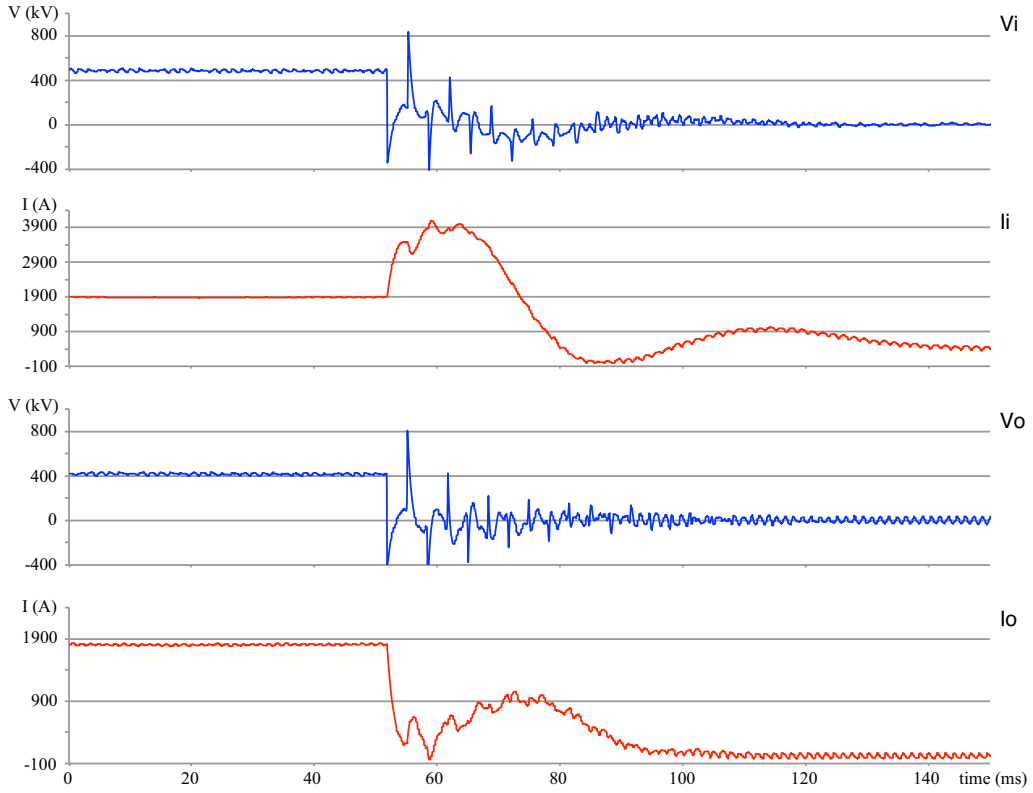

Figure 5.12: Simulated fault record from both line-ends.

In order to illustrate the test, Figure 5.13 shows a graphic result of one of the analysis made. For this case, the fault was located at 400 km. The graph shows the voltage profiles of the line during the first 500 μs of fault. The voltage was calculated using records from each line-end, the blue side was calculated with the rectifier's record, and the red side was calculated with the inverter's record. The point where the two colors meet is the fault point. Figure 5.14 shows the same fault as the fault evolves during the first 1000 μs of the fault event. Here is possible to see that the effect of the fault, although not instantaneous, it is of high speed, and in only 1 ms is almost spotted at the line-ends, with distances of around 400 km from the fault point[9].

For this test, the developed method had the most accurate results. Results are about 40% more accurate than those of commercially available methods. The method of [2] also proved to be more accurate than commercial methods, but even in this case, the developed method's results are slightly better.

[9]To be more precise, being $v_t = 1/\sqrt{LC}$ and taking the values of Table 5.1, then it is known that $v_t = 236995$ km/s. So the wavefront takes about 1.6 ms to travel from the center of the line to the ends (which is about 400 km)

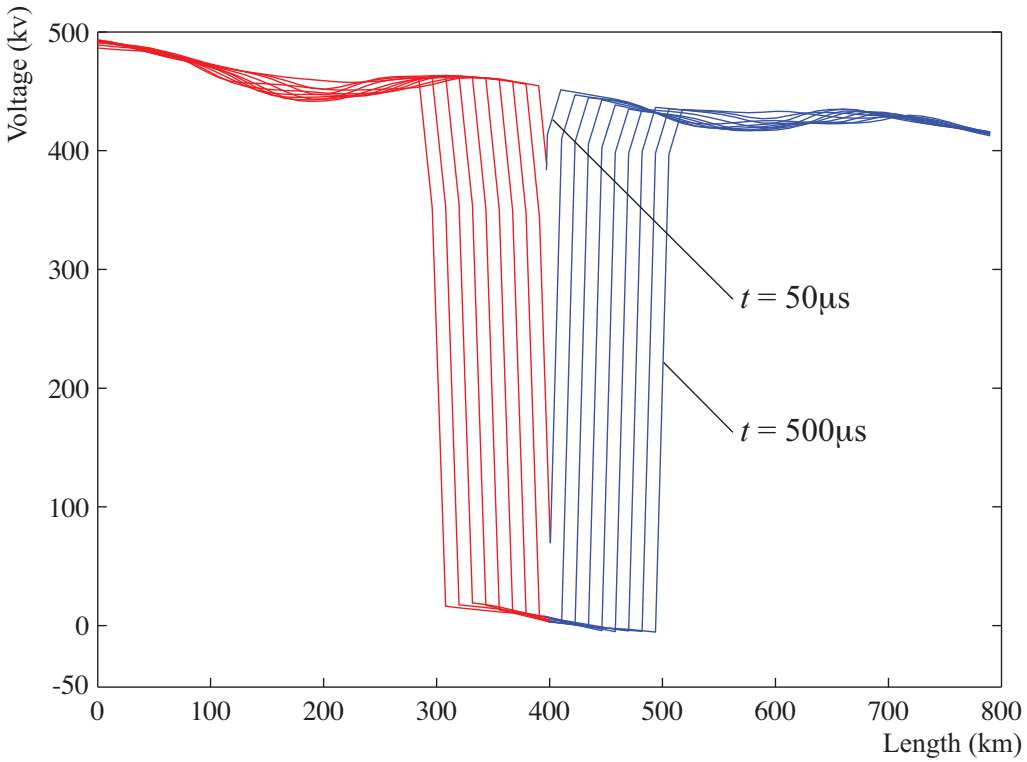

Figure 5.13: Line's voltage profiles as the fault evolves.

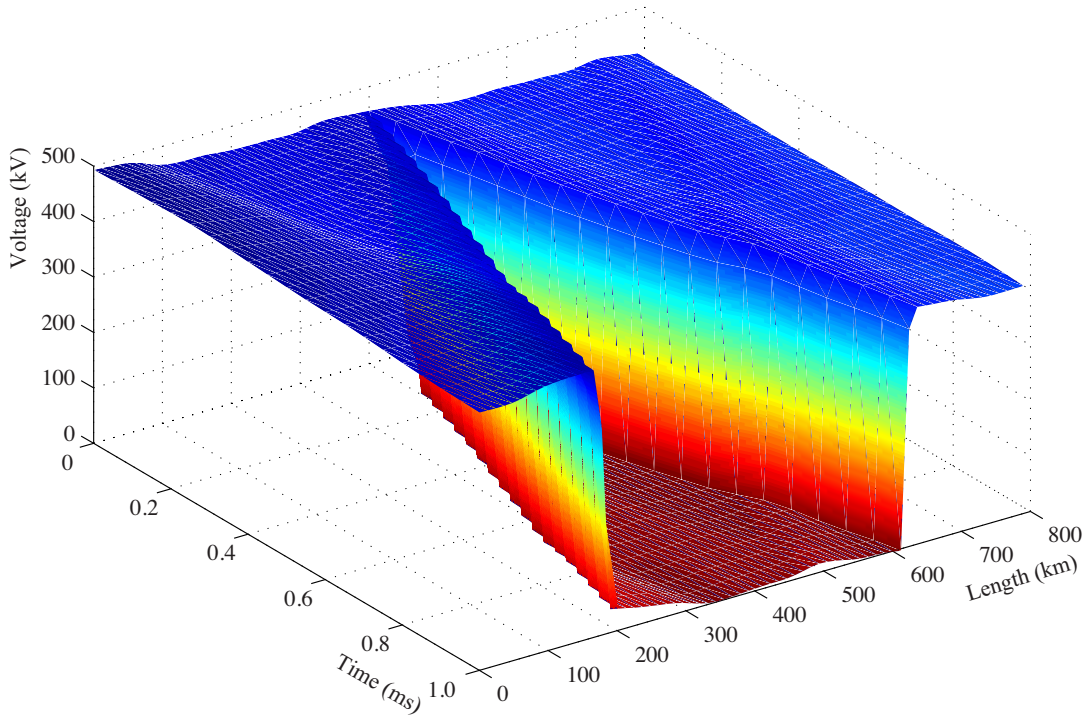

Figure 5.14: Evolution of the fault on the line through time.

Table 5.3 shows a summary of the percentage of errors in the fault location, for faults at each 10 km of the HVDC line. Table 5.3 also shows the faults' total average results.

Table 5.3: Fault location average errors test.

Distance (km)	Developed method	Bergeron's model	1-end traveling wave	2-ends traveling wave
10	0.0307	0.0472	0.2341	0.0148
20	0,2508	0,2526	0,4683	0,2194
30	0,1507	0,1535	0,0475	0,4535
40	0,0347	0,0381	0,1866	0,0623
50	0,0822	0,0788	0,4207	0,1718
60	0,2000	0,1976	0,0951	0,4060
70	0,2256	0,2238	0,1390	0,1099
80	0,2336	0,2355	0,3732	0,1243
90	0,1977	0,2005	0,6073	0,3916
100	0,0818	0,0852	0,8415	0,1574
110	0,0340	0,0306	0,3256	0,0767
120	0,1514	0,1487	0,5598	0,3109
130	0,2450	0,2432	0,0440	0,5450
140	0,0099	0,0041	0,2781	0,0292
150	0,2446	0,2464	0,2377	0,2633
160	0,1280	0,1302	0,0036	0,2525
170	0,0115	0,0138	0,2305	0,0184
180	0,1057	0,1041	0,2853	0,2158
190	0,2233	0,2226	0,0511	0,3001
200	0,2075	0,2077	0,1830	0,6841
210	0,2427	0,2428	0,4171	0,1682
220	0,1740	0,1745	0,0987	0,4024
230	0,0575	0,0583	0,6145	0,1135
240	0,0592	0,0587	0,3696	0,1207
250	0,1764	0,1765	0,1462	0,3548
260	0,2412	0,2419	0,0879	0,1610
270	0,2105	0,2095	0,4279	0,0731
280	0,2200	0,2198	0,1938	0,3073
290	0,1040	0,1041	0,0404	0,2086
300	0,0118	0,0115	0,4755	0,0256
310	0,1282	0,128	0,2413	0,2597
320	0,2451	0,2449	0,0072	0,4939
330	0,0213	0,0248	0,2270	0,0220
340	0,2490	0,2492	0,2889	0,2122
350	0,1521	0,1527	0,8047	0,3037
360	0,0356	0,0362	0,1794	0,0695
370	0,0808	0,0804	0,3364	0,1646
380	0,1977	0,1973	0,1023	0,3512
390	0,2284	0,228	0,1319	0,6329
400	0,2298	0,2303	0,3660	0,1171
410	0,1992	0,1995	0,1498	0,3988
420	0,0823	0,0823	0,0843	0,1646
430	0,0347	0,0348	0,4315	0,0695
440	0,1514	0,1515	0,1974	0,3037

Fault location average errors test. (follow up)

Distance (km)	Developed method	Bergeron's model	1-end traveling wave	2-ends traveling wave
450	0,2480	0,248	0,7132	0,2122
460	0,0204	0,0237	0,4791	0,0220
470	0,2464	0,2465	0,2449	0,2561
480	0,1297	0,1294	0,0108	0,2597
490	0,0129	0,0127	0,2234	0,0256
500	0,1036	0,1039	0,2925	0,2086
510	0,2199	0,2199	0,6916	0,3073
520	0,2103	0,2099	0,1758	0,0731
530	0,2410	0,241	0,4100	0,1610
540	0,1764	0,1759	0,1059	0,3952
550	0,0592	0,0579	0,1283	0,6293
560	0,0573	0,0587	0,3876	0,1135
570	0,1739	0,1753	0,1534	0,3476
580	0,2427	0,2438	0,0807	0,5818
590	0,0623	0,0729	0,3149	0,0659
600	0,2230	0,2214	0,2010	0,3001
610	0,1055	0,103	0,0332	0,2158
620	0,0111	0,0138	0,2673	0,0184
630	0,1273	0,1298	0,2485	0,2525
640	0,2434	0,2451	0,0144	0,2633
650	0,0109	0,0029	0,2198	0,7208
660	0,2466	0,2448	0,2961	0,5450
670	0,1527	0,1501	0,0619	0,3109
680	0,0349	0,0317	0,1722	0,0767
690	0,0813	0,0838	0,3436	0,1574
700	0,1961	0,1977	0,1095	0,3916
710	0,2310	0,2317	0,1247	0,1243
720	0,1018	0,1183	0,3912	0,1099
730	0,2019	0,2007	0,1570	0,3440
740	0,0846	0,0827	0,0771	0,1718
750	0,0321	0,0343	0,4387	0,0623
760	0,1488	0,1505	0,2046	0,2965
770	0,2486	0,2488	0,0296	0,2194
780	0,0291	0,0448	0,2637	0,0148
Average:	0,1423	0,1430	0,2577	0,2379

Figure 5.15 shows a comparative graphic of the percentage of error of fault location results for faults at each 10 km of the HVDC line.

5.2.3 Sensitive Test to Fault Resistance

As mentioned before, the developed method aims to bring improvements in high impedance fault locations. In order to evaluate the fault locator's performance at different fault resistance (R_F) levels, a comparative analysis is made using fault simulated data. For this test, faults were simulated in the HVDC system at every 50 km by varying R_F, from 0 to 400 Ω in steps of 20 Ω increments. Then the faults were analyzed using each method and the results were compared.

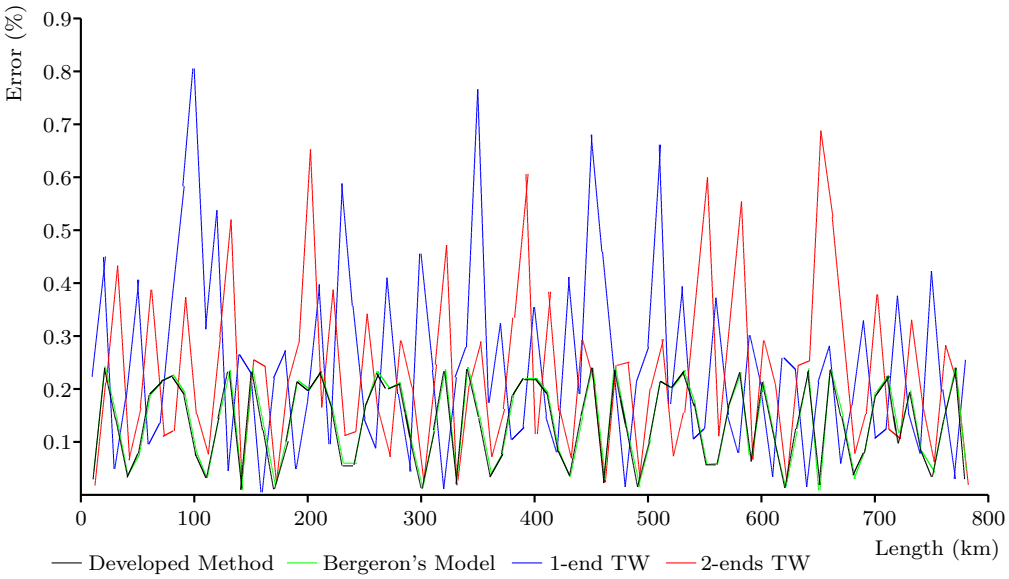

Figure 5.15: Fault location errors test.

In order to illustrate the test, Figure 5.16 shows a composition of several fault location results. For this case, the faults were located at 400 km. The graph shows how the onset of the fault changes, as R_F increases from 0 to 400 Ω. All records were analyzed 50 μs after the fault starts.

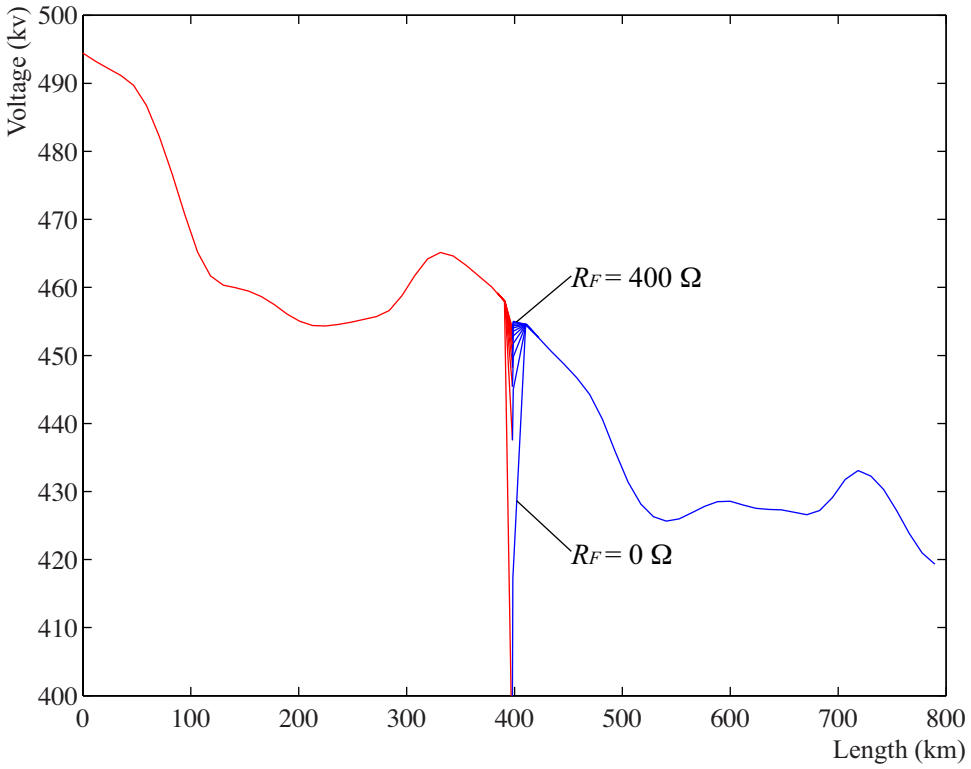

Figure 5.16: Line's voltage profiles as R_F changes.

Figure 5.17 shows the test results for all fault location methods. Each graphic shows the error level along the line and as R_F increases. The blue areas denote less error, and red areas denote larger error as shown in the right-side bar. The results show that for the two-ends traveling wave method, the faults were detected in 67.8 % of the cases, and for the one-end traveling wave method, the faults were detected in 73.9 % of the cases. In both tests, the undetected faults were those of higher impedance. This makes impossible the location of the fault in those cases where it was not possible to detect. For the developed method, and for method of [2], the faults were detected in all cases.

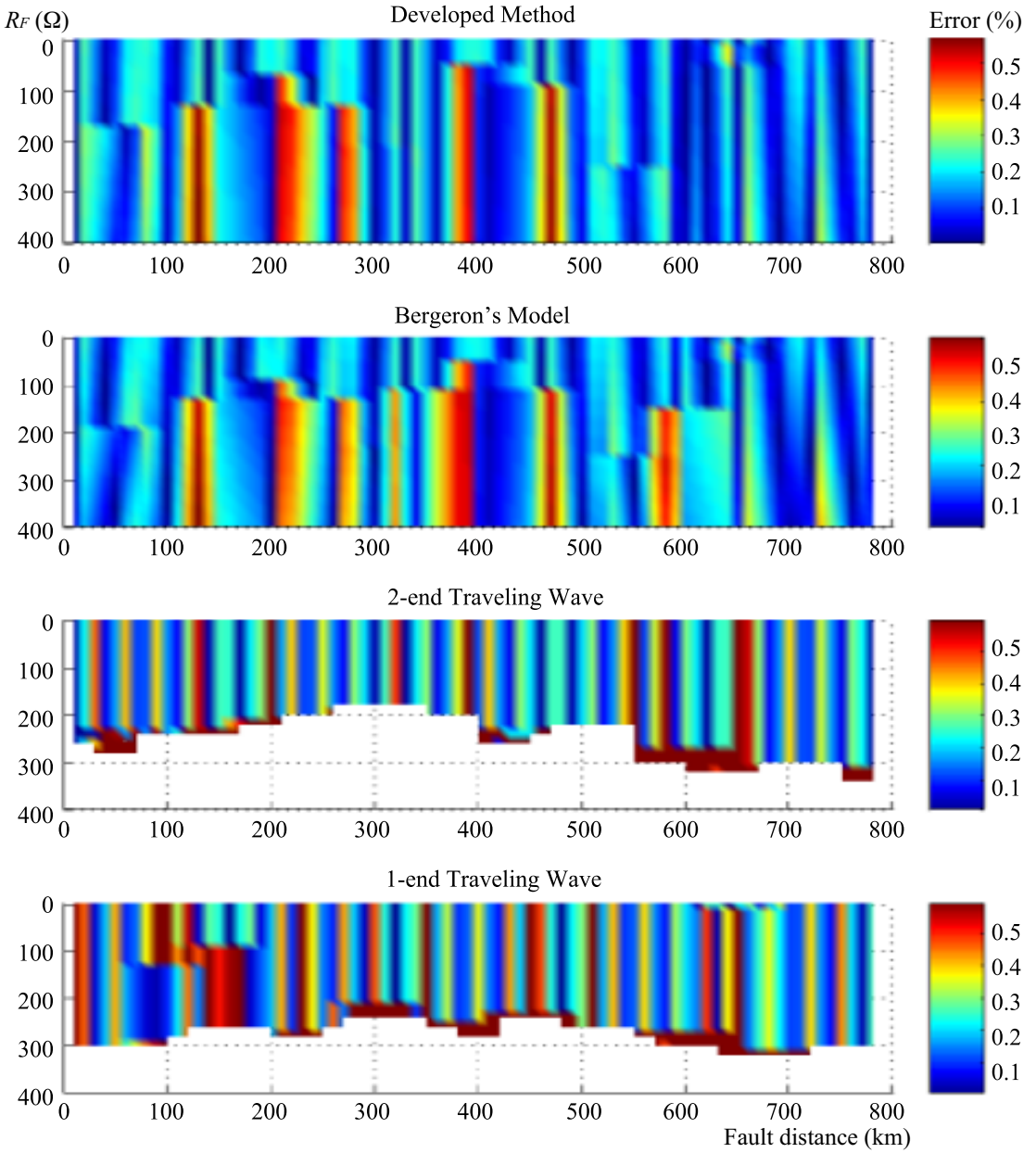

Figure 5.17: Sensitive test results for fault resistance.

In order to illustrate the test, Table 5.4 shows the minimum and maximum error for each method, and the fault distance and R_F where those errors were obtained. Table 5.4 also shows the total average error for all fault location results for the case where the methods work.

Table 5.4: Fault location test errors.

Method	Minimum Error			Maximum Error			Average
	d (km)	R_F (Ω)	Error (%)	d (km)	R_F (Ω)	Error (%)	Error (%)
Developed Method	10	280	0.0001	450	80	0.2440	0.0916
Bergeron's Model	780	120	0.0004	350	400	0.2461	0.1052
2-end Trav. Wave	10	0	0.0148	780	340	6.7351	0.4566
1-end Trav. Wave	100	140	0.0915	550	280	8.8715	0.6724

For this test, the developed method had the most accurate results. The method proved to be more accurate than commercial methods and the method of [2]. The commercially available methods lose accuracy as R_F increase. The one-end traveling wave method identified high impedance faults in more occasions than the two-ends traveling wave method, but with the worse accuracy.

Bibliography Chapter 5

[1] F. Magnago and A. Abur, "Fault location using wavelets," *IEEE Transactions on Power Delivery*, vol. 13, no. 4, pp. 1475–1480, 1998.

[2] S. Jiale, G. Shuping, S. Guobing, J. Zaibin, and K. Xiaoning, "A novel fault-location method for HVDC transmission lines," *IEEE Transactions on Power Delivery*, vol. 25, no. 2, pp. 1203–1209, 2010.

[3] C. Peixoto, "Itaipu 6300 MW HVDC transmission system feasibility and planning aspects," *Symposium on Incorporating HVDC Power Transmission Into System Planning*, pp. 211–236, 1980.

[4] A. Praça, H. Arakaki, S. Alves, K. Eriksson, J. Graham, and G. Biledt, "Itaipu HVDC transmission system 10 years operational experience," in *V Symposium of Specialists in Electric Operational and Expansion Planning*, p. 12, 1996.

[5] T. Montelius, "DC line fault locator," tech. rep., ABB, Functional Description, 2011.

[6] G. Sarcinelli Luz and N. da Silva, "First benchmack model for HVDC controls in ATP program," in *X Symposium of Specialists in Electric Operational and Expansion Planning*, p. 10, 2006.

[7] IEEE, "IEEE guide for determining fault location on AC transmission and distribution lines," *IEEE Std C37.114-2004*, pp. 1–36, June 2005.

Chapter 6

Conclusions & Future Research

This chapter is devoted to evaluate the main contributions that result from this work. It includes a brief summary of the analysis, developments, and findings that constitute the core of this work. It also specifies the original contributions that have resulted while pursuing the general objective of this work. Finally, a number of future lines of research stemming from the developments presented are identified.

This work has addressed the problem of Fault location in two-terminals HVDC lines. This issue is currently of relevance due to advances in the DC power transmission technology, and the increase of HVDC line projects around the world. This is also relevant and of great concern of the European countries, where HVDC projects seek to exploit the potential of renewable energy around the continent. The advantage of using DC technology in these type of projects is the ability to connect remote renewable power resources such as wind power in the North Sea, solar power in North Africa, by crossing large bodies of water. These projects are strongly encouraged as a sustainable way to face the global warming problem.

DC technologies are necessary to deal with the environmental problems derived of traditional power systems. However, development of new power systems represent a challenge from the operational point of view, and for the search for new paradigms.

This work proposes an impedance-based method to solve the problem of fault location. This approach permits to overcome the problems in the commercially available fault locators which are traveling wave-based. The Impedance-based method proposes the use of a time-domain distributed-parameters line model. The distributed-parameters nature of this line model comes from the fact that approximations are not used to solve the line differential equations.

The proposed method has been developed considering the following three innovative features:

- Use of an operation principle different from that of commercially available methods, in order to avoid the weaknesses of those methods.
- Use of a time-domain transmission line model specifically developed for the method, in order to achieve high levels of accuracy.

- Use of fault data currently available in all HVDC system, avoiding the use of special equipment dedicated for fault location analysis, in order to reduce costs and facilitate the method's implementation in real HVDC lines.

Whereas the impedance-based fault location methods constitute the class most commonly used in AC systems fault location, due to its simplicity and low cost, its application in HVDC has not been sufficiently studied because of difficulties in the implementation of the DC line models that are necessary for this methodology. Although designed for AC lines, these methods can also be applied to locate faults on DC lines since there is no essential difference in line primary parameters between AC and DC lines. But AC lines models used in these methods are a function of the system's frequency, so they cannot be applied directly as models for HVDC lines since DC lines don't have a fundamental frequency. The main problem in this formulation is to find a model that fulfills the functions of the traditional frequency-domain line models but in the time-domain in order to adapt it to an impedance-based fault locator.

The telegraph equation needs to be solved in order to find a time-domain line model. But the telegraph equation is a second order linear partial differential equation with a coordinate of space and other of time, making it difficult to obtain a complete solution for them in terms of V and I as functions of x and t. To find an accurate solution to this equation is the main problem of transmission line modeling. The presented solution begins by dividing the partial differential equation into two equations: one in time-domain and the other in space-domain. Then, the general solutions of each one compensate each other, in order to describe the complete behavior of the line. Therefore, the general solution is given by the general solutions of its components in time and space.

With the time-domain line model, the proposed impedance-based fault location method can be used for HVDC line analysis. The method has shown the better performance when compared with existing commercial methods, using both actual and simulated fault records.

6.1 Contributions and Findings

Specific contributions and findings are summarized below:

1. This work develops an impedance-based fault location method for two-ended HVDC lines. The method was tested using both actual and simulated fault records, this records were analyzed using both the proposed method and commercial methods and the results were compared. For this test the proposed method proved to be more accurate than the currently available methods. The average of the results using the proposed method was about 40% more accurate than those of commercial methods. The novelty of this method is found in the use of a time-domain line model in order to obtain a high accuracy in the HVDC fault location.

2. This work develops a fault location method with more robustness against high impedance faults. Traveling wave-based methods have problems detecting high impedance faults since this kind of faults don't generate large wavefronts. But impedance-based methods are less affected by this problem. This type of faults are more common in overhead lines. The method was tested using simulated fault records and varying R_F from 0 to 400 Ω in steps of 20 Ω increments, these records were analyzed using both the proposed method and commercial methods and the results were compared. These tests showed that commercial methods can not detect high impedance faults, while the proposed method has a better performance in accuracy and detecting high impedance faults.

3. Another improvement that the proposed method could bring involves short HVDC lines. Short HVDC lines represent an important research area since almost 50% of the world's HVDC cables have a length of 100 km or less. The use of traveling wave-based methods in short HVDC lines have an added difficulty because the wavefront's velocity is very high, a high sampling frequency of measurement is required in order to record each wavefront's arrival to each line-ends. The proposed method is based on another operation principle and does not need special measurement equipment. Since the line model can be applied to both overhead and cables, they could also be used in fault location for short HVDC cables.

4. With the advantages showed with the use of the proposed method, this method could replace the current traveling wave-based methods or, at least, complement them in cases when traditional methods don't work.

5. The proposed method reduces process costs in HVDC line's operation. Utilities are showing some reluctance to move from an established working technology to the promise of an unfamiliar technology as they deal with their limited resources. There are many new developments, however, that can help them become more effective, efficient, and creative, but it is human nature to resist change. Utilities have the responsibility for keeping the lights on, so moving out of that comfort zone is difficult. The challenge is being able to determine what technology is a suitable solution that best fulfills the mission of providing the customer with high-quality power and the proposed method proved to be a possible option with economical advantages. The method provides economical and technical advancements in the fault analysis field, by offering more accuracy and faster solutions to the problem and with less special and dedicated field measurement equipment requirements, leading to improvements in the repair and operational processes of HVDC systems.

6. In this work a time-domain transmission line model was developed based entirely on distributed parameters. This model was designed specifically to be used in the fault location method of this work. However, as seen in section 4.1, to deduct the model was not required the use of premises to limit the model to only fault analysis, making possible the use of the model in the simulation of

other transient phenomena occurred in transmission lines. In this regard, the model has potential for improvements in areas such as electromagnetic transient simulation or any other analysis that requires a high accuracy in predicting the transmission lines behavior in time-domain.

6.2 Future Lines of Research

The developments of this work lead to a number of future lines of research whose exploration is likely to produce interesting results. This list summarizes the most important.

1. In this work was developed a functional fault location method for HVDC lines. The use of this method is limited to two-terminal lines. A possible extension of this work would be to develop a fault location method for multi-terminal HVDC lines.

   The recent advent of equipment oriented to the DC transmission (namely, the appearance of the first HVDC breaker commercially available), foresees a promising future for HVDC grids. With the use of DC breakers is expected topologies formed by large multiterminals HVDC grids where each line section can be operated as two-terminal lines like on AC grids, in these cases the method could be applied directly. But, also like on AC grids, there are always specific conditions that may favor the use of multi-terminal and tapped HVDC lines. In this context, the development of an impedance-based fault location method for multi-terminal HVDC line would introduce additional benefits to this area which is in full development.

2. This work shows the deduction of a model for fundamental frequency parameters and single-phase. This is a sufficient and appropriate modeling for the needs of the proposed method. A multi-conductors model for this purpose is not required because there isn't mutual coupling between DC conductors since there are not electromagnetic fields between them. Also, a frequency depended parameters model is not required because in DC system there is no frequency.

   But as said before, to deduct the model was not required the use of premises to limit the model to only fault analysis, making possible the use of the model in the simulation of other transient phenomena occurred in transmission lines. In this regard, the model has potential for improvements in areas such as electromagnetic transient simulation or any other analysis that requires a high accuracy in predicting the transmission lines behavior in time-domain, and not only for DC systems but also for AC systems. A possible extension of this work would be to further expand the model of the line for cases with multi-conductor and frequency depended parameters.

Appendix A

Test HVDC line Model

As explained, in section 5.1, the validation stage of the method developed in this work was carried out in cooperation with the company Eletrobras Furnas. The Itaipu HVDC model was used in the fault simulations in order to validate the method's performance.

The model was developed using the software Simulink/MATLAB, and was adapted from the model used by Eletrobras Furnas. The model used by the company was developed using the software ATP, and is based on the model of the PSCAD/EMTDC software found in the HVDC example directory, provided by the software's developer company and implemented by CIGRE. The CIGRE benchmark model for HVDC control studies became over time the standard HVDC benchmark for control studies, and provides a useful model as a result of its many special characteristics.

The HVDC line model was developed using MATLAB in order to unify all testing procedures in one software. Since all fault location algorithms were programmed using this software, and the test required to analyze 418 faults using 4 different methods, having everything programmed using the same language significantly facilitates the testing process because it makes possible to automate the simulation and analysis of faults.

For the model's development, were used many of the available components in the library of the SimPowerSystems module of the Simulink/MATLAB software.

A.1 Description of the HVDC System

The system is shown in Figure A.1. A 2000 MW dipole HVDC line (500 kV, 2 kA each pole) is used to transmit power from a 500 kV, 5000 MVA, 50 Hz network (Itaipu Dam) to a 245 kV, 10000 MVA, 60 Hz network (São Paulo City). The AC networks are represented by damped L-R equivalents with an angle of 80 degrees at fundamental frequency (50 Hz or 60 Hz) and at the third harmonic. A circuit breaker is used to apply DC line faults.

The rectifier and the inverter are 12-pulse converters using two Universal Bridge

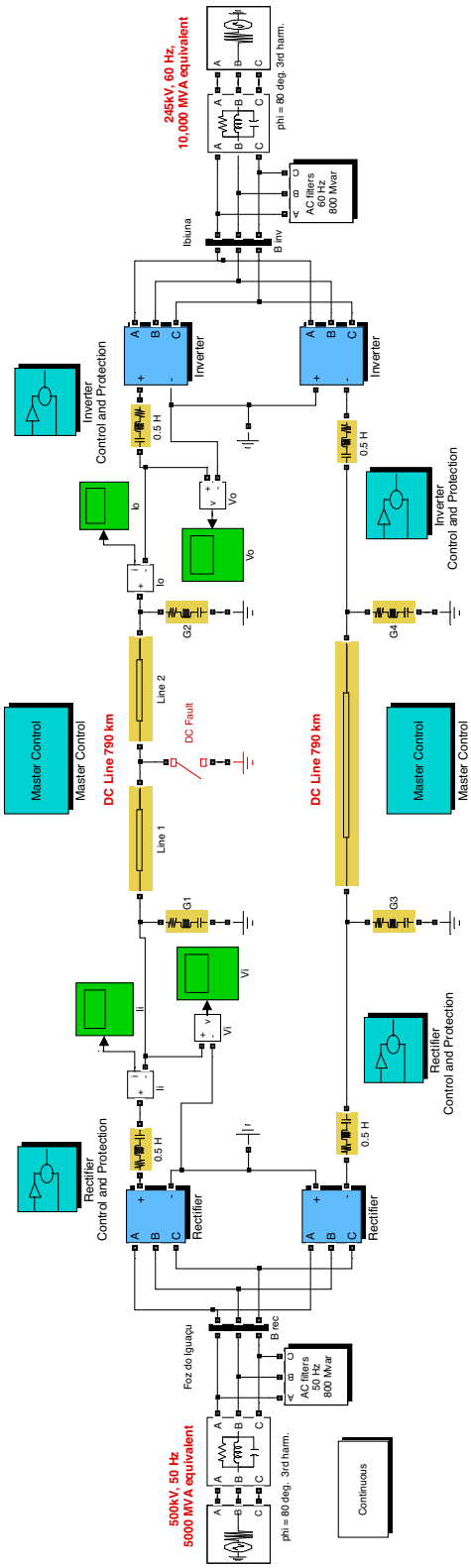

Figure A.1: MATLAB HVDC system model.

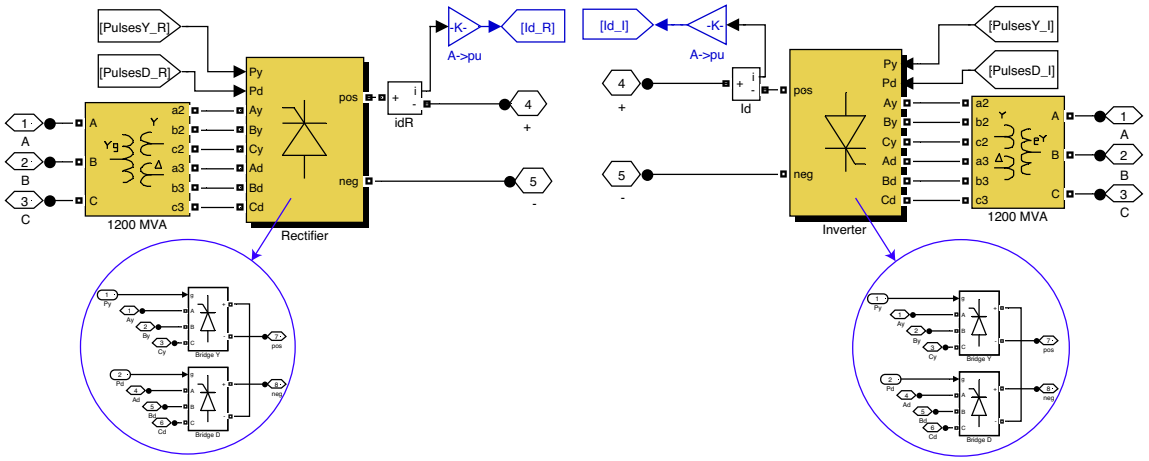

(a) Rectifier. (b) Inverter.

Figure A.2: Converters diagram blocks.

blocks connected in series (see Figure A.2). Since the HVDC system is a dipole line, two rectifiers and two inverters are needed. The converters are interconnected through two 0.5 H smoothing reactors and a 790 km line. A resistance has been added from each line-end to ground in order to simulate the line's conductance. The converter transformers (Wye grounded/Wye/Delta) are modeled with Three-Phase Transformer (Three-Windings) blocks. The transformer tap changers are not simulated. The tap position is rather at a fixed position determined by a multiplication factor applied to the primary nominal voltage of the converter's transformers (0.90 on the rectifier side; 0.96 on the inverter side).

The synchronization and generation of the twelve firing pulses is performed in the 12-Pulse Firing Control system. This block uses the primary voltages to synchronize and generate the pulses according to the alpha firing angle computed by converter controller. The synchronizing voltages are measured at the primary side of the converter transformer because the waveforms are less distorted. A Phase Locked Loop is used to generate three voltages synchronized on the fundamental component of the positive-sequence voltages. The firing pulse generator is synchronized to the three voltages generated by the PLL. At the zero crossings of the commutating voltages a ramp is reset. A firing pulse is generated whenever the ramp value becomes equal to the desired delay angle provided by the controller.

From the AC point of view, an HVDC converter acts as a source of harmonic currents. From the DC point of view, it is a source of harmonic voltages. So the harmonic order is $n = k * p \pm 1$ for the AC current, and $n = k * p$ for the direct voltage. Where n is the order number, p the pulse number, and k is an integer. In this model, $p = 12$ so that injected harmonics on the AC side are 11, 13, 23, 25, and on the DC side are 12, 24 (see Figure A.3).

AC filters are used to prevent the odd harmonic currents from spreading out on the network. The filters are grouped in two subsystems. These filters also appear as large capacitors at fundamental frequency, thus providing reactive power compensation for

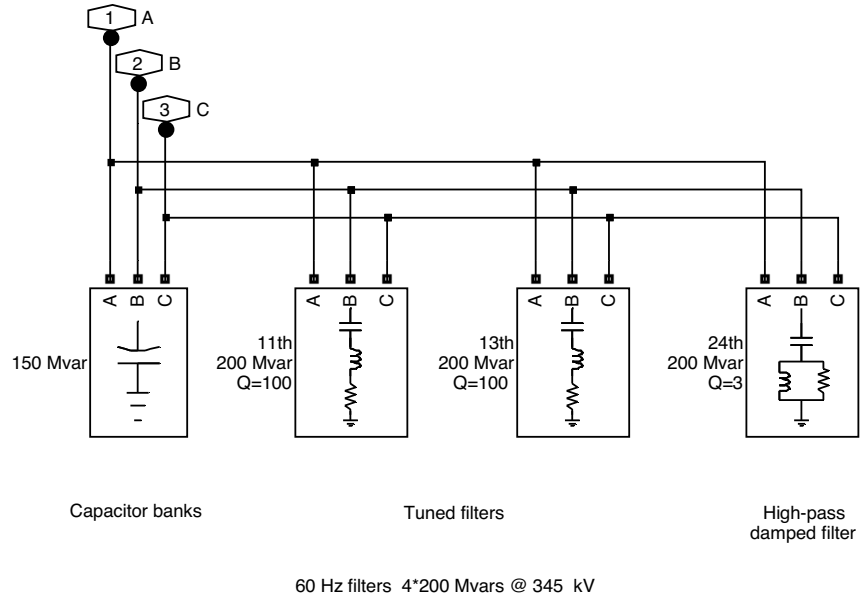

Figure A.3: Filters diagram blocks.

the rectifier consumption due to the firing angle α. For $\alpha = 30$ degrees, the converter reactive power demand is approximately 60% of the power transmitted at full load. Extra reactive power is also provided by capacitor banks.

A.2 Control and Protection Systems

Control and protection systems used are the Discrete HVDC Controller block of the Blocks library. A control and protection system is used for each pole in order to work independently. The control systems of the rectifier and of the inverter use the same Discrete HVDC Controller block. The block can operate in either rectifier or inverter mode. At the inverter, the Gamma Measurement block is used and it's found in the same library. The Master Control system generates the current reference for all converters and initiates the starting and stopping of the DC power transmission.

A.2.1 Protection System

At the rectifier, the DC fault protection detects a fault on the line and takes the necessary action to clear the fault. The DC fault protection constitutes the protective functions at the rectifier. The DC fault protection detects a fault on the DC line and tries to extinguish the fault current by ordering a forced alpha operation during a fixed duration. The Commutation faults prevention control constitutes the protective functions at the inverter. After a fault detection, an angle value is sent to the converter control in order to be deducted from the maximum delay angle limit (see Figure A.4).

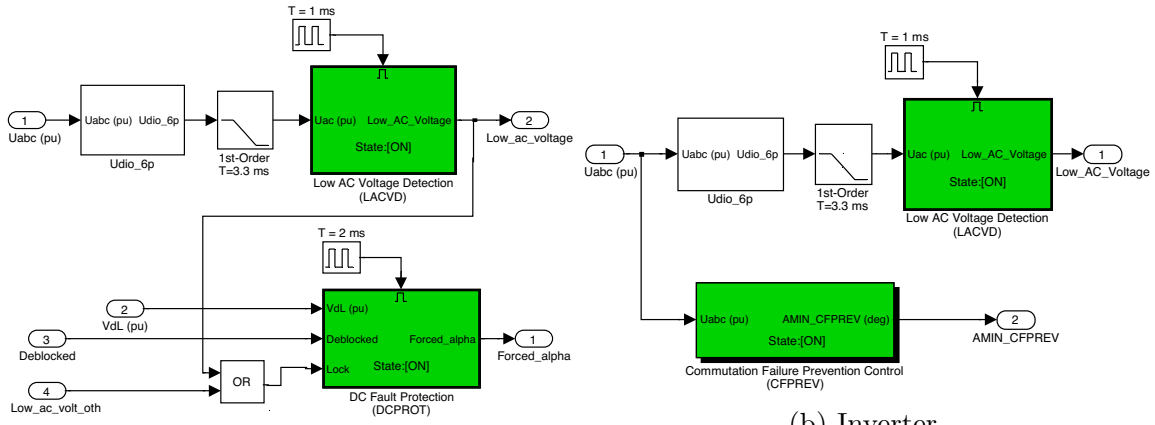

(a) Rectifier.

(b) Inverter.

Figure A.4: Protections diagram blocks.

A.2.2 Master Control

The rectifier's and inverter's current reference are generated in the master control. The reference should be equal in both converters to avoid the loss of the margin. The converter's starting and stopping is initiated and the current reference can be ramped up or down. A current step can be added to the current reference for testing purposes (see Figure A.5).

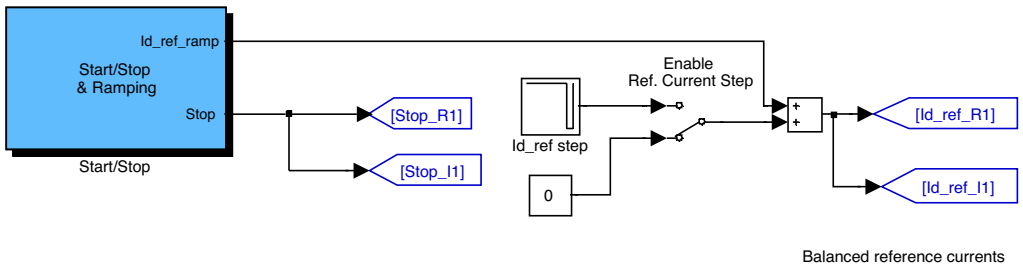

Figure A.5: Master control diagram blocks.

A.2.3 Controller Block Inputs and Outputs

Figure A.6 is the controller block diagram used in the model.

The input signals are explained bellow:

- Inputs 1 and 2 (VdL and Id) are the DC line voltage and current. The measured DC currents and voltages are scaled to p.u. before they are used in the controllers. The inputs are filtered before being processed by the regulators.
- Inputs 3 and 4 (Id_ref and Vd_ref) are the voltage and current reference values in p.u.

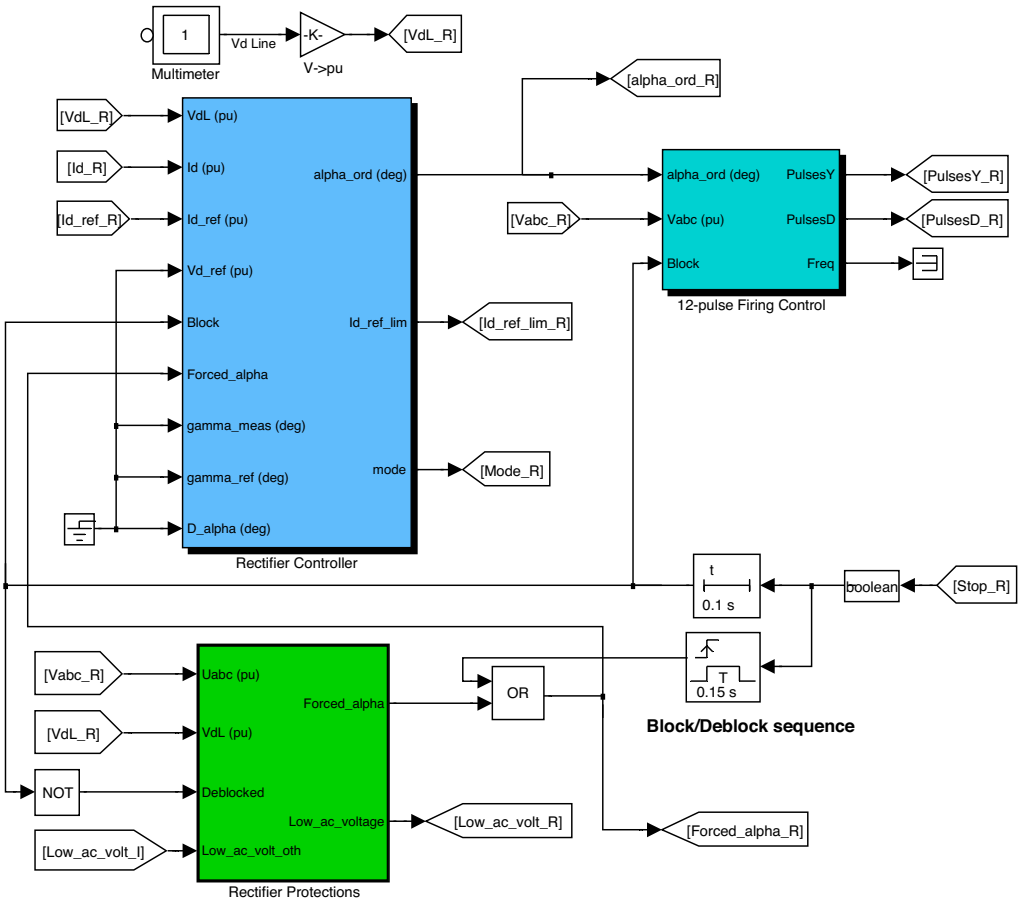

Figure A.6: Control diagram blocks.

- Input 5 (*Block*) accepts a logical signal (0 or 1) used to block the converter when Block is 1.
- Input 6 ($Forced - alpha$) is also a logical signal that can be used for protection purposes. If this signal is high, the firing angle is forced at the value defined in the block dialog box.
- Input 7 (*gamma_meas*) is the measured minimum extinction angle of the converter's 12 valves. It is obtained by combining the outputs of two 6-pulse Gamma Measurement blocks.
- Input 8 ($gamma\_ref$) is the extinction angle reference in degrees. To minimize the reactive power absorption, the reference is set to a minimum acceptable angle.
- Input 9 (D_alpha) is a value that is subtracted from the delay angle maximum limit to increase the commutation margin during transients.

In normal operation, the rectifier controls the current at the Id_ref reference value, whereas the inverter controls the voltage or gamma at the Vd_ref or *Gamma_meas*

reference value. They are set at 0.1 p.u., 0.05 p.u., and 1.0 deg., respectively.

The output signals are explained bellow:

- Output 1 ($alpha\_ord$) is the firing delay angle in degrees ordered by the regulator.
- Output 2 (Id_ref_lim) is the actual reference current value.
- Output 3 ($Mode$) is an indication of the actual state of the converter control mode.

The state is given by a number (from 0 to 6) as follows:

- 0 Blocked pulses
- 1 Current control
- 2 Voltage control
- 3 Alpha minimum limitation
- 4 Alpha maximum limitation
- 5 Forced or constant alpha
- 6 Gamma control

The system normally operates at point 1. However, during a severe contingency producing a voltage drop on the AC network feeding the rectifier, the operating point moves to point 2. The rectifier is forced to a minimum mode and the inverter is in current control mode. Similarly, a voltage drop on the AC network feeding the inverter will force a control mode change to Gamma regulation to limit the angle to min. During severe contingency, a faster response is necessary to increase the commutation margin and, consequently, to reduce the probability of a commutation fault. The Commutation Failure Prevention Control subsystem generates a signal that decreases the maximum limit of the delay angle during the voltage drop.

A.3 Model Test

Having the complete system modeled, several cases were simulated in PSCad and MATLAB to compare the results, but only the most severe one, the solid fault, is presented in order to make easier the comparison of the results. Figure A.7 presents, side by side in the same scale, simulation results in both softwares. Graphs of DC voltage and current from the rectifier and inverter line-ends during the fault are presented. The ones on the left side are PSCAD results, and the ones on the right side are MATLAB results.

The comparison between the results presented by both programs shows they have quite similar responses for the fault.

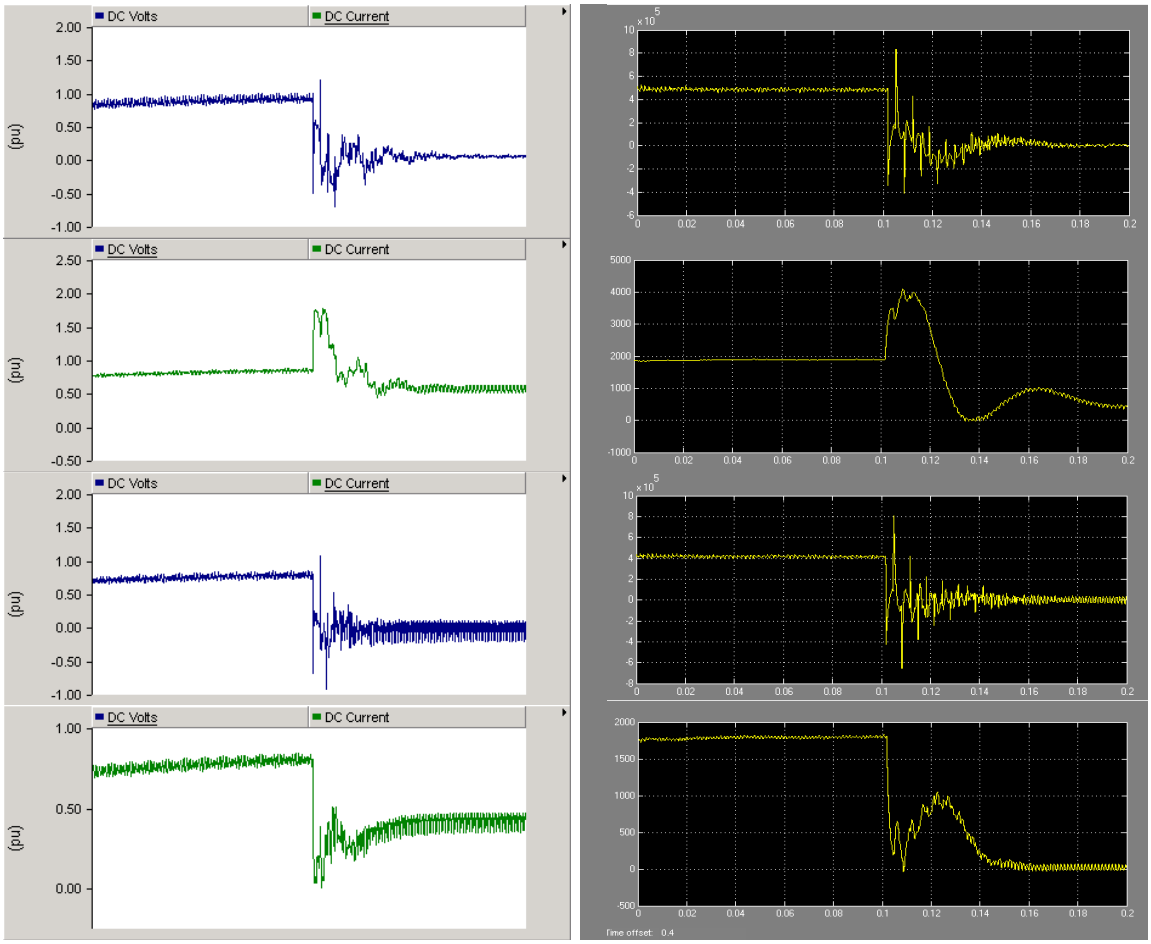

(a) PSCad model. (b) MATLAB model.

Figure A.7: Models behavior comparison.

Appendix B

COMTRADE Standard

IEEE Standard Common Format for Transient Data Exchange (COMTRADE) is intended for use by digital computer based devices which generate or collect transient data from electric power system. The standard should facilitate exchange of the transient data for the purpose of simulation, testing, validation, or archival storage. It is expected that the standard will be particularly useful for users of digital relays, digital fault recorders, or digital simulation programs of electrical transient phenomena.

COMTRADE provides a common language in which those interested in power system and protection analysis may exchange information, in the form of digital data files of power system events. The standard is not a standard for communication systems, its purpose is that all manufacturers involved in the fabrication of recording, analysis, and testing systems will provide a bridge between their own proprietary system and COMTRADE. Several manufacturers have already committed to support this standard. These data files comprised of records of voltage and current waveforms, logical events -such as alarms-, prospective relay operations or breakers operations, in a time coherent record.

The need for a common format resulted from the burgeoning interest in the analysis of the performance of power systems and their protection subsystems. This led to the proliferation of devices for the acquisition or simulation of power systems event data. For valid commercial reasons, different manufacturers use widely divergent formats and media for data storage. However, the situation with interconnected utilities who share a common interconnection but use equipment from different manufacturers, makes difficult for simulation programs to exchange data about a common power system event. This standard provides a means to share such information.

B.1 Standard Files Summary

The standard recommends the use of a set of files for a given event consisting on three types of files with the same prefix and their required extensions .cfg, .dat, and .hdr. Each file type stores different data related to the event.

B.1.1 Configuration Files

The configuration file (.cfg) is in a pre-defined fixed ASCII format so that it can be read by a computer program, or a human being. This file contains station name and the record's ID, or simulation information defining the format of the data event. This includes date and time, sampling rate, frequency, number and type of channels in the data section of the record, and whether the data is stored in binary or ASCII format. It provides all of the information necessary to print or make an analog reproduction of the record. The format is fixed so that it can be read by a computer for automated reproduction.

B.1.2 Data Files

The data files (.dat) contain the actual data samples of the recorded or simulated event. These are digital time tagged samples of the instantaneous values of analogue and logical events. Each discrete analogue or logical source monitored is called a channel. Analogue channels are commonly voltage and currents. These may have many different values depending upon the resolution of the originating recorder or program, and are represented by integer values. Conversion information for these numbers is contained in the .cfg and .hdr files. Logical channels are typically relay or breaker contacts, these have only two states (active or inactive), and they are represented by ones and zeros.

The data files consist of rows and columns. Each represents a time tagged series of samples. The number of rows in a record depends on the sampling rate and the total time recorded. There will be as many rows as there are samples in the record. Each row contains one column for the sample number, one column for the time since the beginning of the record, and one column for each analogue or digital channel. The data file must conform exactly to the format defined by the information in the .cfg file so that it can be read by a computer program.

B.1.3 Header Files

The header file (.hdr) is a free form ASCII file containing any textual information that the originator wants to convey to the end user. The contents may include information on the recording or simulation system, and the power system location from which the event data was originated. Power system impedances, transformer ratios, and similar information may be included. To ensure compatibility, information on the data recording format and data file must be included.

B.2 Sampling Rate

The range of sampling rate of the original data depends on the source of that data, and the exact sample used depends upon the equipment used at the source. Therefore,

a file generated in one system may have too high or low sample rate for application in another system.

For instance, simulations may need to sample at very high rate to maintain accuracy. The time resolution of samples resulting from such a study is much more detailed than what would be useful in any plotting or reproduction system. The sampling rate, and therefore the number of samples, would normally be reduced before exchange or cross application of this data. It must be taken into account that reduction of the sample rate by any method means loss of frequency response. Also, once the data is converted to a low sampling rate there is no way to restore the loss of frequency response by recovering back to the original data. Simple decimation of the sample rate by throwing away every second, or second and third data point is not a valid method of sample rate conversion. This method leads to the generation of large artificial frequency components in the data.

Similarly, while digital fault recorders from different manufacturers have a similar range of sampling frequencies, they don't all have a common base frequency. These sampling rates are similar to the ranges of sampling frequency used in analog reproduction systems for relay testing. However, in both cases the data sampling frequency may have to be modified for a cross application. The range of sampling frequencies in the current generation of digital relays which store fault data is lower than that commonly used in digital fault recorders and reproduction system. Therefore, the sampling rate of data from digital fault recorders will probably need to be changed for a digital relaying application.

Recorders or relays usually have anti-aliasing filters in the sampling circuit to limit the frequency components of the input signal. These filters prevent the generation of spurious frequency components in the data caused by the interaction of the sampling frequency and the high order frequency components of the original signal.

The standard suggests methods suitable for conversion between one sampling rate and another.

B.3 Illustrative Example

An illustrative example of the formats of .cfg and .dat files for records in COMTRADE standard is shown below. It shows a variety of lines with different characters that provide the record information separated by commas. At the end of the examples is shown the significance of each line, with a meaning of each term of the lines and the information found on them. The meaning of some lines is not explained, it is because these are equal to its previous line.

B.3.1 .cfg File Format

$$
\begin{aligned}
&Name, ID < CR/LF > && (A1)\\
&XX, xxA, xxD < CR/LF > && (A2)\\
&CN, CName, P, ET, Und, K_1, K_2, To, MIN, MAX < CR/LF > && (A3)\\
&CN, CName, P, ET, Und, K_1, K_2, To, MIN, MAX < CR/LF >\\
&\vdots\\
&\vdots\\
&CN, CName, P, ET, Und, K_1, K_2, To, MIN, MAX < CR/LF >\\
&CN, CName, M < CR/LF > && (A4)\\
&CN, CName, M < CR/LF >\\
&\vdots\\
&\vdots\\
&CN, CName, M < CR/LF >\\
&FR < CR/LF > && (A5)\\
&Tm < CR/LF > && (A6)\\
&SS1, ENDSS1 < CR/LF > && (A7)\\
&MM/DD/YY, HH : MI : SS.SSS < CR/LF > && (A8)\\
&MM/DD/YY, HH : MI : SS.SSS < CR/LF > && (A9)\\
&TP < CR/LF > && (A10)
\end{aligned}
$$

Meaning:

($A1$) Substation's name and identification

$Name$: substation's name

ID: identification of substation's register equipments

($A2$) Number and types of channels

XX: total number of channels

xxA: total number of analog channels

xxD: total number of digital channels

($A3$) Information of each analog channel

CN: channel's number

$CName$: channel's name

P: phase monitored by the channel

ET: type of system equipment monitored by the channel (Bus, Trf, Line, etc)

Und: signal's units after applying the conversion factor (Voltage or Amper)

K_1: conversion factor for units at Und

K_2: conversion factor for units at Und

With K_1*(.dat)+K_2 the actual measurement is obtained from the integer values stored at the .dat file

To: time when sampling starts, with respect to the beginning of the file (μs)

MIN: minimum integer value of the scale for that channel samples

MAX: maximum integer value of the scale for that channel samples

($A4$) Information of each digital channel

CN: channel's number

$CName$: channel's name

M: indicates the normal state of the channel (0 to inactive and 1 to active)

($A5$) System's frequency

FR: system's frequency

($A6$) Record's time

Tm: multiple of the record's time in seconds

($A7$) Sampling rates velocity

$SS1$: sampling frequency in Hz

$ENDSS1$: number of the last sample to the sampling frequency

($A8$) Date and time of start of event

MM: Event's start month

DD: Event's start day

YY: Event's start year

HH: Event's start hour

MI: Event's start minute

$SS.SSS$: Event's start second, up to six decimals

($A9$) Date and time of end of event

MM: Event's end month

DD: Event's end day

YY: Event's end year

HH: Event's end hour

MI: Event's end minute

$SS.SSS$: Event's end second, up to six decimals

($A10$) .dat file type

TP: type of code used in the .dat file (ASCII or BINARY)

B.3.2 .dat File Format

$$1, 0, 4882, 13581, -18555, \cdots, 100, 121, -216, 0, 0, \cdots, 0, 0 < CR/LF > \quad (A1)$$
$$2, 347, 2589, 15085, -17763, \cdots, 70, 144, -211, 0, 0, \cdots, 0, 0 < CR/LF >$$
$$3, 694, 152, 16233, -16456, -26, \cdots, 41, 166, -202, 0, 0, \cdots, 0, 0 < CR/LF >$$
$$4, 1041, -2280, 17067, -14840, \cdots, 13, 184, -191, 0, 0, \cdots, 0, 0 < CR/LF >$$
$$\vdots \quad \vdots \quad \vdots \quad \vdots \quad \vdots \quad \vdots \quad \vdots \quad \vdots \quad \vdots \quad \vdots \quad \vdots$$
$$2685, 931348, -12426, 19369, -6999, \cdots, -54, 124, -61, 0, 0, \cdots, 0, 0 < CR/LF >$$
$$2686, 931695, -13890, 18621, -4793, \cdots, -69, 119, -42, 0, 0, \cdots, 0, 0 < CR/LF >$$
$$2687, 932042, -15108, 17325, -2290, \cdots, -84, 114, -23, 0, 0, \cdots, 0, 0 < CR/LF >$$
$$2688, 932389, -16111, 15695, 324, \cdots, -99, 109, -4, 0, 0, \cdots, 0, 0 < CR/LF >$$

Meaning:

(A1) $CN, TI, A1, A2, \cdots, AN, D1, D2, \cdots, DN < CR/LF >$

CN: sample number

TI: time in μs for the sample interval

$A1, A2, \cdots, AN$: samples' integer values for each analog channel

$D1, D2, \cdots, DN$: samples' integer values for each digital channel